SCUOLA DOTTORALE IN BIOLOGIA

SEZIONE "BIOLOGIA APPLICATA ALLA SALUTE DELL'UOMO"

CICLO XXV

Tesi di Dottorato di Ricerca

# Effetto dello stress ossidativo caratterizzante il Diabete Mellito sulla struttura e funzione del VWF: rilevanza nell'insorgenza di complicanze trombotiche in questo contesto clinico


***Dottoranda***
Dott.ssa Laura Oggianu

***Docente guida presso "Università degli Studi Roma Tre"***
Ch.mo Prof. Paolo ASCENZI

***Docente guida presso "Università Cattolica del Sacro Cuore"***
Ch.mo Prof. Raimondo DE CRISTOFARO

***Coordinatore del corso***
Ch.mo Prof. Paolo VISCA

DOCTORAL SCHOOL IN BIOLOGY

COURSE "BIOLOGY APPLIED TO HUMAN HEALTH"

CYCLE XXV

Doctoral Thesis

# Effect of oxidative stress occurring in diabetes mellitus on VWF structure and function: its relevance for thrombotic complications in this clinical setting


***Ph.D. Student***
Dr. Laura Oggianu

***Tutor at "Università degli Studi Roma Tre"***
Prof. Paolo ASCENZI

***Tutor at "Università Cattolica del Sacro Cuore"***
Prof. Raimondo DE CRISTOFARO

***Course Coordinator***
Prof. Paolo VISCA

# APPENDIX

# 1. INTRODUCTION

## 1.1 VON WILLEBRAND FACTOR

### 1.1.1 STRUCTURE, ASSEMBLY, STORAGE AND SECRETION

Von Willebrand Factor (VWF) is a multimeric glycoprotein with very high molecular weight that plays an essential role in platelet-dependent hemostasis. VWF is synthesized in all vascular endothelial cells [1] and megakaryocytes [2].
Inside RER, a monomer of pro-VWF (275 kDa) forms dimers (550 kDa) via disulfide bonds at the carboxyl terminus ("tail-to-tail" dimerisation) [3, 4]. After transport to the Golgi apparatus, pro-VWF dimers form homo-polymers through an additional disulfide bond at the amino terminus, in a process termed "head-to-head" multimerisation [5]. This is followed by N-linked and O-linked glycosylation and by the proteolytic removal of the large VWF pro-peptide by furin [5].
The majority, up to 95%, is then constitutively secreted, whereas the remainder 5% is stored in cytoplasmic granules called Weibel-Palade bodies, that are specific for endothelium [6, 7]. A similar packaging form has been found at in the platelet α-granules [8].
The VWF stored inside endothelial cells is secreted in response to a variety of stimuli, including adrenergic stress or thrombin generation. VWF secreted by endothelial cells is almost exclusively constituted by ultra large multimers (UL-VWF), which can be up to approximately 20 000 kDa in size [9, 10] and are the most adhesive and hemostatically reactive forms of VWF.
When in the bloodstream, UL-VWF appears as a tangled condensed coil. Instead, under fluid shear stress, UL-VWF forms string-like structures attached to the endothelial cell surface, perhaps through interaction with P-selectin [11].
In such a condition, it may be cleaved by ADAMTS13 at the Tyr1605-Met1606 bond in the A2 domain [12], generating the less adhesive range of VWF multimer sizes that normally circulate in the blood, with a half-life of ≈12h and a concentration of ≈10μg/ml [13].

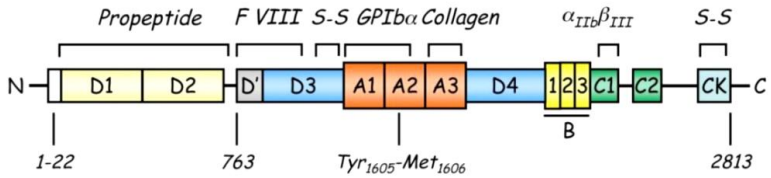


**Figure 1. Structure-function relationships of von Willebrand factor.** The pre-pro-VWF polypeptide is indicated with amino acids numbered from the amino- (aa 1) to carboxy-terminal portions (aa 2813). Binding sites are indicated for factor VIII (D' and D3 domains), platelet glycoprotein Ibα (GPIbα) (A1 domain), collagen (A1 and A3 domains) and integrin αIIbβIII (RGD sequence within the C2 domain). The cleavage site (Tyr1605-Met1606) for ADAMTS13 is located at the central A2 domain of von Willebrand factor. The locations of inter-subunit disulfide bonds (S-S) are shown in the CK and D3 domains, which are important for the formation of VWF dimers and multimers respectively [12].

### 1.1.2 BIOLOGICAL ACTIVITIES AND STRUCTURE-FUNCTION RELATIONSHIPS

VWF exerts its hemostatic functions through binding to platelet surface glycoproteins and to constituents of connective tissue. The binding of VWF to platelets is regulated by both its initial interaction to connective tissue and shear stress in flowing blood [14].
In the absence of injury VWF does not interact with circulating platelets, while damages to the endothelium allow A3 VWF domain binding to constituents of sub-endothelial connective tissue [15].
Once immobilized in the sub-endothelial connective tissue, VWF requires the presence of strong hydrodynamic forces allowing its elongation and the consequent exposition of its platelet binding site [16].
Platelets can then adhere to VWF thanks to their surface glycoprotein (GP) Ib-IX-V complex, that interacts with the A1 VWF domain [17].
The shear stress dependency of VWF-mediated platelet adhesion is due to the fact that shear rate (expressed in units of cm/s per cm, or inverse seconds, $s^{-1}$) is maximal at the vessel wall.
The kinetically rapid interaction between GPIbα and VWF promotes the reversible tethering of platelets that approach the vessel wall. The slowly moving tethered platelets may then adhere irreversibly through the kinetically slow binding of other platelet integrins to ligands in connective tissue. [18].

The puzzle remains that VWF does not appear to support platelet adhesion at low shear rates, yet it is extremely effective at high shear rates.
In the absence of shear stress, VWF deposited on a hydrophobic surface had a globular, condensed conformation [19]. Above a critical shear stress value, VWF adopted an extended chain conformation with the exposure of intra-molecular globular domains (Figure 2). The shear stress required to induce this conformational transition appears comparable to the threshold of shear stress for VWF-dependent platelet adhesion to vessel segments. Thus, shear-induced conformational changes in VWF contributes to the regulation of VWF binding to platelet GPIbα [19].

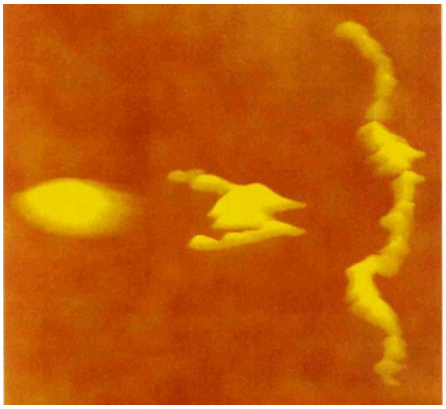

**Figure 2. Effect of shear stress on VWF conformation.** Atomic force microscopy (AFM) in tapping mode exerts negligible shear force on the sample and images VWF as a globular protein (left). AFM in contact mode applies shear forces of a few nanoNewtons and can slightly extend the VWF molecule (center). Shear force of 35 dyn/cm$^2$ applied by a rotating disk before imaging extends the VWF molecule in the direction of the shear field, with molecular lengths ranging from 146 to 774 nm [19].

## 1.2 ADAMTS13

### 1.2.1 BIOSYNTHESIS, SECRETION, STRUCTURE AND FUNCTION

ADAMTS13 (A Disintegrin-like And Metalloprotease with Thrombo-Spondin type 1 motif 13) is the 13$^{th}$ member of the ADAMTS family of zinc proteases and it specifically cleaves VWF at the Tyr1605-Met1606 bond in the A2 domain. The proteolytic activity requires the presence of both $Ca^{2+}$ and $Zn^{2+}$ cations [20] and moreover, it requires VWF in a denatured conformation, achieved by conditions of high shear stress [12].
ADAMTS13 is synthesized predominantly in the liver [21, 22], although variable expression has been observed in endothelial cells [23, 24], megakaryocytes, or platelets [25, 26] and it is secreted into plasma as an already active enzyme. Considering the large surface area of vascular endothelial beds, plasma ADAMTS13 might be derived mainly from endothelial cells, even though each endothelial cell produces little amounts of ADAMTS13 compared to other sites [23, 24].
Like the other members of its family, ADAMTS13 lacks a trans-membrane domain and, therefore, it is secreted rather than membrane bound. Moreover, ADAMTS13 pro-peptide does not impair its secretion or activity, demonstrating that it is not required for the enzyme folding or secretion and likely, it does not confer enzymatic latency and inactive zymogen characteristics to ADAMTS13 [20]. In common with the other ADAMTS proteases, ADAMTS13 presents a structure comprising a metalloprotease domain (M), a disintegrin-like domain (Dis), a cysteine-rich domain (Cys-R), a spacer domain (Spa) and a thrombospondin type 1 (TSP1) repeat [21].
The metalloprotease domain is the catalytic center for the hydrolyzation of VWF, however, this region alone is not sufficient to recognize and hydrolyze the VWF at its cleavage site in the A2 domain. Instead, the presence of the TSP1, the Cys-R and (in particular) the Spa domains mediates the molecular recognition and proteolytic processing of VWF multimers [22, 20]. The catalytic domain is followed by the disintegrin-like domain (so called because it presents 25% to 45% identity to the snake venom disintegrins), that probably plays its function in both enzyme activity and specificity [22]. CUB (complement C1r/C1s, Uegf (EGF-related sea urchin protein) and BMP-1 (bone morphogenic protein-1)) domains are unique to ADAMTS13 and allow it to interact with intracellular sorting receptors that direct apical targeting. This way, ADAMTS13 synthesized in endothelial cells is directly delivered to the apical domain of polarized cells (i.e., toward the lumen of the vessels) [23]. TSP1 motifs are known to mediate protein-protein interactions, especially among proteins in the extracellular matrix. In the case of ADAMTS13, TSP1 repeats (from 2 to 8) are those that interact with VWF under fluid shear stress [23].

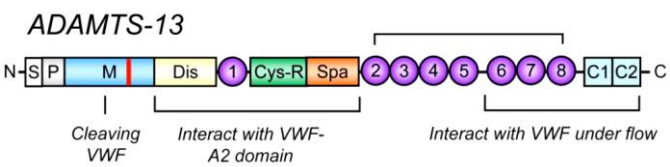


**Figure 3. ADAMTS13 structure** The structural domains are indicated: signal peptide (**S**), propeptide (**P**), metalloprotease (**M**) (location of zinc-binding motif shown in red), disintegrin domain (**Dis**), first thrombospondin type 1 (TSP1) repeat (**1**), cysteine-rich domain (**Cys-R**), spacer domain (**Spa**), (**2**) through (**8**), the second to eighth TSP1 repeats and two CUB domains (**C1** and **C2**) [21].

### 1.2.2 ENZYMATIC ACTIVITY REGULATION

Modulation of the ADAMTS13/VWF interaction is critical for an efficient proteolysis: ADAMTS13 binds to VWF under both static or high shear stress conditions, however, this interaction, is unproductive for proteolysis unless shear stress is high enough to stretch VWF and expose the buried A2 domain for cleavage at its Tyr1605-Met1606 bond [27]. The unique requirement of shear forces finely regulates ADAMTS13 activity and impedes an uncontrolled VWF proteolysis to take place [28].
On the other hand, in the absence of ADAMTS13 activity due to genetic mutations or formation of anti-ADAMTS13 autoantibodies, a life-treatening disease, referred to as thrombotic thrombocytopenic purpura (TTP), does occur, causing UL-VWF retention (the forms with higher pro-haemostatic potential) and an uncontrolled microvascular thrombosis [29].
Thrombin, factor Xa, leukocyte elastase, and plasmin can cleave and inactivate ADAMTS13, regulating its activity at the site of thrombus formation, where it shows concentrations particularly elevated. The susceptibility of ADAMTS13 to elastase proteolysis in vivo is particularly evident in patients with sepsis-induced disseminated intravascular coagulation, in which leukocyte elastase activity is increased, suggesting that cleavage of ADAMTS13 by leukocyte elastase might contribute to the relatively severe deficiency of ADAMTS13 activity [30].

## 1.3 LEUKOCYTE SERINE PROTEASES

Human neutrophil elastase (HNE), proteinase 3 (PR3) and cathepsin G (CG) are three serine proteases of the chymotrypsin family that are stored in the primary (azurophil) granules of polymorphonuclear neutrophils (PMNs), from where they are liberated into the extracellular space, or associated with the outer PMN plasma membrane [31]. Their activities depend upon a catalytic triad composed of aspartate, histidine and serine residues, which are widely separated in the primary sequence, but are brought together at the active site of the enzymes in their tertiary structures. They were first identified as degradative enzymes responsible for eliminating intracellular pathogens and breaking down tissues at inflammatory sites [32, 33] and were soon recognized as possible molecular targets for anti-inflammatory agents [34]. Circulating PMNs are the first cells to reach a site of inflammation by extravasation, thus providing a primary line of defense against bacterial infection.
Leukocyte serine proteases (LSPs) act intracellularly, within phagolysosomes, to digest phagocytized micro-organisms in combination with microbicidal peptides and the membrane-associated NADPH-oxidase system, that produces oxygen metabolites [35].
LSPs released from cells are involved in the regulation of innate immunity, inflammation and infection, in addition to their well recognized destructive function of extracellular matrix components at inflammatory sites, to which they are recruited [35].
This dual, apparently antinomic, protective/destructive function has attracted great interest over the past decade as new specific targets were discovered [36].
It is now clear that LSPs are not only destructive proteases with broad, unspecific and redundant proteolytic activity as initially stated, but that each has specific functions in spite of their similar gene expressions, subcellular locations, 3D structures, physicochemical properties and antigenic substrate specificities. Even if all three LSPs have bactericidal properties, they act through different mechanisms that may or may not involve their proteolytic activity [36, 37].
In addition to their degradative/bactericidal properties, LSPs are also important regulators of the local inflammatory response. They can modulate biological functions, such as the control of cellular signaling through the processing of chemokines, modulating the cytokine network and activating specific cell surface receptors [31, 36].
Exposure of PMNs to cytokines and chemoattractants results in the rapid mobilization of azurophil granules to the cell surface, the release of granule proteins and the appearance of LSPs on the cell surface, which are catalytically active just like soluble proteases [31].

## 1.4 OXIDATIVE STRESS

The paradox of aerobic life, or “Oxygen Paradox”, is that higher eukaryotic aerobic organisms cannot exist without oxygen, yet oxygen is inherently dangerous to their existence. This “dark side” of oxygen relates directly to the fact that each oxygen atom has one unpaired electron in its outer valence shell and molecular oxygen has two unpaired electrons [38]. Thus, atomic oxygen is a free radical and molecular oxygen is a (free) bi-radical.
Concerted tetravalent reduction of oxygen by the mitochondrial electron-transport chain, to produce water, is considered to be a relatively safe process; however, the univalent reduction of oxygen generates reactive intermediates [38].

The reductive environment of the cellular milieu provides ample opportunities for oxygen to undergo unscheduled univalent reduction. So, oxygen, while essential for life, is at the same time involved in the toxic effects of exposure to ionizing radiation, UV light, and a variety of chemical substances [38].
All of these agents cause an increased production of oxygen-derived free radicals and a modified pro-oxidant state. Oxygen-derived free radicals are also generated as part of a normal physiological process, such as during mitochondrial electron transport, by cellular oxido-reductase such as xanthine oxidase and by oxidative action of neutrophils at sites of inflammation.
Reactive oxygen species (ROS) are formed and degraded by all aerobic organisms, leading to either physiological concentrations required for normal cell function, or excessive quantities corresponding to the state of oxidative stress. As the term ROS implies, intracellular production of those oxygen intermediates threatens the integrity of various biomolecules, including proteins [39], lipids, as well as lipoproteins involved in atherosclerosis [40] and DNA [41].
The chemical consequences of protein oxidation include the formation of carbonyl groups (aldehydes and ketones) on some amino acids (e.g. proline, arginine, lysine or threonine) and the conversion of methionine to methionine sulfoxide, histidine to oxohistidine or asparagine, tyrosine to dityrosine, and cysteine to dislufides [42]. Biologically, these modification lead to alterations in enzyme activities and binding properties of the proteins. Moreover, many disabling pathological conditions, such as atherogenesis [43], diabetes [44] and chronic kidney disease (CKD) [45-48] are known to result in oxidation of cellular and extracellular components.
ROS include a number of chemically reactive molecules derived from oxygen [49]. Some of those molecules are extremely reactive, such as the hydroxyl radical, while some are less reactive (superoxide and hydrogen peroxide). Intracellular free radicals (i.e., free low molecular weight molecules with an unpaired electron) are often ROS and vice versa and the two terms are therefore commonly used as equivalents. Free radicals and ROS can readily react with most biomolecules, starting a chain reaction of free radical formation [50].
In order to stop this chain reaction, a newly formed radical must either react with another free radical, eliminating the unpaired electrons, or reacting with a free radical scavenger, a chain-breaking or primary antioxidant. As it is impossible to prevent all free radical production in vivo, it is not surprising that a range of antioxidant defenses have evolved in the body [51].
Both enzymic and non-enzymic antioxidants are present. Antioxidant enzymes include superoxide dismutase, glutathione peroxidase and catalase. The main non-enzymic antioxidants include GSH, vitamin C and vitamin E [52]. The antioxidant defenses of the body are usually adequate to prevent substantial tissue damage, without any excess of antioxidant defenses. However, an overproduction of free radicals, or a drop in the level of the antioxidant defenses will lead to an imbalance and cause deleterious effects, determining the occurrence of a oxidative stress condition [52].

### 1.4.1 OXIDATIVE STRESS AND TYPE 2 DIABETES MELLITUS

Diabetes Mellitus (DM) is a severe metabolic disease characterized by the presence of high oxidative stress and complicated by dramatic thrombotic micro- and macro-agiopathies [53]. DM is responsible for tissues and organs damage through several physiopathological mechanisms, such as an increased flux of glucose and other sugars through the polyol pathway, increased intracellular formation and activity of advanced glycation endproducts (AGEs), activation of protein kinase (PK)C isoforms and finally, overactivity of the hexosamine pathway. Altogether, these mechanisms were reported to be linked to an upstream mitochondrial overproduction of ROS [54]. In particular, in the diabetic microvasculature, this is a direct consequence of intracellular hyperglycemia.
On the other hand, in the DM microvasculature, ROS overproduction would stem from increased oxidation of fatty acids, main consequence of insulin resistance [54]. Moreover, hyperglycemia in DM promotes also an impairment of the antioxidant systems, such as glutathione reduced form (GSH) [55].
Oxidative stress is involved in the pathogenesis of endothelial dysfunction, characterized, besides increased vascular stiffness and tone, by the presence of a pro-thrombotic and anti-fibrinolytic status [56].
Endothelial dysfunction plays a key role in the pathogenesis of atherosclerosis and its presence has been documented in diabetic patients [57].
Oxidative stress induces chemical modifications also of plasma proteins and enzymes, including those involved in haemostasis and coagulation, as VWF and fibrinogen, which are potentially involved in the mechanisms favoring both micro- and macro-angiopathic diseases [58].
The oxidative stress causes in these proteins formation of ROS- and nitrogen oxidative species (NOS)-modified amino acids, such as 3-nitrotyrosine (3-N-Tyr) and sulfoxy-methionine (Met-SO). The presence of these oxidation-modified amino acids may affects some of the functional properties of these proteins. In particular, both oxidized fibrinogen and VWF show pro-thrombotic tendency [59].
On the other hand, the formation of Met-SO at position 1606 in the A2 domain of VWF is responsible for a severe resistance to proteolysis by ADAMTS-13, causing an accumulation of ultra-large VWF multimers that have high platelet pro-aggregating tendency in the microvasculature [59].

Although it is known that ED/thrombosis and oxidative stress are present in subjects with DM, it is still debated whether these conditions are linked to the clinical evidence of micro- and macro-vascular complications in this setting.

### 1.4.2 OXIDATIVE STRESS AND CHRONIC KIDNEY DISEASE

Chronic kidney disease (CKD) is a pathology characterized by progressive impairment of renal function over time, with the glomerular filtration rate (GFR) being the best measure of kidney function. The early stages of chronic kidney disease (stages 2 and 3) are manifested by mild to moderate decreased GFR and may be both asymptomatic or associated with a pro-inflammatory state [60] and with the perturbation of vascular endothelium [61]. Its diagnosis results therefore important to treat cardiovascular risk factors, to delay progression of CKD and to prevent cardiovascular events. Advanced stages of CKD (4 and 5) are characterized by severely decreased GFR accompanied by clinical complications (hypertension, anaemia, vascular and bone disease), requiring renal replacement therapy when end-stage renal disease is reached [62, 63].

The end-stage renal disease (ESRD) is associated with oxidative stress, as a result of both increased oxidant production and decreased antioxidant defenses [64-66], which may arise either from deficiencies of antioxidants (such as glutathione, ascorbate or α-tocopherol) or increased formation of ROS and RNS (reactive nitrogen species) such as peroxynitrite (ONOO-), hydrogen peroxide ($H_2O_2$), hypochlorous acid (HOCL) or superoxide anions ($O_2$·-) [67]. [48, 68]. Extracellular reduced thiols (e.g., free cysteine and homocysteine and albumin-bound cysteine), constituting an important component of the natural antioxidant defense [69, 70], are depleted in hemodialyzed (HD) patients, whereas the corresponding oxidized thiols accumulate, with a resulting global prothrombotic effect [45, 71].

Moreover, increased plasma levels of the VWF have been found in uremic patients, representing a key marker of vascular endothelium perturbation occurring in CKD [72]. VWF found in HD patients contains high carbonyl levels and increased proportion of UL-VWF polymers, which are also the most resistant forms to ADAMTS-13 cleavage [73].

High levels of many other oxidative stress markers such as F2-isoprostanes, advanced glycosylation end products, malonyldialdehyde and oxidized LDL have been demonstrated to accumulate in the plasma of patients with mild to moderate CKD and in ESRD patients [74], primarily as a result of their concomitant increased production and diminished renal clearance [45], but also for the enhanced release of myeloperoxidase from phagocytes, that are activated during HD treatment [75].

The oxidative stress characterizing the CKD is probably due to increased production of ROS as increased NAD(P)H oxidase activity has been reported in the vascular endothelium of patients with even mild CKD [76], together with high levels of the pro-inflammatory cytokine IL-6 and acute-phase C-reactive protein [45]. Whether there is also a deficiency in the antioxidant defense system is still a matter of debate [74]. While some studies demonstrate a reduction in intracellular or plasma antioxidant factors such a superoxide dismutase, catalase or glutathione peroxidase other studies showed no reduction in total antioxidant capacity [77, 78].

All together, oxidative stress, inflammation and endothelial dysfunction characterizing CKD may be taken into account as “non-traditional” risk factors for the cardiovascular diseases (CVD) that accounts for up to 60% of deaths in CKD [61, 79, 80]. Although existing data suggest a probable role for oxidative stress in increased atherogenecity in CKD patients, further studies are needed to examine the pathophysiological role of oxidative stress and its effects in reducing treatment strategies in CKD.

## 1.5 REFERENCES


1. Jaffe EA et al., *Synthesis of von Willebrand factor by cultured human endothelial cells.* Proc Natl Acad Sci U S A, 1974. **71**(5):1906-9.
2. Nachman R et al., *Synthesis of factor VIII antigen by cultured guinea pig megakaryocytes.* J Clin Invest, 1977. **60**(4):914-21.
3. Marti T et al., *Identification of disulfide-bridged substructures within human von Willebrand factor.* Biochemistry, 1987. **26**(25):8099-109.
4. Voorberg J et al., *Assembly and routing of von Willebrand factor variants: the requirements for disulfide-linked dimerization reside within the carboxy-terminal 151 amino acids.* J Cell Biol, 1991. **113**(1):195-205.
5. Rehemtulla A and Kaufman RJ, *Preferred sequence requirements for cleavage of pro-von Willebrand factor by propeptide-processing enzymes.* Blood, 1992. **79**(9):2349-55.
6. Sporn LA et al., *Inducible secretion of large, biologically potent von Willebrand factor multimers.* Cell, 1986. **46**(2):185-90.
7. Wagner DD et al., *Immunolocalization of von Willebrand protein in Weibel-Palade bodies of human endothelial cells.* J Cell Biol, 1982. **95**(1):355-60.
8. Cramer EM et al., *Eccentric localization of von Willebrand factor in an internal structure of platelet alpha-granule resembling that of Weibel-Palade bodies.* Blood, 1985. **66**(3):710-3.
9. Ruggeri ZM and Zimmerman TS, *The complex multimeric composition of factor VIII/von Willebrand factor.* Blood, 1981. **57**(6):1140-3.
10. Tsai HM et al., *Multimeric composition of endothelial cell-derived von Willebrand factor.* Blood, 1989. **73**(8):2074-6.
11. Padilla A et al., *P-selectin anchors newly released ultralarge von Willebrand factor multimers to the endothelial cell surface.* Blood, 2004. **103**(6):2150-6.
12. Tsai HM, *Physiologic cleavage of von Willebrand factor by a plasma protease is dependent on its conformation and requires calcium ion.* Blood, 1996. **87**(10):4235-44.
13. Borchiellini A et al., *Quantitative analysis of von Willebrand factor propeptide release in vivo: effect of experimental endotoxemia and administration of 1-deamino-8-D-arginine vasopressin in humans.* Blood, 1996. **88**(8):2951-8.
14. Kalafatis M et al., *Localization of a collagen-interactive domain of human von Willebrand factor between amino acid residues Gly 911 and Glu 1,365.* Blood, 1987. **70**(5):1577-83.
15. Pareti FI et al., *Isolation and characterization of two domains of human von Willebrand factor that interact with fibrillar collagen types I and III.* J Biol Chem, 1987. **262**(28):13835-41.
16. Roth GJ et al., *Localization of binding sites within human von Willebrand factor for monomeric type III collagen.* Biochemistry, 1986. **25**(26):8357-61.
17. Marchese P et al., *Identification of three tyrosine residues of glycoprotein Ib alpha with distinct roles in von Willebrand factor and alpha-thrombin binding.* J Biol Chem, 1995. **270**(16):9571-8.
18. Ruggeri ZM, *von Willebrand factor.* J Clin Invest, 1997. **99**(4):559-64.
19. Siedlecki CA et al., *Shear-dependent changes in the three-dimensional structure of human von Willebrand factor.* Blood, 1996. **88**(8):2939-50.
20. Zheng X et al., *Cleavage of von Willebrand factor requires the spacer domain of the metalloprotease ADAMTS13.* J Biol Chem, 2003. **278**(32):30136-41.
21. Levy GG et al., *Mutations in a member of the ADAMTS gene family cause thrombotic thrombocytopenic purpura.* Nature, 2001. **413**(6855):488-94.
22. Zheng X et al., *Structure of von Willebrand factor-cleaving protease (ADAMTS13), a metalloprotease involved in thrombotic thrombocytopenic purpura.* J Biol Chem, 2001. **276**(44):41059-63.
23. Shang D et al., *Apical sorting of ADAMTS13 in vascular endothelial cells and Madin-Darby canine kidney cells depends on the CUB domains and their association with lipid rafts.* Blood, 2006. **108**(7):2207-15.
24. Turner N et al., *Human endothelial cells synthesize and release ADAMTS-13.* J Thromb Haemost, 2006. **4**(6):1396-404.
25. Liu L et al., *Platelet-derived VWF-cleaving metalloprotease ADAMTS-13.* J Thromb Haemost, 2005. **3**(11):2536-44.
26. Suzuki M et al., *Detection of von Willebrand factor-cleaving protease (ADAMTS-13) in human platelets.* Biochem Biophys Res Commun, 2004. **313**(1):212-6.
27. Tsai HM, *Shear stress and von Willebrand factor in health and disease.* Semin Thromb Hemost, 2003. **29**(5):479-88.
28. Tsai HM et al., *Shear stress enhances the proteolysis of von Willebrand factor in normal plasma.* Blood, 1994. **83**(8):2171-9.
29. Moake JL, *Thrombotic microangiopathies.* N Engl J Med, 2002. **347**(8):589-600.

30. Ono T et al., *Severe secondary deficiency of von Willebrand factor-cleaving protease (ADAMTS13) in patients with sepsis-induced disseminated intravascular coagulation: its correlation with development of renal failure.* Blood, 2006. **107**(2):528-34.
31. Korkmaz B et al., *Neutrophil elastase, proteinase 3 and cathepsin G: physicochemical properties, activity and physiopathological functions.* Biochimie, 2008. **90**(2):227-42.
32. Baggiolini M et al., *Cellular mechanisms of proteinase release from inflammatory cells and the degradation of extracellular proteins.* Ciba Found Symp, 1979. **75**:105-21.
33. Janoff A and Scherer J, *Mediators of inflammation in leukocyte lysosomes. IX. Elastinolytic activity in granules of human polymorphonuclear leukocytes.* J Exp Med, 1968. **128**(5):1137-55.
34. Virca GD et al., *Similarities between human and rat leukocyte elastase and cathepsin G.* Eur J Biochem, 1984. **144**(1):1-9.
35. Pham CT, *Neutrophil serine proteases: specific regulators of inflammation.* Nat Rev Immunol, 2006. **6**(7):541-50.
36. Bank U and Ansorge S, *More than destructive: neutrophil-derived serine proteases in cytokine bioactivity control.* J Leukoc Biol, 2001. **69**(2):197-206.
37. Reid PT and Sallenave JM, *Neutrophil-derived elastases and their inhibitors: potential role in the pathogenesis of lung disease.* Curr Opin Investig Drugs, 2001. **2**(1):59-67.
38. Davies KJ, *Oxidative stress: the paradox of aerobic life.* Biochem Soc Symp, 1995. **61**:1-31.
39. Stadtman ER and Levine RL, *Protein oxidation.* Ann N Y Acad Sci, 2000. **899**:191-208.
40. Yla-Herttuala S, *Oxidized LDL and atherogenesis.* Ann N Y Acad Sci, 1999. **874**:134-7.
41. Marnett LJ, *Oxyradicals and DNA damage.* Carcinogenesis, 2000. **21**(3):361-70.
42. Lee Y and Shacter E, *Role of carbohydrates in oxidative modification of fibrinogen and other plasma proteins.* Arch Biochem Biophys, 1995. **321**(1):175-81.
43. Parthasarathy S et al., *The role of oxidized low-density lipoproteins in the pathogenesis of atherosclerosis.* Annu Rev Med, 1992. **43**:219-25.
44. Johansen JS et al., *Oxidative stress and the use of antioxidants in diabetes: linking basic science to clinical practice.* Cardiovasc Diabetol, 2005. **4**(1):5.
45. Himmelfarb J and Hakim RM, *Oxidative stress in uremia.* Curr Opin Nephrol Hypertens, 2003. **12**:593-8.
46. Himmelfarb J et al., *Oxidative stress is increased in critically ill patients with acute renal failure*. J Am Soc Nephrol, 2004. **15**:2449-56.
47. Massy ZA et al., *The role of oxidative stress in chronic kidney disease.* Semin Dial, 2009. **22:**405-8.
48. Walker LM et al., *Oxidative stress and reactive nitrogen species generation during renal ischemia*. Toxicol Sci, 2001. **63:**143-8.
49. Betteridge DJ, *What is oxidative stress?* Metabolism, 2000. **49**(2 Suppl 1):3-8.
50. Fridovich I, *Fundamental aspects of reactive oxygen species, or what's the matter with oxygen?* Ann N Y Acad Sci, 1999. **893**:13-8.
51. Halliwell B, *Antioxidants in human health and disease.* Annu Rev Nutr, 1996. **16**:33-50.
52. Halliwell B, *Antioxidant defence mechanisms: from the beginning to the end (of the beginning).* Free Radic Res, 1999. **31**(4):261-72.
53. Brownlee M, *Biochemistry and molecular cell biology of diabetic complications*. Nature, 2001. **414**:813-20.
54. Brownlee M, *The pathobiology of diabetic complications: a unifying mechanism.* Diabetes, 2005. **54**:1615-25.
55. Lewis P et al., *Lack of the antioxidant enzyme glutathione peroxidase-1 accelerates atherosclerosis in diabetic apolipoprotein E-deficient mice.* Circulation, 2007. **115**:2178-87.
56. Leopold JA and Loscalzo J, *Oxidative risk for atherothrombotic cardiovascular disease.* Free Radic Biol Med, 2009. **47**:1673-1706.
57. Calles-Escandon J and Cipolla M, *Diabetes and endothelial dysfunction: a clinical perspective*. Endocr Rev, 2001. **22**:36-52.
58. Parastatidis I et al., *Fibrinogen beta-chain tyrosine nitration is a prothrombotic risk factor.* J Biol Chem, 2008. **283**:33846-53.
59. Lancellotti S et al., *Formation of methionine sulfoxide by peroxynitrite at position 1606 of von Willebrand factor inhibits its cleavage by ADAMTS-13: A new prothrombotic mechanism in diseases associated with oxidative stress.* Free Radic Biol Med, 2010. **48**:446-56.
60. Zimmermann J et al., *Inflammation enhances cardiovascular risk and mortality in hemodialysis patients*. Kidney Int, 1999. **55***:*648-658.
61. Annuk M et al., *Oxidative stress and endothelial function in chronic renal failure*. J Am Soc Nephrol, 2001. **12**:2747-52.
62. Weiner DE, *Causes and consequences of chronic kidney disease: implications for managed health care*. J Manag Care Pharm, 2007. **13**(3 Suppl):S1‑S9.
63. Luke RG, *Chronic renal failure - a vasculopathic state.* N Engl J Med, 1998. **339**:841-3.
64. Vaziri ND, *Oxidative stress in uremia: nature, mechanisms, and potential consequences*. Semin Nephrol, 2004. **24**:469‑73

65. Galle J, *Oxidative stress in chronic renal failure*. Nephrol Dial Transplant, 2001. **16**:2135‑7.
66. Palleschi S et al., *Reliability of oxidative stress biomarkers in hemodialysis patients: a comparative study*. Clin Chem Lab Med, 2007. **45**:1211‑8.
67. Halliwell B, *The role of oxygen radicals in human disease, with particular reference to the vascular system.* Haemostasis, 1993. **23**(Suppl 1):S118-26.
68. Vinas JL et al., *Mitochondrial NOS upregulation during renal I/R causes apoptosis in a peroxynitrite-dependent manner.* Kidney Int, 2006. **69**:1403-9.
69 Ueland PM et al., *Reduced, oxidized and protein-bound forms of homocysteine and other aminothiols in plasma comprise the redox thiol status - a possible element of the extracellular antioxidant defense system.* J Nutr, 1996. **126** (4 Suppl):1281S-4S
70 Halliwell B, *Albumin - an important extracellular antioxidant?* Biochem Pharmacol, 1998. **37**:569-71.
71 Bostom AG and Lathrop L, *Hyperhomocysteinemia in end-stage renal disease: Prevalence, etiology and potential relationship to arteriosclerotic outcomes.* Kidney Int, 1997. **52**:10-20.
72 Małyszko JS et al., *Markers of endothelial damage in patients on hemodialysis and hemodiafiltration*. J. Nephrol, 2006. **19**:150-4.
73 Kirmizis D et al., *Validity of plasma fibrinogen, D-dimer, and the von Willebrand factor as markers of cardiovascular morbidity in patients on chronic hemodialysis.* Med Sci Monit, 2006. **12**:CR55-62.
74. Cachofeiro V et al., *Oxidative stress and inflammation, a link between chronic kidney disease and cardiovascular disease*. Kidney Int, 2008. **111**(Suppl):S4-S9.
75 Ward R and McLeish K, *Hemodialysis with cellulose membranes primes the neutrophil oxidative burst*. Artif Organs, 1995. **19**:801-7.
76. Fortuno A et al., *Increased phagocytic nicotinamide adenine dinucleotide phosphate oxidasedependent superoxide production in patients with early chronic kidney disease.* Kidney Int Suppl, 2005. **99**:S71-S5.
77. Karamouzis I et al., *Increase in oxidative stress but not in antioxidant capacity with advancing stages of chronic kidney disease.* Am J Nephrol, 2008. **28**:397-404.
78. Dounousi E et al., *Oxidative stress is progressively enhanced with advancing stages of CKD*. Am J Kidney Dis, 2006. **48**:752-60.
79 Go AS et al., *Chronic kidney disease and the risks of death, cardiovascular events, and hospitalization.* N Engl J Med, 2004. **351**:1296-1305.
80 Foley R et al., *Epidemiology of cardiovascular disease in chronic renal disease.* J Am Soc Nephrol, 1998. **32(12 Suppl.)**:S16-S23.

## 2. PUBLICATIONS

- Lancellotti S, De Filippis V, Pozzi N, Oggianu L, Rutella S, Scaglione GL, Maset F, Peyvandi F and De Cristofaro R, *Oxidized von Willebrand factor is efficiently cleaved by serine proteases from primary granules of leukocytes: divergence from ADAMTS-13.* Journal of Thrombosis and Haemostasis, 2011. **9**:1620–7.
  - Article
  - Supporting Information

- Oggianu L, Lancellotti S, Pitocco D, Zaccardi F, Rizzo P, Martini F, Ghirlanda G and De Cristofaro R, *The Oxidative modification of don Willebrand factor is associated with thrombotic angiopathies in Diabetes Mellitus.* Accepted publication by PLOS ONE on December 24th, 2012.

- De Filippis V, Lancellotti S, Maset F, Spolaore B, Pozzi N, Gambaro G, Oggianu L, Calò LA, De Cristofaro R, *Oxidation of Met1606 in von Willebrand factor is a risk factor for thrombotic and septic complications in chronic renal failure*. Biochemical Journal, 2012. **442**(2):423-32.

.

*Journal of Thrombosis and Haemostasis*, **9**: 1620–1627 DOI: 10.1111/j.1538-7836.2011.04367.x

ORIGINAL ARTICLE

# Oxidized von Willebrand factor is efficiently cleaved by serine proteases from primary granules of leukocytes: divergence from ADAMTS-13

S. LANCELLOTTI,*[1] V. DE FILIPPIS,†[1] N. POZZI,† L. OGGIANU,*‡ S. RUTELLA,§¶ G. L. SCAGLIONE,* F. MASET,† F. PEYVANDI,**†† P. M. MANNUCCI,‡‡ and R. DE CRISTOFARO*

*Institute of Internal Medicine and Geriatrics, and Hemostasis Research Center, Catholic University School of Medicine, Rome; †Department of Pharmaceutical Sciences, University of Padua, Padua; ‡Section of Biology Applied to Human Health, 'Rome Tre' University, Rome; §Department of Hematology, Catholic University School of Medicine, Rome; ¶IRCCS San Raaele Pisana, Rome; **A. Bianchi Bonomi Hemophilia and Thrombosis Center, University of Milan, Milan; ††Department of Medicine and Medical Specialties, IRCCS Maggiore Hospital, Mangiagalli and Regina Elena Foundation, Luigi Villa Foundation, Milan; and ‡‡Scientific Direction, IRCCS Cà Granda Maggiore Policlinico Hospital Foundation, Milan, Italy

**To cite this article:** Lancellotti S, De Filippis V, Pozzi N, Oggianu L, Rutella S, Scaglione GL, Maset F, Peyvandi F, Mannucci PM, De Cristofaro R. Oxidized von Willebrand factor is efficiently cleaved by serine proteases from primary granules of leukocytes: divergence from ADAMTS-13. *J Thromb Haemost* 2011; **9**: 1620–7.

**Summary.** *Background:* The leukocyte serine proteases (LSPs) elastase, proteinase 3 and cathepsin G cleave von Willebrand factor (VWF) near or at the same cleavage site (Tyr1605–Met1606) as ADAMTS-13, the metalloprotease that specifically controls the proteolytic processing of VWF. Recent studies have shown that oxidation of VWF at Met1606 with formation of methionine sulfoxide (MetSO) severely impairs its proteolysis by ADAMTS-13. *Methods:* This study was aimed at assessing whether or not oxidation of VWF by reactive oxygen species (ROS) can also affect its cleavage by elastase, proteinase 3, and cathepsin G. In this study, the catalytic specificity of hydrolysis by LSPs of the VWF peptide substrate VWF74 and full-length VWF, both unaltered and in the oxidized form, was measured by RP-HPLC, electrophoretic and mass spectrometry methods. *Results:* LSPs cleaved both VWF multimers and VWF74 near or at the same peptide bond as is cleaved by ADAMTS-13, with $k_{cat}/K_m$ values similar to those of the metalloprotease. However, unlike ADAMTS-13, cathepsin G cleaved VWF74 containing a MetSO residue at position 1606 with a $k_{cat}/K_m$ value higher than that for VWF74, whereas the catalytic efficiencies of both elastase and proteinase 3 were unaffected by the replacement of Met1606 with MetSO. Likewise, oxidation of VWF multimers by hypochlorous acid and ROS, produced by activated leukocytes, improved their hydrolysis by LSPs. *Conclusions:* Oxidation by leukocyte ROS has a net positive effect on the cleavage of VWF multimers by LSPs, under conditions where high concentrations of oxidant species would severely reduce the proteolytic efficiency of ADAMTS-13.

**Keywords**: ADAMTS-13, cathepsin G, elastase, methionine sulfoxide, oxidative stress, polymorphonuclear cells, proteinase 3, thrombotic microangiopathy, von Willebrand factor.

Correspondence: Raimondo De Cristofaro, Hemostasis Research Center, Institute of Internal Medicine and Geriatrics, Catholic University School of Medicine, Largo F. Vito 1, 00168 Rome, Italy. Tel.: +30 06 30154438; fax: +39 06 30155915.
E-mail: rdecristofaro@rm.unicatt.it

[1]These authors contributed equally to this study.

Received 19 November 2010, accepted 28 April 2011

## Introduction

Activated polymorphonuclear cells (PMNs) are extensively involved in the defense of the human body against infections, and use several biochemical strategies to pursue this aim [1]. In response to diverse stimuli, activated PMNs secrete granule proteases and a series of cytotoxins, as well as superoxide anion ($O_2^{\cdot-}$) and other reactive oxygen species (ROS) [2,3]. Moreover, PMNs are not merely defensive cells, but also participate in hemostatic functions by interacting with both platelets and endothelial cells in primary hemostasis [3,4]. Recent studies have documented specific cleavage by the PMN leukocyte serine proteases (LSPs) human leukocyte elastase (HLE), proteinase 3 (PR3) and cathepsin G (CG) of the A2 domain of von Willebrand factor (VWF) [5]. The cleavage sites are located near or at the same Tyr1605–Met1606 peptide bond as is hydrolyzed by ADAMTS-13, the zinc protease that specifically controls the proteolytic processing of VWF under high shear stress [5]. On the other hand, recent studies have shown that oxidation of Met1606 with the formation of methionine sulfoxide (MetSO) inhibits VWF proteolysis by ADAMTS-13 [6,7]. VWF, besides its well-known involvement in primary hemostasis, participates in other biological phenomena, such as bacterial infections, leukocyte extravasation, [8] and angiogen-

esis [9]. The high molecular weight VWF multimers are involved, for instance, in bacterial adhesion and tissue invasion mediated by surface adhesin molecules called microbial surface components recognizing adhesive matrix molecules [10,11]. *Staphylococcus aureus* expresses numerous adhesins, such as staphylococcal protein A (Spa), which binds to soluble and immobilized VWF multimers [12]. The process of bacterial adhesion causes migration and activation of PMNs, which secrete enzymes and ROS to eliminate the pathogens. Thus, in this study, we investigated whether PMN-induced oxidative stress influences VWF hydrolysis by LSPs.

## Methods

The pseudo-wild-type peptide VWF74, containing the amino acid exchange Cys1669 → Ala and encompassing the VWF A2 domain sequence 1596–1669 (DREQAPNLV**YM**VT GNPASDEIKRLPGDIQVVPIGVGPNANVQELERIGWP NAPILIQDFETLPREAPDLVLQRA), and its derivative containing MetSO at position 11 (1606), were synthesized as previously detailed [7]. The Michaelis–Menten parameters for the hydrolysis of VWF74 and VWF74-MetSO by LSPs and ADAMTS-13 were determined by quantifying the cleavage products by RP-HPLC, as described previously [7]. Purification of plasma VWF multimers and their oxidation with hypochlorous acid (HClO) or the myeloperoxidase/$H_2O_2$/Cl system (MOPSY) were performed as described previously [7]. After oxidation, VWF samples (20 μg $mL^{-1}$) were separately incubated at 37 °C with 10 nM ADAMTS-13, HLE, PR3, and CG, in the absence or presence of 1.5 mg $mL^{-1}$ sulfate-free ristocetin. At time intervals (i.e. 0, 1 and 2 h), aliquots (50 μL) of these solutions were sampled and the reaction was stopped with 0.3 M acetic acid or 10 mM EDTA, when ADAMTS-13 had reacted. In all cases, proteolysis of oxidized VWF was assessed by SDS–agarose electrophoresis in 1.5% agarose gel, as described previously [7]. Purified VWF multimers (20 μg $mL^{-1}$) were also incubated with human PMNs, isolated from healthy volunteers and stimulated with 50 ng $mL^{-1}$ 12-phorbol-13-myristate acetate (PMA) or 1 μM fMet-Leu-Phe peptide (Sigma, St. Louis, MO, USA) in Hepes-buffered saline. PMNs were purified by following a procedure published elsewhere, with only minor modifications [13].

Intracellular superoxide anion production and $H_2O_2$ production by PMA-activated PMNs were monitored by labeling the cells with 2′,7′-dichlorofluorescein diacetate (20 μM final concentration) and hydroethidine (10 μM final concentration), respectively [14]. Superoxide anions secreted by stimulated PMNs were measured spectrophometrically at 25 °C by ferricytochrome *c* reduction, as reported previously [14]. The concentrations of HLE bound to the specific inhibitor $\alpha_1$-antiprotease 1, present in the supernatants of PMA-stimulated PMNs, and HLE hydrolytic activity for a synthetic substrate were measured with both ELISA and chromogenic assays.

The conformational state of both intact and oxidized VWF multimers was studied by far-UV circular dichroism, intrinsic fluorescence and dynamic light scattering (DLS) spectroscopy Denaturation experiments on VWF and oxidized VWF were carried out by intrinsic fluorescence spectroscopy, and the data were analyzed according to a two-state model, as reported previously [15]. Assessment of Met1606 oxidation by MOPSY and the oxidative burst by PMA-activated PMNs was performed by targeted mass spectrometry (MS) analysis. All methodological details are given in the Supporting Information.

## Results

### *Determination of the sites for LSP cleavageof VWF74 and VWF74-MetSO*

Proteolysis reactions of wild-type synthetic VWF74 and VWF74-MetSO with LSPs (20 nM) and ADAMTS-13 (5 nM) were carried out under identical experimental conditions, and the products were fractionated by RP-HPLC (Fig. 1A–H). MS analysis of the peptides eluted from the column allowed us to unequivocally establish the chemical identity of the proteolytic fragments (Table 1) and to identify the cleavage site(s) in the VWF74 peptide sequence (Fig. 1I). After 1 h of reaction at 37 °C, ADAMTS-13 cleaved VWF74 exclusively at Tyr1605–Met1606 (Fig. 1A), generating the N-terminal peptide Asp1596–Tyr1605 (p1 = 1203.58 a.m.u.) and the C-terminal peptide Met1606–Ala1669 (p2 = 6969.94 a.m.u.). Cleavage of VWF74-MetSO was markedly impaired (Fig. 1E), in agreement with the results recently reported by us and others [6,7]). However, the cleavage site for ADAMTS-13 was unchanged (p1* = 1203.63 a.m.u.). Similar behavior was observed for the cleavage of VWF74-MetSO by other LSPs (i.e. CG and PR3). As found with ADAMTS-13, CG (almost) exclusively cleaved both VWF74 and VWF74-MetSO at Tyr1605–Met1606 (Fig. 1B,F). However, unlike what we observed with ADAMTS-13, CG cleaved VWF74-MetSO with significantly higher efficiency than was seen with the unmodified VWF74. Figure 1C,G shows that PR3 cleaved both VWF74 and VWF74-MetSO with comparable efficiency, predominantly at Va1607–Thr1608, even though very minor cleavage at Ala1612–Ser1613 was also observed. Whereas ADAMTS-13, CG and PR3 cleaved wild-type and oxidized VWF74 at a single peptide bond with nearly absolute specificity, HLE cleaved the substrate at multiple sites (e.g. Val1607–Thr1608, Val1626–Pro1627, Ala1647–Pro1648, and Ile1649–Leu1650) with comparable efficiencies (Fig. 1D,H), reflecting the wider substrate specificity of this protease [3]. As for PR3, oxidation of Met1606 did not influence cleavage by HLE (Fig. 1D,H).

### *Determination of the Michaelis–Menten parameters for the cleavage of VWF74 and VWF74-MetSO by LSPs*

In proteolysis experiments with ADAMTS-13, VWF74 was cleaved with the best-fit Michaelis–Menten parameter values, $k_{cat}$ = 0.81 ± 0.02 $s^{-1}$ and $K_m$ = 6.55 ± 0.32 μM, in agreement with our previous data [7]. In contrast, no kinetic parameter could be calculated for VWF74-MetSO under the same experimental conditions over a concentration range from 2.5 to 40 μM, as previously reported by us and others [6,7]. LSPs

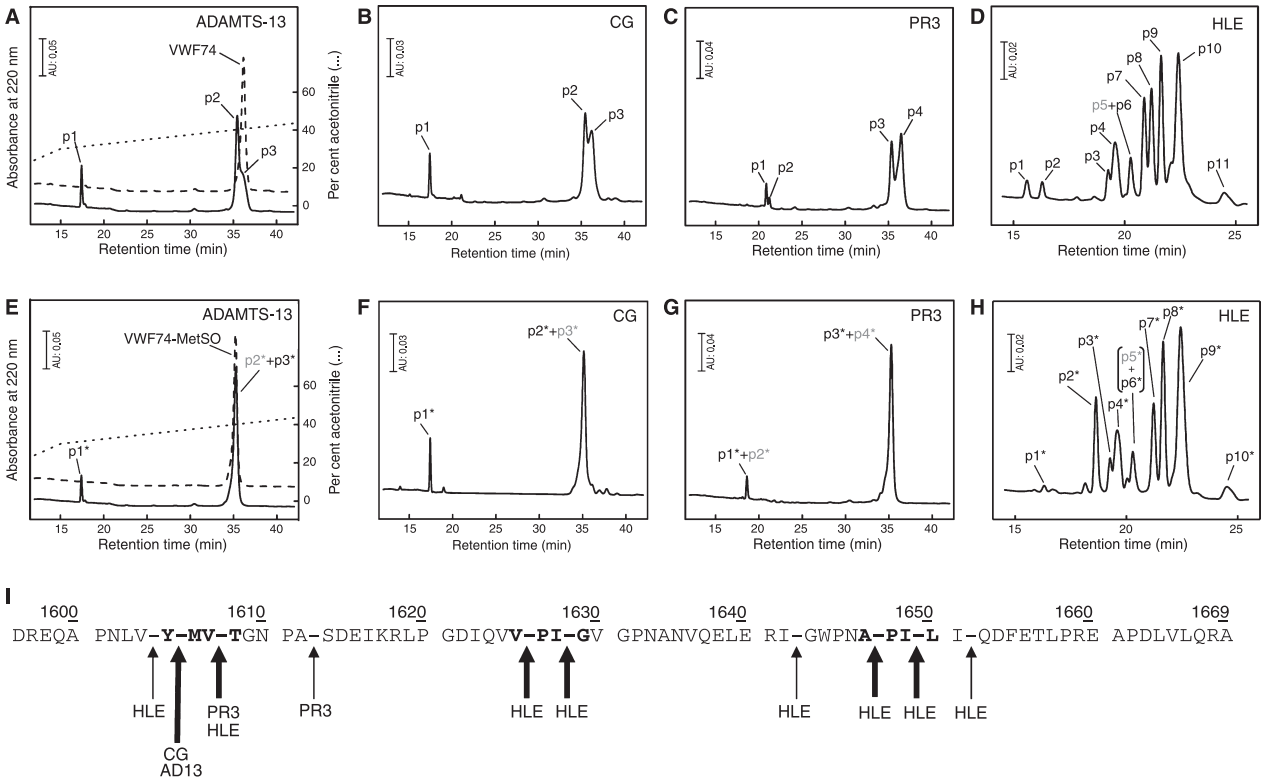


**Fig. 1.** Products of the proteolysis reactions of von VWF74 and VWF74-MetSO by ADAMTS-13 and leukocyte serine proteases. RP-HPLC analysis of the proteolysis reactions of von Willebrand factor (VWF)74 (upper panels) and VWF74-methionine sulfoxide (VWF74-MetSO) (lower panels) with ADAMTS-13 (A, E), and the leukocyte serine proteases (LSPs) cathepsin G (CG) (B, F), proteinase 3 (PR3) (C, G), and human leukocyte elastase (HLE) (D, H). Proteolysis was conducted under identical experimental conditions (20 μM substrate, 37 °C in Hepes-buffered saline, pH 7.4) with ADAMTS-13 (5 nM, 1 h) and LSPs (20 nM, 1.5 h). Acid-quenched aliquots were fractionated by RP-HPLC, and the proteolytic fragments analyzed by mass spectrometry (MS) (see Table 1). When two peptide species are coeluted in the same peak, the less abundant fragment (as judged from MS spectra) is indicated in gray. For each protease, the absorbance scale relative to proteolysis with VWF74 and VWF74-MetSO is the same. For clarity, the chromatograms of the reference peptides at reaction time = 0 is shown only in (A) and (E). (I) Identification of the cleavage sites of VWF74 and VWF74-MetSO after proteolysis with ADAMTS-13 and LSPs, as deduced from MS data. The major cleavage sites are indicated by thick arrows and bold labels.

cleaved VWF74 efficiently, with $k_{cat}/K_m$ values even higher than that of ADAMTS-13 (Fig. 2; Table 2). In the case of HLE, owing to cleavage at multiple sites (Fig. 1D,H), only a pseudo-first-order rate constant, $k_{obs}$, of VWF74 disappearance at 25 °C could be determined (0.125 ± 0.01 $min^{-1}$). At variance with what was previously observed with ADAMTS-13 [6,7], oxidation of Met1606 did not inhibit the cleavage of VWF74 by LSPs. Instead, the specific oxidation of Met1606 slightly increased the $k_{cat}/K_m$ value of CG, mainly because of a slight increase in the $k_{cat}$ value, whereas the values of $k_{cat}/K_m$ and $k_{obs}$ for PR3 and HLE remained essentially unchanged within the range of experimental error, if compared to that of VWF74 (Table 2). These findings were in qualitative agreement with those obtained with oxidized VWF multimers, as described below.

### *Cleavage of VWF multimers by LSPs and activated PMNs*

Preliminary experiments showed that, unlike ADAMTS-13, LSPs do not strictly need a stretched conformation of VWF to cleave this substrate. Even under static conditions and in the absence of ristocetin, which stabilizes the stretched conformation of VWF [16], the latter was indeed cleaved by HLE, PR3 and CG released from activated PMNs (Fig. 3C). This finding is in qualitative agreement with recent results obtained by others [5]. In particular, we observed that, in the absence of the antibiotics under the same experimental conditions, the rates of VWF cleavage by elastase, CG and PR3 were approximately six-fold, seven-fold and five-fold lower, respectively, than in its presence. However, ristocetin significantly accelerated the proteolytic reaction in vitro with purified LSPs, as shown in Fig. 3A. The oxidative modifications induced on purified VWF by HClO strongly inhibited VWF cleavage by ADAMTS-13 but left unaltered, or even slightly accelerated, the cleavage of VWF by LSPs (Fig. 3A). The differential effects of oxidation on VWF hydrolysis by ADAMTS-13 and LSPs were even more evident when the cleaved VWF samples were analyzed in the reduced form (Fig. 3B). A similar effect was observed when PMA-activated PMNs were used as a source of both ROS and LSPs, which extensively cleaved plasma-derived VWF multimers after 45 min of incubation (Fig. 3C). Production of superoxide anions by PMA-activated PMNs was monitored by a flow cytometry-based assay, as well as by using horse cytochrome *c* as a superoxide tracer (Fig. 4A,B). Our results indicate that, after PMA or fMet-Leu-Phe peptide addition,

**Table 1** Mass spectrometry data of the proteolytic fragments obtained by reaction of von Willebrand factor (VWF)74 and VWF74-methionine sulfoxide (VWF74-MetSO) with ADAMTS-13 and leukocyte serine proteases†

| VWF74 | | | VWF74-MetSO | | |
|---|---|---|---|---|---|
| Peak ID | Mass (a.m.u.)‡ | Fragment sequence | Peak ID | Mass (a.m.u.) | Fragment sequence |
| ADAMTS-13 | | | | | |
| p1 | 1203.58 (1203.59) | Asp1596–Tyr1605 | $p1^{ox}$ | 1203.63 (1203.59) | Asp1596–Tyr1605 |
| p2 | 6969.94 (6969.98) | Met1606–Ala1669 | $p2^{ox}$§ | 6985.63 (6985.97) | Met1606–Ala1669 |
| p3 | 8156.06 (8156.26) | Asp1596–Ala1669 | $p3^{ox}$ | 8172.62 (8172.25) | Asp1596–Ala1669 |
| Cathepsin G | | | | | |
| p1 | 1203.59 (1203.59) | Asp1596–Tyr1605 | $p1^{ox}$ | 1203.61 (1203.59) | Asp1596–Tyr1605 |
| p2 | 6969.92 (6969.98) | Met1606–Ala1669 | $p2^{ox}$ | 6986.25 (6985.97) | Met1606–Ala1669 |
| p3 | 8156.74 (8156.26) | Asp1596–Ala1669 | $p3^{ox}$ | 8172.91 (8172.25) | Asp1596–Ala1669 |
| Proteinase 3 | | | | | |
| p1 | 1433.42 (1433.70) | Asp1596–Val1607 | $p1^{ox}$ | 1449.73 (1449.69) | Asp1596–Val1607 |
| p2 | 1873.90 (1873.90) | Asp1596–Ala1612 | $p2^{ox}$ | 1889.90 (1889.89) | Asp1596–Ala1612 |
| p3 | 6739.56 (6739.65) | Thr1608–Ala1669 | $p3^{ox}$ | 6986.25 (6985.97) | Thr1608–Ala1669 |
| p4 | 8156.78 (8156.26) | Asp1596–Ala1669 | $p4^{ox}$ | 8172.47 (8172.25) | Asp1596–Ala1669 |
| Human leukocyte elastase | | | | | |
| p1 | 411.19 (411.18) | Tyr1605–Val1607 | $p1^{ox}$ | 1040.52 (1040.52) | Val1596–Asp1604 |
| p2 | 1040.57 (1040.52) | Val1596–Asp1604 | $p2^{ox}$ | 1449.70 (1449.69) | Asp1596–Val1607 |
| p3 | 1494.83 (1494.78) | Gly1629–Ile1642 | $p3^{ox}$ | 1494.83 (1494.78) | Gly1629–Ile1642 |
| p4 | 753.43 (753.38) | Gly1643–Ile1649 | $p4^{ox}$ | 753.40 (753.38) | Gly1643–Ile1649 |
| p5 | 1333.84 (1333.80) | Lys1617–Ile1628 | $p5^{ox}$ | 1333.82 (1333.80) | Lys1617–Ile1628 |
| p6 | 2097.16 (2097.08) | Gln1652–Ala1669 | $p6^{ox}$ | 2097.07 (2097.08) | Gln1652–Ala1669 |
| p7 | 1433.73 (1433.70) | Asp1596–Val1607 | $p7^{ox}$ | 2218.20 (2218.19) | Thr1608–Ile1628 |
| p8 | 2218.30 (2218.19) | Thr1608–Ile1628 | $p8^{ox}$ | 2323.28 (2323.25) | Leu1650–Ala1669 |
| p9 | 2323.37 (2323.25) | Leu1650–Ala1669 | $p9^{ox}$ | 2230.17 (2230.15) | Pro1627–Ala1647 |
| p10 | 2230.24 (2230.15) | Pro1627–Ala1647 | $p10^{ox}$ | 979.61 (979.60) | Gly1643–Ile1651 |
| p11 | 979.61 (979.60) | Gly1643–Ile1651 | | | |

†The peptide materials corresponding to the chromatographic peaks reported in Fig. 1 were collected, lyophilized, and analyzed by ESI-TOF MS. ‡Mass spectrometry data of the proteolytic fragments obtained by reaction of von Willebrand factor (VWF)74 and VWF74-methionine sulfoxide (VWF74-MetSO) with ADAMTS-13 and leukocyte serine proteases†. §The label indicates the minor of two components coeluting in the RP-HPLC chromatograms reported in Fig. 1.

PMNs undergo a rapid oxidative burst, as demonstrated by flow cytometry showing that, in the PMN cells, the generation of both $H_2O_2$ and superoxide anions began rapidly after 5 min. In particular, ROS secretion by PMNs reached a plateau concentration of superoxide anion of about 30 μM after approximately 20 min of stimulation (Fig. 4B). Notably, extracellular scavenging of ROS by a mixture of superoxide dismutase, catalase and L-Met caused a net decrease in VWF cleavage by activated PMNs (Fig. 3C). The positive effect of ROS activity on VWF proteolysis by activated PMNs was more evident than in experiments with single LSPs and MOPSY-oxidized VWF as substrate. This apparent discrepancy may derive from a positive effect of different ROS released by PMNs, superoxide, HClO, and peroxynitrite) on the simultaneous release of large amounts of different LSPs from activated PMNs. The presence of either serine protease inhibitors (i.e. aprotinin and phenylmethanesulfonyl fluoride) alone or in combination with ROS scavengers completely inhibited the cleavage of VWF by LSPs (Fig. 3C). Additional experiments aimed at assessing the amount and activity of HLE released by activated PMNs showed that active enzyme was rapidly secreted, reaching a very high concentration of approximately 350 nM after about 2 min of incubation of $2 \times 10^3$ $\mu L^{-1}$ PMNs with 1 μM fMet-Leu-Phe or 5 min of incubation with 50 ng $mL^{-1}$ PMA. The very high levels of active HLE secreted by PMNs were sufficient to cause significant cleavage of VWF, as experimentally demonstrated even in the absence of shear stress or ristocetin. After the plateau was reached at 5 min, a slight but progressive decrease in HLE activity was measured for up to 30 min, although the active enzyme was always present at concentrations > 100 nM (Fig. 4C). Notably, ELISA data showed that HLE–$\alpha_1$-protease inhibitor ($\alpha_1$-PI) complex was not found in the same supernatants of activated PMNs. Thus, no natural inhibitor secreted by PMNs was responsible for the decrease in HLE activity. Instead, the partial decrease in HLE activity could be attributable to progressively higher levels of ROS generated by PMNs, which may also react with amino acids engaged in the catalytic machinery of serine proteases [17]. In vitro experiments showed that both MOPSY and ROS-secreting PMNs induced significant inhibition of HLE activity (Fig. S1A). However, the PMN-induced oxidation of α-PI induced much more severe impairment of its inhibitor activity (Fig. S1B), probably because of oxidation of the α-PI Met residue engaged in the inhibition of the active site of the protease. These findings provided a mechanistic explanation of

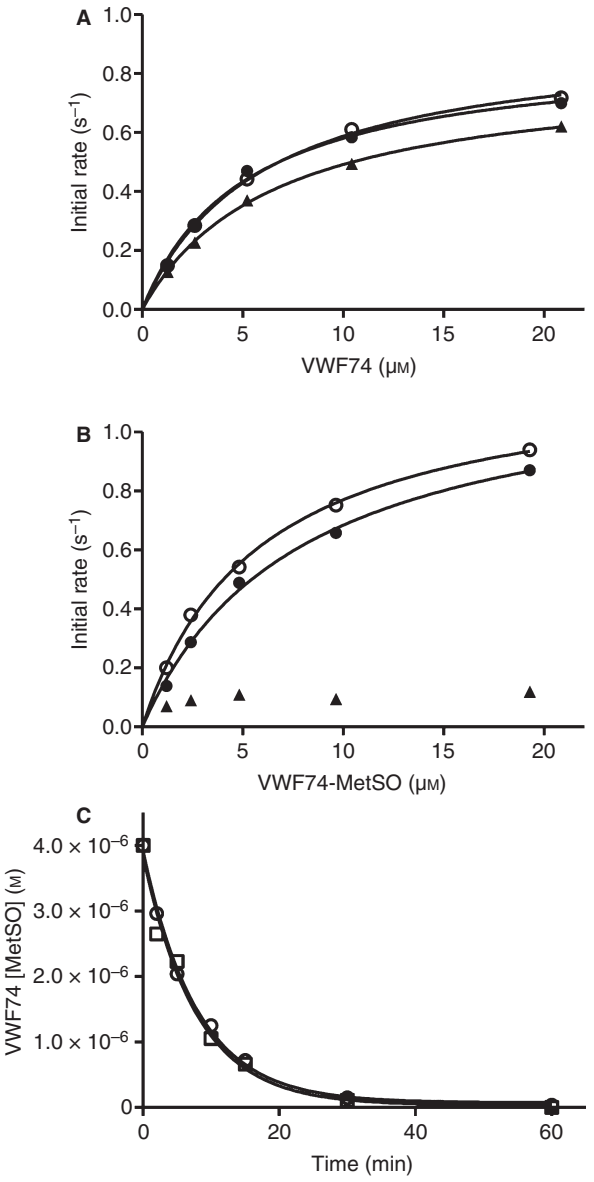


**Fig. 2.** Determination of the Michaelis -Menten parameters of VWF74 and VWF74-MetSO cleavage by ADAMTS13 and serine proteases. (A, B) Determination of the Michaelis–Menten parameters of von Willebrand factor (VWF)74 (A) and VWF74-methionine sulfoxide (VWF-MetSO) (B) cleavage by ADAMTS13 (▲), cathepsin G (○), and proteinase 3 (●). The steady-state kinetic parameters were calculated by measuring, with RP-HPLC, the concentration of the N-terminal peptide released in the proteolysis reaction. The continuous lines were drawn according to the best-fit Michaelis parameters listed in Table 2. (C) Concentration of uncleaved peptides (initial concentration of 4 μM; [O] VWF74, [□] VWF74-MetSO) as a function of time in the presence of 10 nM human leukocyte elastase (HLE). The continuous lines were drawn according to a single exponential decay equation, using the best-fit $k_{obs}$ values listed in Table 2.

the results shown in Fig. 4C, and also indicated that the ROS burst by PMNs globally would favor the LSPs activity in vivo, causing an imbalance between α-PI and HLE activity in favor of the latter.

Notably, treatment of VWF with activated PMNs, under conditions where the release of proteases (but not that of ROS) is inhibited (see Supporting Information), caused a net increase in the number of carbonyl groups in the protein (0.25 pmol μg$^{-1}$ vs. 0.05 pmol μg$^{-1}$ in the control). Furthermore, with a targeted MS approach [18], we established that, after incubation of VWF with activated PMNs, as above, Met1606 was oxidized to MetSO (Fig. S2; Table S1C).

**Table 2** Michaelis–Menten parameters and pseudo-first-order rate constant, $k_{obs}$, of von Willebrand factor (VWF)74 and VWF74-methionine sulfoxide (VWF74-MetSO) hydrolysis by leukocyte serine proteases and ADAMTS-13

| Enzyme | $k_{cat}$ (s$^{-1}$) | $K_m$ (μM) | $k_{cat}/K_m$ (M$^{-1}$ s$^{-1}$) |
|---|---|---|---|
| VWF74 | | | |
| ADAMTS-13 | 0.81 ± 0.02 | 6.55 ± 0.32 | $1.24 \times 10^5$ |
| HLE | | | $k_{obs}$ (min$^{-1}$) = 0.125 ± 0.01 |
| CG | 0.93 ± 0.03 | 5.88 ± 0.44 | $1.58 \times 10^5$ |
| PR3 | 0.88 ± 0.04 | 5.18 ± 0.64 | $1.70 \times 10^5$ |
| VWF74-MetSO | | | |
| ADAMTS-13 | ND | ND | ND |
| HLE | | | $k_{obs}$ (min$^{-1}$) = 0.128 ± 0.02 |
| CG | 1.21 ± 0.06 | 5.76 ± 0.87 | $2.10 \times 10^5$ |
| PR3 | 1.22 ± 0.06 | 7.84 ± 0.87 | $1.56 \times 10^5$ |

CG, cathepsin G; HLE, human leukocyte elastase; ND, not determined; PR3, proteinase 3.

### *Spectroscopic properties of unaltered and HClO-oxidized VWF multimers*

To ascertain whether the change in the proteolytic efficiency of VWF observed with ADAMTS-13 and CG was caused by the different chemical properties (e.g. hydrophilicity) of MetSO as compared with those of Met, or by an alteration of the VWF conformation, possibly occurring upon oxidation, we investigated the conformational properties of unaltered and HClO-treated VWF by UV absorption, circular dichroism, fluorescence spectroscopy, and DLS (Fig. S3). Even though significant spectroscopic differences were observed (Fig. S3A–C), these were probably caused by the formation of oxidized Trp derivatives (i.e., mono-oxyindolyl-alanine and di-oxyindolyl-alanine) rather than by gross conformational changes of VWF. This conclusion is also supported by DLS measurements showing that increasing HClO concentrations did not alter the hydrodynamic radius of VWF ($r$ = 100 ± 39 nM) (Fig. S3D) and by denaturation experiments indicating that both unaltered and oxidized VWF display similar resistance to guanidinium-induced unfolding (Fig. S4).

## Discussion

ADAMTS-13 has been considered in the recent past to be the only enzyme responsible for the proteolytic processing of VWF [19]. However, recent studies have shown that LSPs efficiently cleave VWF multimers near or even at the same peptide bond cleaved by ADAMTS-13 [5]. The results of MS analysis agree with those recently reported [5], showing that ADAMTS-13

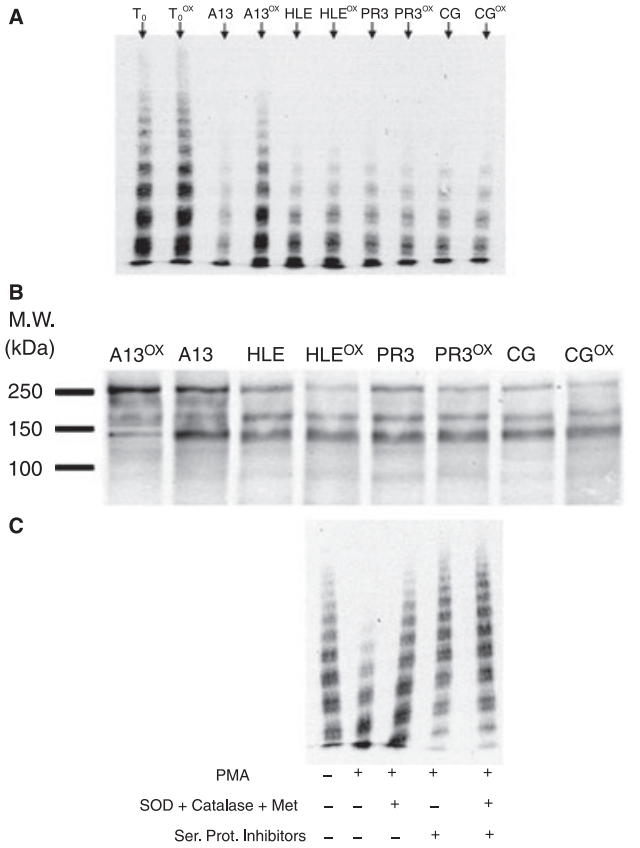


**Fig. 3.** Analysis of multimer structure of intact and oxidized VWF treated with ADAMTS-13 and leukocyte serine proteases. (A) Multimeric structure of intact and oxidized von Willebrand factor (VWF) treated with ADAMTS-13, human leukocyte elastase (HLE), proteinase 3 (PR3), and cathepsin G (CG). In vitro oxidation of VWF was achieved by treatment for 15 min with 40 μM HClO, as detailed in Methods. For each enzyme, the multimer VWF pattern obtained after 2 h of digestion in the presence of 1.5 mg $mL^{-1}$ ristocetin is shown. Electrophoresis was performed with 1.5% SDS–agarose, and this was followed by immunoblotting with polyclonal anti-VWF antibodies. This gel is representative of four different experiments that yielded similar results. (B) Western blot of intact and oxidized VWF treated with ADAMTS-13, HLE, PR3, and CG, as indicated in the legend to (A). SDS-PAGE was performed with 4–12% gradient gels, and the samples were treated under reducing conditions. (C) Multimeric structure of purified VWF (20 μg $mL^{-1}$) treated for 45 min with $1 \times 10^6$ $mL^{-1}$ polymorphonuclear cells in the absence and presence of 12-phorbol-13-myristate acetate (PMA) (50 ng $mL^{-1}$), reactive oxygen species (ROS) scavengers, and serine protease inhibitors. The proteolysis reaction was conducted as detailed in Methods. Superoxide dismutase (SOD) (6 U $mL^{-1}$), catalase (200 nM) and free Met (1 mM) were used as ROS scavengers, and phenylmethanesulfonyl fluoride and aprotinin (500 μM) as serine protease inhibitors. Electrophoretic runs were carried out with 0.8% (stacking gel) to 1.5% (running gel) agarose gel. The results shown in this gel are representative of five different experiments that yielded similar results.

and CG cleave FRETS-VWF73 at Tyr1605–Met1606, whereas both HLE and PR3 cleave the same substrate selectively at Val1607–Thr1608. Strikingly, our results also show for the first time that, at variance with ADAMTS-13, the selective oxidation of Met1606 to MetSO does not affect, or even enhances, cleavage of VWF74 by isolated LSPs (Figs 1 and 2).

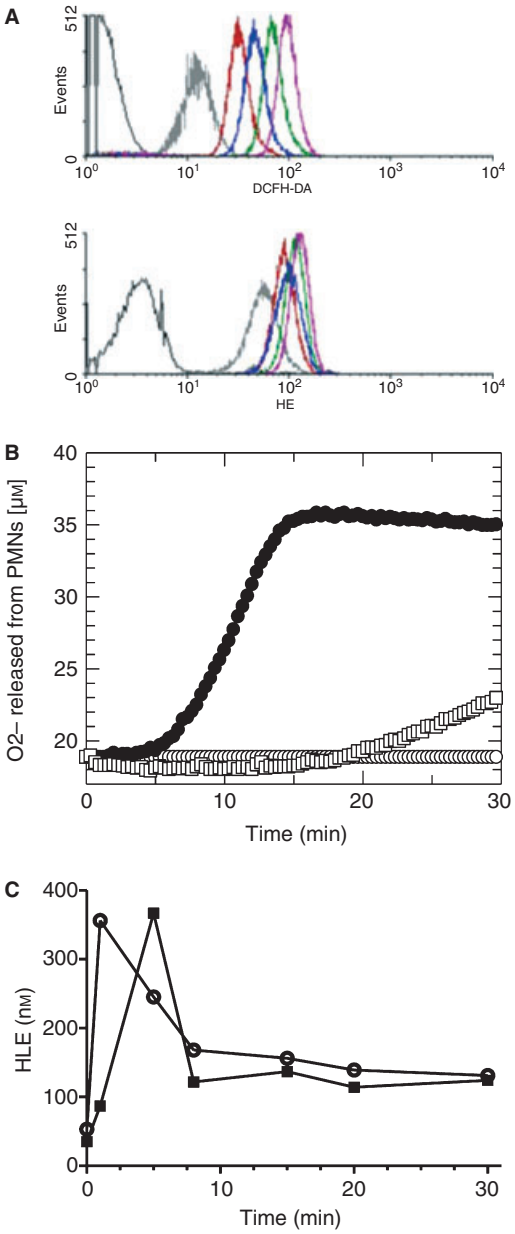


**Fig. 4.** Evaluation of oxidative metabolism in polymorphonuclear cells (PMNs). (A) Flow cytometry analysis of PMN cells loaded with 2′,7′-dichlorofluorescein diacetate (DCFH-DA) and hydroethidine (HE), to monitor $H_2O_2$ and superoxide anion production, respectively, prior to their activation with 50 ng $mL^{-1}$ 12-phorbol-13-myristate acetate (PMA). Samples were run through a FACS Canto flow cytometer at time 0, and then every 5 min from the addition of PMA for up to 25 min (from left to right). The histograms are representative of three independent experiments performed with PMN preparations from different consenting volunteers. (B) Measurement of superoxide release from PMNs. The time-dependent release of superoxide from PMNs with (□) or without (●) the addition of 6 U $mL^{-1}$ superoxide dismutase, 200 nM catalase and 1 mM Met is shown. The arrow indicates the time point when von Willebrand factor was separated from PMNs for the analysis of its multimer pattern. Typical results from three independent experiments are shown. (C) Human leukocyte elastase (HLE) release from PMA-stimulated (■) and fMet-Leu-Phe-stimulated (○) PMNs. The concentration of active enzyme was measured by spectrophotometric determination of the hydrolysis rate of 200 μM *N*-(methoxysuccinyl)-Ala-Ala-Pro-Val 4-nitroanilide at 405 nm, as detailed in Methods.

PMN stimulation causes the production of ROS, mostly stemming from activation of NADPH oxidase ($H_2O_2$) [20]. Neutrophils also produce peroxynitrite from superoxide anion by reaction with NO and hydroxyl radical from $H_2O_2$ in the presence of transition metals [21]. Activated PMNs also release HClO, one of the most powerful oxidant molecules in vivo, generated by myeloperoxidase in the presence of chloride ions and $H_2O_2$. The results shown in Fig. 3 demonstrate that the proteolytic processing of VWF by LSPs isolated (Fig. 3A,B) or released by activated PMNs (Fig. 3C) is not only permitted in the presence of ROS, but is even significantly accelerated by the action of ROS released by activated PMNs. Importantly, our MS analysis unequivocally showed, that upon incubation of VWF with activated PMNs, Met1606 is quantitatively converted into its sulfoxide derivative MetSO (Fig. S2; Table S1).

Overall, the results reported herein, although further confirming and extending the findings of previous studies [5–7], are unprecedented, and demonstrate that the same oxidative modification of a single amino acid in VWF (i.e. Met1606 → MetSO) produces very different effects on the interaction with different enzymes (i.e. ADAMTS-13 and LSPs) involved in its proteolytic processing. The analysis of UV-absorption, fluorescence and circular dichroism spectra of unaltered and oxidized VWF revealed significant differences (Fig. S3A–C). These findings might suggest the occurrence of conformational changes induced by oxidative reactions. However, the results of DLS (Fig. S3D) and guanidinium-induced denaturation of unaltered and oxidized VWF (Figs S3 and S4) allow us to conclude that the enhanced proteolysis of oxidized VWF is caused by the altered chemical properties (i.e. hydrophilicity, charge, and polarizability) of MetSO as compared with Met, and not by any gross distortion of either the tertiary structure or the polymerization state of oxidized VWF, which would otherwise affect proteolysis [22]. In the case of ADAMTS-13, our recent model-building and docking studies suggest that replacing an apolar amino acid such as Met with a highly polar and partially negative residue such as MetSO strongly hampers productive binding of the cleavable Tyr–Met bond into the hydrophobic S1′ site of the protease (N. Pozzi, S. Lancellotti, R. De Cristofaro, V. De Filippis, unpublished data). Opposite, albeit conceptually similar, considerations hold for the effect of Met oxidation on VWF hydrolysis by LSPs. These are extremely basic enzymes, with pI values ranging from 9.5 for PR3 to 12 for CG [3]. In particular, CG (1kyn.pdb) has a strong positive electrostatic potential in the region surrounding the primary specificity S1′ site of the protease, and this feature is expected to favor binding of substrates with a negatively charged side chain at P1′, such as MetSO [23]. In contrast, the S1′ site of PR3 (1fuj.pdb) [24], and especially that of HLE (2rg3.pdb) [25], is less electropositive than in CG. These properties are consistent with the kinetic data reported in Table 2, showing that Met oxidation makes VWF74 a better substrate for CG, without dramatically increasing the catalytic efficiency of PR3 or HLE with the same substrate.

Could these findings have any pathophysiologic implications? Under physiologic conditions, a discrete and 'tonic' activation of leukocytes may contribute to proteolytic processing of circulating VWF, because HLE, PR3 and CG are able to cleave VWF with a catalytic specificity similar to or even higher than that of ADAMTS-13. Notably, De Meyer *et al.* [26] detected satellite bands in plasma from thrombotic thrombocytopenic purpura patients and ADAMTS13$^{-/-}$ mice by using VWF multimer analysis. It is reasonable to assume that they are generated in the above setting by LSPs. On the other hand, if massive and uncontrolled release of LSPs and ROS does occur in particular clinical settings, as in promyelocytic leukemia, then this phenomenon causes extensive and pathologic degradation of VWF, which contributes to the development of severe hemorrhagic syndromes [27]. Finally, it is known that VWF multimers also have extra hemostatic functions, and may cooperate with endothelial cells in different biological processes. In particular, VWF is engaged by bacterial pathogens to adhere to vascular vessel and transmigrate into tissues. Spa from *S. aureus* binds with high affinity to soluble and immobilized VWF, especially to ultralarge VWF multimers [12]. Thus, LSP-mediated VWF proteolysis may be considered as a mechanism aimed at limiting the VWF-mediated adhesion and invasion of such common bacteria in a highly oxidant milieu, where ADAMTS-13 could not efficiently cleave VWF. Accordingly, previous studies showed that experimental group C *Streptococcus*-induced endocarditis failed to develop in pigs with von Willebrand disease [28].

Our results are consistent with the existence of two different pathways of coupled oxidative/proteolytic reactions: (i) chronic oxidative stress by peroxynitrite, mainly arising from endothelial cells in chronic inflammatory settings (e.g. vascular aging and diabetes), reduces cleavage of VWF multimers by ADAMTS-13, with a resulting accumulation of ultralarge VWF and a prothrombotic effect [6,7]; and (ii) rapid and simultaneous release of ROS and LSPs from activated leukocytes results in a positive effect on VWF proteolysis, under conditions (e.g. sepsis) where high concentrations of ROS would impede the activity of ADAMTS-13. Further studies are in progress to explore the in vivo relevance and physiopathologic consequences of VWF proteolysis by LSPs in different clinical settings.

## Addendum

S. Lancellotti: performed research, analyzed data, and revised the manuscript; V. De Filippis: performed MS analysis and revised the manuscript; N. Pozzi, L. Oggianu, F. Maset, and G.L. Scaglione: performed research; S. Rutella: performed research and revised the manuscript; F. Peyvandi and P. M. Mannucci: analyzed data and revised the manuscript; R. De Cristofaro: designed the research, obtained steady-state kinetic data, analyzed the data, and wrote the paper.

## Acknowledgements

V. De Filippis thanks C. D'Orlando for performing some circular dichroism measurements, and B. Spolaore for performing some MS analyses.

## Disclosure of Conflict of Interests

Financial support from MIUR (Ministero Italiano Università e Ricerca, PRIN-2007) to F. Peyvandi (no. 2007T9HTFB_001), V. De Filippis (no. 2007T9HTFB_002) and R. De Cristofaro (no. 2007T9HTFB_003) is gratefully acknowledged. The other authors state that they have no conflict of interest.

## Supporting Information

Additional Supporting Information may be found in the online version of this article:

**Figure S1.** Amidolytic activity of untreated and PMN-oxidized HLE towards *N*-(methoxysuccinyl)-Ala-Ala-Pro-Val 4-nitroanilide.
**Figure S2.** Targeted mass spectrometry (TMS) analysis of untreated (VWF) and oxidized (VWF-Ox) von Willebrand factor with PMNs.
**Figure S3.** Conformational characterization of intact and HClO-oxidized VWF.
**Figure S4.** Guanidinium-induced denaturation of native and oxidized VWF multimers.
**Table S1.** Fragmentation patterns for the proteotipic peptides Met-PTP and MetSO-PTP.

Please note: Wiley-Blackwell are not responsible for the content or functionality of any supporting materials supplied by the authors. Any queries (other than missing material) should be directed to the corresponding author for the article.

## References

1 Nathan C. Neutrophils and immunity: challenges and opportunities. *Nat Rev Immunol* 2006; **6**: 173–82.
2 Dahlgren C, Karlsson A. Respiratory burst in human neutrophils. *J Immunol Methods* 1999; **232**: 3–14.
3 Korkmaz B, Moreau T, Gauthier F. Neutrophil elastase, proteinase 3 and cathepsin G: physicochemical properties, activity and physiopathological functions. *Biochimie* 2008; **90**: 227–42.
4 Zarbock A, Polanowska-Grabowska RK, Ley K. Platelet–neutrophil-interactions: linking hemostasis and inflammation. *Blood Rev* 2007; **21**: 99–111.
5 Raife TJ, Cao W, Atkinson BS, Bedell B, Montgomery RR, Lentz SR, Johnson GF, Zheng XL. Leukocyte proteases cleave von Willebrand factor at or near the ADAMTS13 cleavage site. *Blood* 2009; **114**: 1666–74.
6 Chen J, Fu X, Wang Y, Ling M, McMullen B, Kulman J, Chung DW, Lopez JA. Oxidative modification of von Willebrand factor by neutrophil oxidants inhibits its cleavage by ADAMTS13. *Blood* 2010; **115**: 706–12.
7 Lancellotti S, De Filippis V, Pozzi N, Peyvandi F, Palla R, Rocca B, Rutella S, Pitocco D, Mannucci PM, De Cristofaro R. Formation of methionine sulfoxide by peroxynitrite at position 1606 of von Willebrand factor inhibits its cleavage by ADAMTS-13: a new prothrombotic mechanism in diseases associated with oxidative stress. *Free Radic Biol Med* 2010; **48**: 446–56.
8 Petri B, Broermann A, Li H, Khandoga AG, Zarbock A, Krombach F, Goerge T, Schneider SW, Jones C, Nieswandt B, Wild MK, Vestweber D. von Willebrand factor promotes leukocyte extravasation. *Blood* 2010; **116**: 4712–19.
9 Starke RD, Ferraro F, Paschalaki KE, Dryden NH, McKinnon TA, Sutton RE, Payne EM, Haskard DO, Hughes AD, Cutler DF, Laffan MA, Randi AM. Endothelial von Willebrand factor regulates angiogenesis. *Blood* 2010; **117**: 1071–80.
10 George NP, Wei Q, Shin PK, Konstantopoulos K, Ross JM. *Staphylococcus aureus* adhesion via Spa, ClfA, and SdrCDE to immobilized platelets demonstrates shear-dependent behavior. *Arterioscler Thromb Vasc Biol* 2006; **26**: 2394–400.
11 Heilmann C, Herrmann M, Kehrel BE, Peters G. Platelet-binding domains in 2 fibrinogen-binding proteins of *Staphylococcus aureus* identified by phage display. *J Infect Dis* 2002; **186**: 32–9.
12 Hartleib J, Kohler N, Dickinson RB, Chhatwal GS, Sixma JJ, Hartford OM, Foster TJ, Peters G, Kehrel BE, Herrmann M. Protein A is the von Willebrand factor binding protein on *Staphylococcus aureus*. *Blood* 2000; **96**: 2149–56.
13 Klock JC, Bainton DF. Degranulation and abnormal bactericidal function of granulocytes procured by reversible adhesion to nylon wool. *Blood* 1976; **48**: 149–61.
14 Watson F, Robinson J, Edwards SW. Protein kinase C-dependent and -independent activation of the NADPH oxidase of human neutrophils. *J Biol Chem* 1991; **266**: 7432–9.
15 Di Stasio E, Bizzarri P, Misiti F, Pavoni E, Brancaccio A. A fast and accurate procedure to collect and analyze unfolding fluorescence signal: the case of dystroglycan domains. *Biophys Chem* 2004; **107**: 197–211.
16 Di Stasio E, Romitelli F, Lancellotti S, Arcovito A, Giardina B, De Cristofaro R. Kinetic study of von Willebrand factor self-aggregation induced by ristocetin. *Biophys Chem* 2009; **144**: 101–7.
17 De Cristofaro R, Landolfi R. Oxidation of human alpha-thrombin by the myeloperoxidase–$H_2O_2$–chloride system: structural and functional effects. *Thromb Haemost* 2000; **83**: 253–61.
18 Huttenhain R, Malmstrom J, Picotti P, Aebersold R. Perspectives of targeted mass spectrometry for protein biomarker verification. *Curr Opin Chem Biol* 2009; **13**: 518–25.
19 Chung DW, Fujikawa K. Processing of von Willebrand factor by ADAMTS-13. *Biochemistry* 2002; **41**: 11065–70.
20 Klebanoff SJ. Myeloperoxidase: friend and foe. *J Leukoc Biol* 2005; **77**: 598–625.
21 Carreras MC, Pargament GA, Catz SD, Poderoso JJ, Boveris A. Kinetics of nitric oxide and hydrogen peroxide production and formation of peroxynitrite during the respiratory burst of human neutrophils. *FEBS Lett* 1994; **341**: 65–8.
22 Auton M, Cruz MA, Moake J. Conformational stability and domain unfolding of the Von Willebrand factor A domains. *J Mol Biol* 2007; **366**: 986–1000.
23 Greco MN, Hawkins MJ, Powell ET, Almond HR Jr, Corcoran TW, de Garavilla L, Kauffman JA, Recacha R, Chattopadhyay D, Andrade-Gordon P, Maryanoff BE. Nonpeptide inhibitors of cathepsin G: optimization of a novel beta-ketophosphonic acid lead by structure-based drug design. *J Am Chem Soc* 2002; **124**: 3810–11.
24 Fujinaga M, Chernaia MM, Halenbeck R, Koths K, James MN. The crystal structure of PR3, a neutrophil serine proteinase antigen of Wegener's granulomatosis antibodies. *J Mol Biol* 1996; **261**: 267–78.
25 Huang W, Yamamoto Y, Li Y, Dou D, Alliston KR, Hanzlik RP, Williams TD, Groutas WC. X-ray snapshot of the mechanism of inactivation of human neutrophil elastase by 1,2,5-thiadiazolidin-3-one 1,1-dioxide derivatives. *J Med Chem* 2008; **51**: 2003–8.
26 De Meyer SF, Budde U, Deckmyn H, Vanhoorelbeke K. In vivo absence of ADAMTS13 does not abrogate VWF size heterogeneity. *J Thromb Haemost* 2009; **7**: PP-TH-091, 964.
27 Federici AB, Berkowitz SD, Lattuada A, Mannucci PM. Degradation of von Willebrand factor in patients with acquired clinical conditions in which there is heightened proteolysis. *Blood* 1993; **81**: 720–5.
28 Johnson CM, Bowie EJ. Pigs with von Willebrand disease may be resistant to experimental infective endocarditis. *J Lab Clin Med* 1992; **120**: 553–8.

# *SUPPORTING INFORMATION*

## SERINE PROTEASES FROM PRIMARY GRANULES OF LEUKOCYTES EFFICIENTLY CLEAVE OXIDIZED VON WILLEBRAND FACTOR: DIVERGENCE FROM ADAMTS-13

**Stefano Lancellotti[1#], Vincenzo De Filippis[2#], Nicola Pozzi[2], Laura Oggianu [1,3], Sergio Rutella[4,5], Giovanni Luca Scaglione[1], Fabio Maset, Flora Peyvandi[6], Pier Mannuccio Mannucci[6] and Raimondo De Cristofaro[1*]**

*Proteolysis of VWF74 and VWF74-MetSO by human LSPs and identification of the cleavage sites by mass spectrometry*

The pseudo wild-type peptide VWF74, containing the amino acid exchange Cys1669Ala and encompassing the VWF A2 domain sequence 1596-1669 (DREQAPNLV**YM**VTGNPASDEIKRLPGDIQVVPIGVGPNANVQELERIGWPNAPILIQDFET LPREAPDLVLQRA), and its derivative containing MetSO at position 1606 were synthesized by the solid-phase method and characterized as previously detailed [1]. VWF74 or VWF74-MetSO (120 µl, 20 µM) in 10 mM Hepes, 150 mM NaCl, 5 mM $CaCl_2$, pH 7.4 (HBS) were separately incubated for 90 min at 37°C with 20 nM PMN-derived HLE, CG and PR3 , all purchased from Sigma-Aldrich (Milano, Italy). For comparison, proteolysis reaction was carried for 60 min under identical experimental conditions with 5 nM recombinant human ADAMTS-13 (R&D Systems, Minneapolis, MN). The reaction was stopped by adding 4% aqueous TFA (80 µl) and 6 M Gdn-HCl (200 µl) and fractionated on a Grace-Vydac (The Separation Group, Hesperia, CA) C18 analytical column (4.6 x 250 mm), using an acetonitrile-0.1%TFA gradient (10 to 30% in 10 min; 30 to 45% in 30 min, 0.8 ml/min). The peptides eluted in correspondence of the chromatographic peaks were collected, lyophilized and then analyzed by mass spectrometry (MS) on a Mariner ESI-TOF instrument from PerSeptive Biosystems (Stafford, TX).

*Determination of Michaelis-Menten parameters for proteolysis of VWF74 and VWF74-MetSO by human LSPs*

The Michaelis-Menten parameters for the hydrolysis of VWF74 and VWF74-MetSO by LSPs and ADAMTS-13 were determined by quantifying the cleavage products by RP-HPLC, as previously

described [1]. The VWF74- peptide substrates (1.2 -20.8 μM) were treated with HLE, PR3 and CG (5 nM). The steady state hydrolysis of VWF peptides was performed in HBS, pH 7.5 at 37°C. The Michaelis-Menten parameters were calculated by quantifying at 210 nm the N-terminal peptides ($^{1596}$Asp-Tyr$^{1605}$ or $^{1596}$Asp-Val$^{1607}$) released from VWF74 and VWF74-MetSO, respectively. RP-HPLC and MS analyses showed that proteolysis of VWF74 peptides with PR3, CG, and ADAMTS-13 in the time-range of the analysis (30-90 min) occurred exclusively at a single peptide bond, Tyr1605-Met1606 or Val1607-Thr1608 (see Results), allowing us to determine the parameters $k_{cat}$ and $K_m$ pertaining to a single proteolytic process (Table 2). At variance, HLE cleaved VWF74 peptides at multiple sites with comparable efficiency, even after short incubation time (Fig. 1). Thus, in the latter case only an observed pseudo-first order kinetic constant, $k_{obs}$, of VWF74 disappearance was derived at 25 °C and low substrate concentration (4 μM) (Table 2). A lower temperature was chosen in this case to slow down the proteolytic reaction and monitor with higher precision the products' release.

*Oxidation of VWF multimers by hypochlorous acid and the myeloperoxidase/$H_2O_2$/$Cl^-$ system (MOPSY)*

Plasma VWF multimers were purified and characterized as previously detailed [2, 3] and their hypochlorous acid HClO- or MOPSY-mediated oxidation was carried out using a procedure described earlier [4]. Intact VWF samples (200 nM as a monomer) in 10 mM Hepes-buffered saline, pH 7.50, were treated for 15 min at 25°C with increasing concentrations of HClO (i.e., 2.5, 5, 10, 20 and 40 μM), in the absence or presence of L-tyrosine, added to promote the formation of tyrosyl radicals that contribute to oxidative protein damage and dityrosine intermolecular cross-links [5]. When MOPSY was used, human leukocyte myeloperoxidase (MPO, 25 nM, Calbiochem, Milano, Italy) was added to VWF samples (200 nM) in HBS in the presence of $H_2O_2$ (200 μM) and L-tyrosine (100 μM). The concentration of hypochlorous acid and hypochlorite ion in commercial NaOCl solution (Sigma) was determined spectrophotometrically at 230 nm, using a molar absorptivity of 93.3 and 7.2 $M^{-1}\cdot cm^{-1}$, respectively [4]. The concentration of $H_2O_2$ solution was determined by UV-absorption at 240 nm, using a molar absorptivity of 350 $M^{-1}\cdot cm^{-1}$ [6] . Excess HOCl/NaOCl and tyrosine were eliminated by gel-filtration on a Bio-Rad (Richmond, CA) DG10 column. Oxidation of the model compound $N^{\alpha}$-acetyl-tryptophanyl-amide (NATA) to its mono- (Oia) and di-oxyindolylalanine (Dia) derivatives was carried out by the DMSO-HCl procedure [7]. The reaction was conducted for 15 min and quenched by 1:20 (v/v) dilution with water. The products were then analyzed by MS and UV-absorption, revealing the presence of both Oia and Dia in a 3:2 ratio.

*Proteolysis of the HClO- and MOPSY-treated VWF multimers by LPSs and ADAMTS-13*

After treatment with HClO or MOPSY, VWF samples (20 µg/ml) were separately incubated at 37 °C with 10 nM ADAMTS-13, HLE, PR3, and CG in 5 mM Tris-HCl buffer, pH 8.0, containing 3 mM $CaCl_2$, in the absence or presence of 1.5 mg/ml sulfate-free ristocetin (Helena Laboratories, Beaumont, TX). At time intervals (i.e, 0, 1, and 2 hr), aliquots (50 µl) of these solutions were sampled and the reaction stopped by adding 0.3 M acetic acid (final concentration) or 10 mM EDTA, when ADAMTS-13 was reacted. In all cases, proteolysis of oxidized VWF (VWF-Ox) was assessed by SDS-agarose electrophoresis in 1.5% agarose gel, using rabbit anti-human VWF polyclonal antibody and a HRP-conjugated secondary anti-rabbit antibody (Dako, Milano, Italy), as described [2].

*Hydrolysis of VWF multimers by activated PMNs*

Purified VWF multimers (20 µg/ml) were incubated with human PMNs, isolated from healthy volunteers and stimulated with 50 ng/ml 12-phorbol 13-myristate acetate (PMA, Sigma) in HBS in the presence of 1.5 mg/ml ristocetin. PMNs were purified by following a procedure published elsewhere, with only minor modifications [8]: citrate-anticoagulated blood (20 ml) was mixed with PBS (20 ml) and layered over 20 ml of endotoxin tested Ficoll-Paque solution (GE Healthcare, Milan, Italy), and centrifuged at 400 g for 30 min at 20°C. The supernatant and the mononuclear cell/platelet layer were removed by suction, and the bottom fraction containing PMN cells and red cells was diluted with 10 volumes of 150 mM $NH_4Cl$, 10 mM $KHCO_3$, 0.1 mM EDTAto promote red cells lysis. PMNs were collected by centrifugation (800 g for 5 min), washed twice with 10 mM phosphate buffered saline, and resuspended in HBS at a concentration of 1-5x $10^3$ cells/µl. Purity of PMN cell preparations was checked by a FACS Canto® flow cytometer (BD Biosciences, Mountain View, CA) using FITC-conjugated anti-CD11b or isotype control antibody. Data were then collected by recording FITC fluorescence at 525 nm. Time from blood withdrawal to testing was less than 2 hr. Production of superoxide by isolated PMNs in response to PMA was assessed by monitoring the reduction of ferricytochrome c [9], by recording at 25°C the absorbance at 550 nm, on a model Benchmark Plus microplate spectrophotometer (Bio-Rad), expressed as µM *per* $10^6$ PMNs, using an extinction coefficient of 21 $mM^{-1}\cdot cm^{-1}$ for (reduced-oxidized) cytochrome c [10]. The concentration of superoxide was determined in the absence and presence of 6 U/ml SOD, 1 mM L-methionine, and 200 nM catalase, used as superoxide and $H_2O_2$ scavengers, respectively. VWF was added to these PMNs suspensions and immediately afterwards PMA was added to stimulate PMNs. An aliquot of the PMNs suspension was taken and centrifuged at 10,000 rpm for 30 sec, while the supernatant containing added VWF was used to analyze the pattern of VWF

multimers. To inhibit LSP activity, 500 μM aprotinin and phenyl-methyl-sulphenyl-fluoride (PMSF) were added in control samples under identical experimental conditions. The SDS-agarose electrophoresis of VWF multimers treated with activated PMNs was carried out in 0.8 % (stacking gel)-1.5 % (running gel) agarose gel. The Western blot analysis was performed as detailed above.

*Flow cytometry measurements of oxidative metabolism and spectrophotometric measurements of ROS and HLE secretion by PMN cells*

PMNs ($1x10^6$/tube) were labeled with 2′-7′-dichlorofluorescein diacetate (DCFH-DA; 20 μM final concentration) and hydroethidine (HE; 10 μM final concentration) for 15 min at 37°C to measure $H_2O_2$ and superoxide anion production, respectively [11]. Cells loaded with the fluorescent probes were then stimulated with 50 ng/ml PMA. Samples were immediately analyzed on a FACS Canto® flow cytometer to ensure a true zero value and then each tube was run individually to measure DCFH-DA and HE fluorescence, every 5 min for up to 25 min. Control tubes consisted of PMN cells without addition of PMA. Fluorescence emission for DCFH-DA and HE was collected at 525 nm and 620 nm, respectively. A minimum of 10,000 events was acquired in list mode. Samples were analyzed with the FACS Diva software package (BD Biosciences). Superoxide generation in intact cells was measured at 25°C by spectrophotometric assay of ferricytochrome c reduction in 1.0 ml cuvettes containing $2\times10^6$ cells and 50 μM cytochrome c in phosphate-buffered saline (PBS), pH 7.4, supplemented with 1.2 mM $MgCl_2$, 2 mM $CaCl_2$. The mixture was blanked at 550 nm in a microplate reader before adding PMA, and the time-dependent release of superoxide from PMNs was recorded with or without the addition of superoxide dismutase, catalase and methionine, as ROS scavengers. Readings were taken every 20 s for a total run time of 30 min. Superoxide dismutase-inhibitable absorbance was calculated using $\varepsilon=2\cdot11\times10^4\ M^{-1}cm^{-1}$ for reduced cytochrome c.

The concentrations of HLE bound to the specific inhibitor α1-anti-protease 1, present in the supernatants of PMA-stimulated PMNs were measured using "PMN-Elastase ELISA" kit (Abnova, Milano, Italy) according to the manufacturer's instructions. Aliquots of the same supernatant solutions, taken from 5 to 30 min after addition of PMA, were used to measure the level of HLE activity, by monitoring at 405 nm the enzyme activity toward 200 μM of the synthetic substrate N-(methoxysuccinyl)-Ala-Ala-Pro-Val 4-nitroanilide (Sigma-Aldrich). The reference curve was constructed using purified HLE over a concentration ranging from 10 to 100 nM.

*Oxidation of elastase (HLE) and α1-AP by MOPSY and activated PMNs*

Human HLE or *α1-AP* were used at 80 nM concentration in 10 mM Hepes, 0.15 M NaCl, 0.1% PEG 6000, pH 7.40 (buffer A). When HLE or α1-AP were oxidized by myeloperoxidase, at a concentration of 50 nM, the latter was added to the HLE or α1-AP solution and the reaction was started with 200 μM $H_2O_2$. Free L-tyrosine was also added at a physiological concentration (80 μM, final concentration) to promote the formation of tyrosyl radicals. The solution was incubated at 25° C for 2, 5, 10, 15 and 30 min, respectively. The oxidation reaction was stopped using 1 mM sodium azide to poison the heme moiety of myeloperoxidase and 200 nM catalase to decompose any residual $H_2O_2$. HLE or α1-AP solution was gel filtered on a DG10 Bio-Rad column equilibrated in buffer A. The purity of ox-HLE and ox-α1-AP was checked by SDS-PAGE, which showed a single component with a MW of 29 and 52 kDa, respectively. Oxidative modification of purified elastase or α1-AP was also attained by activated PMNs, using the same conditions reported under Methods, although the in the absence of calcium and presence of 1 mM EDTA and 200 μM Rac1 inhibitor NSC23766 (Merck, Darmstadt, Germany). These experimental conditions allow the oxidative burst to take place, though completely inhibiting the release of primary granules [12]. In the latter case, the reaction was carried out for 30 min at 25° C in buffer A and in the presence of 100 μM L-tyrosine. The activity of untreated and oxidized HLE was measured at 405 nm monitoring the hydrolysis of N-(methoxysuccinyl)-Ala-Ala-Pro-Val 4-nitroanilide (Fig. S1 A).

*Kinetics of HLE interaction with untreated and oxidized α1-AP*

HLE and the inhibitor were present at equimolar concentration (80 nM), whereas the substrate N-(methoxysuccinyl)-Ala-Ala-Pro-Val 4-nitroanilide was used at 0.2 mM. Experimental data were fitted to the equation:

$$v_t/v_0\ (\%) = 100 /[1+(E_0 * k_2/K_i*t)] \qquad (2)$$

Where $v_t$ is the rate of substrate's hydrolysis at any time (t) and $v_0$ is the velocity at time=0 (Fig. S1 B). The value of $k_2$/Ki is approximately equal to the second order rate constant of α1-AP association to HLE [13].

*Oxidation of VWF by PMNs and identification of MetSO at position 1606 of in VWF by Targeted Mass Spectrometry (TMS) analysis*

Oxidation of VWF multimers (20 μg/ml) by activated PMNs (2000/μl) was carried out for 30 min at 37°C in 10 mM Hepes buffered saline, pH 7.45, as detailed above, under conditions where the

release of proteases from primary granules is completely inhibited. Oxidized VWF was recoverd from the supernatant of cultured PMNs by centrifugation At 10000 rpm in a Beckman microfuge and the carbonyl content measured by ELISA, as previously detailed [1].

The experimental strategy used to identify MetSO at position 1606 of PMNs-oxidized VWF (VWF-Ox) was based on the Targeted Mass Spectrometry (TMS) approach [14] and involves the following steps: 1) selection and production of reference proteotypic peptides (PTPs) with known physico-chemical properties (e.g., retention time in RP-HPLC, *m/z* ratio and fragmentation pattern in MS) that are unique to VWF with Met1606 in the unmodified (Met-PTP) or sulfoxide (MetSO-PTP) form; 2) proteolysis of VWF and VWF-Ox with Glu-C protease; 3) LC-MS analysis of the proteolysis reactions and identification of PTPs by TMS; 4) determination of the amino acid sequence of PTPs by MS/MS analysis.

From the analysis of the theoretical fragmentation pattern of VWF with Glu-C protease, the peptide sequence $^{1599}$QAPNLV**YM**VTGNPASDE$^{1615}$ has been selected as a suitable PTP. Met-PTP and MetSO-PTP were prepared by proteolysis with Glu-C protease of the synthetic peptides VWF74 and VWF74-MetSO, respectively. Met-PTP [*m/z* = 903.4 ± 0.1 (2+) a.m.u.] and MetSO-PTP [*m/z* = 911.4 ± 0.1 (2+) a.m.u.] were purified on a microgram scale by RP-HPLC and then used as reference peptides in TMS analysis. VWF samples (15μg; 45μg/ml) in 10 mM Hepes, pH 7.5, 125 mM NaCl were reduced for 20 min at 80°C with 5 mM dithiotreitol (DTT) and then alkylated with 10 mM iodoacetamide for 15 min at 37°C in the dark, keeping the solution pH constant at 7.5 by addition of Tris base. The reaction mixtures, containing the reduced and carboxamidomethylated VWF and VWF-Ox (i.e., RCM-VWF and RCM-VWF-Ox), were digested in parallel for 24 h at 37°C with Glu-C endoprotease (Sigma-Aldrich) at a protease:VWF ratio of 1:20 (w/w) and directly analyzed by liquid chromatography mass spectrometry (LC-MS) on a Q-TOF Micro spectrometer from Micromass (Manchester, UK) equipped with a Z-spray nanoflow electrospray ionization interface and connected to a model CapLC capillary HPLC system from Waters (Milford, MA). Spectra were acquired using the nanoelectrospray source operating at capillary, cone, and extractor voltages of 2700, 35, and 1 V, respectively (positive ion mode). Digested vWF samples (7μl ≈ 2μg) were loaded onto a C18 (75μm x 150mm, 3.5μm granulometry) NanoEase column (Waters), eluted with a linear acetonitrile-0.1%HCOOH gradient from 5 to 70% in 42min at a flow rate of 0.2μl/min. The presence of the monoisotopic peptide species at *m/z* values 903.49± 0.01($2^+$) (Fig. S2 A) and 911.49±0.01($2^+$) a.m.u. (Fig. S2 B), eluting from the column in correspondence of the reference PTPs, allowed us to unequivocally identify Met-PTP and MetSO-PTP in the Total Ion Current (TIC) profile of the proteolysis reaction of VWF and VWF-Ox (Fig. S2 A,B). In the final step, the chemical identity of Met-PTP and MetSO-PTP in the proteolysis reactions was confirmed by

MS/MS sequence analysis (Fig. S2 C,D). The mass values of the peptides belonging to the *b*- and *y*-series [15] (see Fig. S2 C, D) reported in Table S1 provided clear-cut evidence for the presence of MetSO at position 1606 of VWF-Ox.

*Conformational and stability characterization*

UV-absorption spectra of intact and oxidized VWF multimers at different HClO concentrations were recorded on a Varian-Cary (Palo Alto, CA) model 2200 spectrophotomer or on a Jasco (Tokyo, Japan) V-630 instrument. For unaltered VWF, an extinction coefficient at 280 nm was calculated as 0.846 $(mg/ml)^{-1}$ $cm^{-1}$ determined by the method of Pace et al. [16]. Intrinsic fluorescence spectra were recorded on a model Eclipse spectrofluorimeter (Varian, Santa Clara, CA), equipped with a Peltier temperature control system at 25 °C. Both intact and HClO-oxidized (HClO, 2.5-40 µM for 15 min) VWF multimers were used at a concentration of 200 nM. VWF solutions were excited at 280 or 295, using excitation and emission slits of 2.5 or 5 nm. Dityrosine production was assessed by exciting the samples at 325 nm and recording the fluorescence intensity at 410 nm [17]. Far-UV CD spectra were taken on a Jasco (Tokyo, Japan) J-810 spectropolarimeter using a 1-mm pathlength cuvette. The final spectra resulted from four accumulations after base line subtraction and CD signal was expressed as the mean residue ellipticity. All spectroscopic measurements were carried out at 25±0.1°C in HBS. Dynamic light scattering measurements on unaltered and oxidized VWF samples were carried out at 25±0.1°C with a Zetasizer Nano S (Malvern Instruments, Malvern, U.K.) at a fixed angle (i.e., 173°) from the incident light (He-Ne laser power: 4 mW; incident light: 633 nm). Samples were manually injected into a 1-cm path length Suprasil quartz cuvette (45 µl) (Hellma Italia, Milan, Italy). Data were collected for at least 15 minutes from injection. Each measurement consisted of a subset of runs automatically determined, each being averaged for 10 s. Peak intensity analysis was used to determine the average hydrodynamic diameters (Z-average diameter) of the scattering particles. Polydispersity index was obtained by a cumulative analysis of the intensity autocorrelation function using the Nano vs. 5.0 software [3]. Denaturation experiments of VWF and VWF-Ox were carried out by recording the fluorescence $\lambda_{max}$ as a function of guanidine hydrochloride (Gdn-HCl) concentration. Unfolding data were analyzed according to a two-state model, as previously reported [18]. Prior to measurements, samples (2 ml) of genuine and HClO-oxidized (i.e., 40 µM HClO for 15 min. at 25°C) plasma VWF (200 nM) at increasing Gdn-HCl concentrations (0-6 M) were equilibrated for 1 hr at 25±0.1°C in 10 mM Hepes, pH 7.50, 0.15 M NaCl and then excited at 295 nm. The fluorescence $\lambda_{max}$ value (i.e., the wavelength of maximum fluorescence intensity) was recorded as a function of denaturant concentration, [D], using an excitation/emission band pass of 2.5 nm. At

each denaturant concentration, the fluorescence signal was subtracted for that of the corresponding blank and corrected for dilution. Fluorescence data points were fitted to the logistic equation 1, that allowed us to estimate the denaturation midpoint value, $[D]_{1/2}$:

$$\lambda_{max}^{obs} = \lambda_{max}^{N} + \frac{(\lambda_{max}^{D} - \lambda_{max}^{N})}{1 + ([D]_{1/2}/[D])^{n}} \quad (1)$$

Where $n$ is an exponential constant, $\lambda_{max}^{N}$ and $\lambda_{max}^{D}$ are the fluorescence $\lambda_{max}$ value of both VWF and VWF-Ox in the absence and in the presence of fully denaturant Gdn-HCl concentrations. Of note, the unfolding of VWF follows a multistep mechanism [19]. Hence, in this case, $[D]_{1/2}$ value should be considered as an approximate, quantitative indicator of the stability of VWF and VWF-Ox to Gdn-HCl induced denaturation and not as a thermodynamic parameter linked to a specific unfolding model.

The UV-absorption spectrum of unaltered VWF showed a $\lambda_{max}$ value centred at 278 nm and a shoulder at 290, typical of Trp contribution. Increasing the concentration of hypochlorous acid (HClO) from 0 to 41 μM, the $\lambda_{max}$ value underwent a small (i.e., 2 nm) blue-shift, whereas the absorbance ratio 280/255 nm progressively decreased by ~35% of the original value (Fig. S3 A). These spectral changes are compatible with the formation of mono- (Oia) and di-oxyindolyl-alanine (Dia), generated by oxidation of Trp residues and maximally absorbing at 250 nm [7]. Likewise, the fluorescence spectra of VWF, recorded after treatment with HClO (0-40 μM) showed a 5-nm blue-shifted $\lambda_{max}$ value, from 345 to 340 nm, and a 45% decrease of fluorescence intensity (Fig. 3B). The formation of poorly emitting oxyndole-derivatives (i.e., Oia and Dia) explains the observed fluorescence spectral changes. The far UV-CD spectrum of unaltered VWF is typical of a protein containing a mixed α/β secondary structure [20], with two negative bands at 208 and 215 nm (Fig. S3C). After treating VWF with 41 μM HClO, the shape of the spectrum was essentially unchanged, whereas ellipticity decreased by ~33%. Oxidation of Trp residues to Oia- and Dia-derivatives was interpreted to be responsible for the decrease of the CD signal pertaining to VWF-Ox [21]. This conclusion is also supported by DLS measurements, showing that increasing HClO concentrations did not alter the hydrodynamic radius of VWF, which remained essentially constant (r=100±39 nm, Fig. S3D). This result ruled out gross alterations in the conformation or aggregation state of VWF. This conclusion is also consistent with the denaturation experiments showing that both unaltered and oxidized VWF display a similar stability to guanidinium-induced unfolding, as shown in Fig S4.

**References**

1 Lancellotti S, De Filippis V, Pozzi N, Peyvandi F, Palla R, Rocca B, Rutella S, Pitocco D, Mannucci PM, De Cristofaro R. Formation of methionine sulfoxide by peroxynitrite at position 1606 of von Willebrand factor inhibits its cleavage by ADAMTS-13: A new prothrombotic mechanism in diseases associated with oxidative stress. *Free Radic Biol Med*. 2010; **48**: 446-56.
2 De Cristofaro R, Peyvandi F, Palla R, Lavoretano S, Lombardi R, Merati G, Romitelli F, Di Stasio E, Mannucci PM. Role of chloride ions in modulation of the interaction between von Willebrand factor and ADAMTS-13. *J Biol Chem*. 2005; **280**: 23295-302.
3 Di Stasio E, Romitelli F, Lancellotti S, Arcovito A, Giardina B, De Cristofaro R. Kinetic study of von Willebrand factor self-aggregation induced by ristocetin. *Biophys Chem*. 2009; **144**: 101-7.
4 De Cristofaro R, Landolfi R. Oxidation of human alpha-thrombin by the myeloperoxidase-H2O2-chloride system: structural and functional effects. *Thromb Haemost*. 2000; **83**: 253-61.
5 Bhattacharjee S, Pennathur S, Byun J, Crowley J, Mueller D, Gischler J, Hotchkiss RS, Heinecke JW. NADPH oxidase of neutrophils elevates o,o'-dityrosine cross-links in proteins and urine during inflammation. *Arch Biochem Biophys*. 2001; **395**: 69-77.
6 Nelson DP, Kiesow LA. Enthalpy of decomposition of hydrogen peroxide by catalase at 25 degrees C (with molar extinction coefficients of H 2 O 2 solutions in the UV). *Anal Biochem*. 1972; **49**: 474-8.
7 Savige WE, Fontana A. Oxidation of tryptophan to oxindolylalanine by dimethyl sulfoxide-hydrochloric acid. Selective modification of tryptophan containing peptides. *Int J Pept Protein Res*. 1980; **15**: 285-97.
8 Klock JC, Bainton DF. Degranulation and abnormal bactericidal function of granulocytes procured by reversible adhesion to nylon wool. *Blood*. 1976; **48**: 149-61.
9 Kessels GC, Krause KH, Verhoeven AJ. Protein kinase C activity is not involved in N-formylmethionyl-leucyl-phenylalanine-induced phospholipase D activation in human neutrophils, but is essential for concomitant NADPH oxidase activation: studies with a staurosporine analogue with improved selectivity for protein kinase C. *Biochem J*. 1993; **292 ( Pt 3)**: 781-5.
10 van GB, Slater EC. The extinction coefficient of cytochrome c. *Biochim Biophys Acta*. 1962; **58**: 593-5.
11 Robinson J. *Oxidative metabolism*. New York: John Wiley & Sons, Inc., 1997.
12 Mitchell T, Lo A, Logan MR, Lacy P, Eitzen G. Primary granule exocytosis in human neutrophils is regulated by Rac-dependent actin remodeling. *Am J Physiol Cell Physiol*. 2008; **295**: C1354-65.
13 Duranton J, Adam C, Bieth JG. Kinetic mechanism of the inhibition of cathepsin G by alpha 1-antichymotrypsin and alpha 1-proteinase inhibitor. *Biochemistry*. 1998; **37**: 11239-45.
14 Huttenhain R, Malmstrom J, Picotti P, Aebersold R. Perspectives of targeted mass spectrometry for protein biomarker verification. *Curr Opin Chem Biol*. 2009; **13**: 518-25.
15 Johnson RS, Martin SA, Biemann K, Stults JT, Watson JT. Novel fragmentation process of peptides by collision-induced decomposition in a tandem mass spectrometer: differentiation of leucine and isoleucine. *Anal Chem*. 1987; **59**: 2621-5.
16 Pace CN, Vajdos F, Fee L, Grimsley G, Gray T. How to measure and predict the molar absorption coefficient of a protein. *Protein Sci*. 1995; **4**: 2411-23.
17 Yan LJ. Analysis of oxidative modification of proteins. *Curr Protoc Protein Sci*. 2009; **Chapter 14**: Unit14 4.
18 Di Stasio E, Bizzarri P, Misiti F, Pavoni E, Brancaccio A. A fast and accurate procedure to collect and analyze unfolding fluorescence signal: the case of dystroglycan domains. *Biophys Chem*. 2004; **107**: 197-211.
19 Auton M, Cruz MA, Moake J. Conformational stability and domain unfolding of the Von Willebrand factor A domains. *J Mol Biol*. 2007; **366**: 986-1000.

20 Brahms S, Brahms J. Determination of protein secondary structure in solution by vacuum ultraviolet circular dichroism. *J Mol Biol*. 1980; **138**: 149-78.
21 De Filippis V, De Dea E, Lucatello F, Frasson R. Effect of Na+ binding on the conformation, stability and molecular recognition properties of thrombin. *Biochem J*. 2005; **390**: 485-92.

**Table S1-A. Predicted fragmentation pattern for the proteotipic peptides Met-PTP and MetSO-PTP***

| | | | | | | | | | | | | | | | | | |
|---|---|---|---|---|---|---|---|---|---|---|---|---|---|---|---|---|---|
| **b** | 129.07 | 200.10 | 297.16 | 411.20 | 524.28 | 623.35 | **786.41** | **917.46** | **1016.52** | **1117.57** | 1174.59 | **1288.64** | 1385.69 | **1456.73** | 1543.76 | 1658.78 | - |
| **b*** | 129.07 | 200.10 | 297.16 | 411.20 | 524.28 | 623.35 | **786.41** | 933.46 | **1032.52** | **1133.57** | 1190.59 | **1304.64** | 1401.69 | 1472.73 | 1559.76 | 1674.78 | - |
| | 1 | 2 | 3 | 4 | 5 | 6 | 7 | 8 | 9 | 10 | 11 | 12 | 13 | 14 | 15 | 16 | 17 |
| | Gln | Ala | Pro | Asn | Leu | Val | **Tyr** | **Met** | Val | Thr | Gly | Asn | Pro | Ala | Ser | Asp | Glu |
| | 17 | 16 | 15 | 14 | 13 | 12 | 11 | 10 | 9 | 8 | 7 | 6 | 5 | 4 | 3 | 2 | 1 |
| **y*** | - | 1693.78 | 1622.74 | 1525.69 | 1411.65 | 1298.56 | **1199.49** | **1036.43** | 889.39 | 790.32 | 689.27 | 632.25 | 518.21 | 421.16 | 350.12 | 263.09 | 148.06 |
| **y** | - | 1677.78 | 1606.74 | 1509.69 | 1395.65 | 1282.56 | **1183.49** | **1020.43** | 889.39 | 790.32 | 689.27 | 632.25 | 518.21 | 421.16 | 350.12 | 263.09 | 148.06 |

**Table S1-B. MS/MS values for Met-PTP**

| Ion | m/z(+1) | Sequence |
|---|---|---|
| y2 | 263.14 | $^{1614}$D-E$^{1615}$ |
| y3 | 350.19 | $^{1613}$S-E$^{1615}$ |
| y5 | 518.32 | $^{1611}$P-E$^{1615}$ |
| y6 | 623.48 | $^{1610}$N-E$^{1615}$ |
| y7 | 689.45 | $^{1609}$G-E$^{1615}$ |
| **b7** | **786.60** | **$^{1599}$Q-Y$^{1605}$** |
| y8 | 790.46 | $^{1608}$T-E$^{1615}$ |
| y9 | 889.62 | $^{1607}$V-E$^{1615}$ |
| **b8** | **917.68** | **$^{1599}$Q-M$^{1606}$** |
| **b9** | **1016.77** | **$^{1599}$Q-V$^{1607}$** |
| **y10** | **1020.61** | **$^{1606}$M-E$^{1615}$** |
| **b10** | **1117.81** | **$^{1599}$Q-T$^{1608}$** |
| **y11** | **1183.73** | **$^{1605}$Y-E$^{1615}$** |
| **b12** | **1288.90** | **$^{1599}$Q-N$^{1610}$** |
| **b14** | **1457.08** | **$^{1599}$Q-A$^{1612}$** |

**Table S1-C. MS/MS values for MetSO-PTP**

| Ion | m/z(+1) | Sequence |
|---|---|---|
| y2* | 263.14 | $^{1614}$D-E$^{1615}$ |
| y3* | 350.20 | $^{1613}$S-E$^{1615}$ |
| y5* | 518.33 | $^{1611}$P-E$^{1615}$ |
| b5* | 524.40 | $^{1599}$Q-L$^{1603}$ |
| b6* | 623.48 | $^{1599}$Q-V$^{1604}$ |
| y7* | 689.41 | $^{1609}$G-E$^{1615}$ |
| **b7*** | **786.57** | **$^{1599}$Q-Y$^{1605}$** |
| y8* | 790.52 | $^{1608}$T-E$^{1615}$ |
| **b9*** | **1032.78** | **$^{1599}$Q-V$^{1607}$** |
| **y10*** | **1036.43** | **$^{1606}$M(SO)-E$^{1615}$** |
| **b10*** | **1133.87** | **$^{1599}$Q-T$^{1608}$** |
| **y11*** | **1199.49** | **$^{1605}$Y-E$^{1615}$** |
| **b12*** | **1304.95** | **$^{1599}$Q-N$^{1610}$** |

***Supportive Information Figure legends***

**Figure S1**
**(A) Amidolytic activity of untreated (A) and PMN-oxidized (B) HLE toward N-(methoxysuccinyl)-Ala-Ala-Pro-Val 4-nitroanilide.** The concentration of HLE was 50 nM in both cases. (**B) Determination of the second-order rate constants for the inhibition of HLE by untreated and PMN-oxidized α1-AP.** The enzyme and the inhibitor were present at equimolar concentration (80 nM), whereas the substrate N-(methoxysuccinyl)-Ala-Ala-Pro-Val 4-nitroanilide was used at 0.3 mM. The curves have been calculated using eq 2 with the best estimates of $k_2/K_i$ equal to 1.14±0.03 x $10^7$ $M^{-1}$ $sec^{-1}$ for the untreated α1-AP (o) and 6±3 x $10^3$ $M^{-1}$ $sec^{-1}$ for the PMN-oxidized α1-AP (□).

**Figure S2**
**Targeted mass spectrometry (TMS) analysis of untreated (VWF) and oxidized (VWF-Ox) von Willebrand factor with PMNs.** In the experiments herein reported, VWF was oxidized upon incubation for 30 min PMNs activated with PMA. MS spectra of Met-PTP **(A)** and MetSO-PTP **(B)** as identified in the TIC MS traces of the proteolysis reaction of VWF and VWF-Ox with Glu-C protease. MS/MS analysis of the peptides Met-PTP **(C)** and MetSO-PTP **(D)** selected in the proteolytic mixture of vWF. The fragments of the *b*- and *y*-series are shown together with their mass values in Table S1.

**Figure S3**
**Conformational characterization of intact and HClO-oxidized VWF.** (**A**) UV-absorption spectra of purified plasma VWF multimers (100 μg/ml) treated for 15 min at 25°C with increasing concentrations of HClO (from top to bottom: 0, 6, 12, 29, and 41 μM). (**B**) Fluorescence spectra ($\lambda_{ex}$=295 nm) of VWF (200 nM) at increasing HClO concentrations (from top to bottom: 0, 2.5, 5, 10, 20 and 40 μM). (**C**) Far-UV CD spectra of unaltered (○) and oxidized (●) VWF (0.14 mg/ml). Oxidation was carried out with 41 μM HClO for 15 min at 25 °C. (**Inset**) Far-UV CD spectra of the model compounds NATA (○) and Oia/Dia (●) recorded at 310 μM concentration. (**D**) DLS spectra of VWF multimers (200 nM) at increasing HClO concentrations (from top to bottom: 40, 2, 0, 4, 20 and 10 μM).

**Figure S4**
**Guanidinium–induced denaturation of native (●) and oxidized VWF multimers (□).** The continuous lines were drawn using eq. 1 with the best-fit parameter values: VWF, [D]1/2 = 2.35±0.1 M, λmaxN = 344±0.3 nm, and λmaxD = 356 ±0.5 nm; VWF-Ox, [D]1/2 = 2.03±0.12 M, λmaxN = 339.6±0.6 nm and λmaxD = 356 ±0.5 nm.

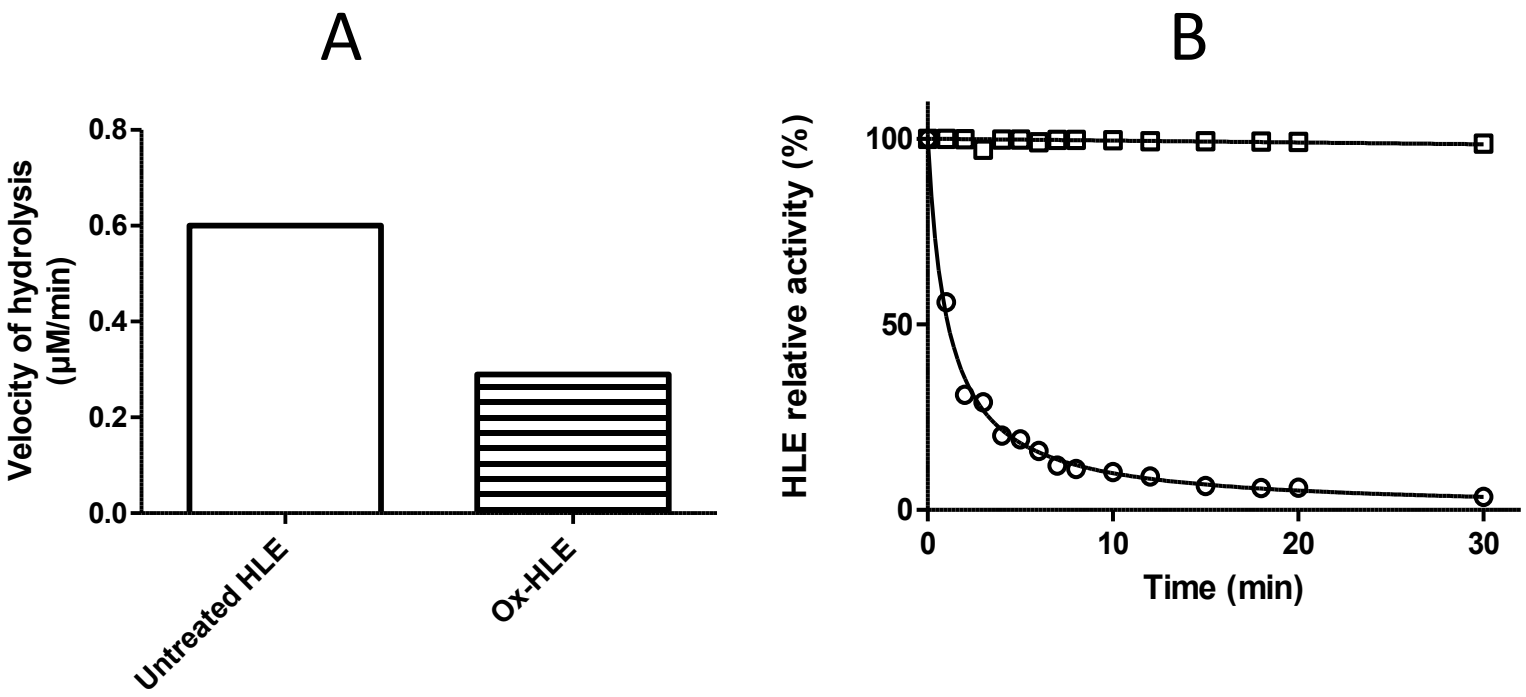
A
B
Velocity of hydrolysis (μM/min)
0.8
0.6
0.4
0.2
0.0
Untreated HLE
Ox-HLE
HLE relative activity (%)
100
50
0
0
10
20
30
Time (min)

Fig. S1

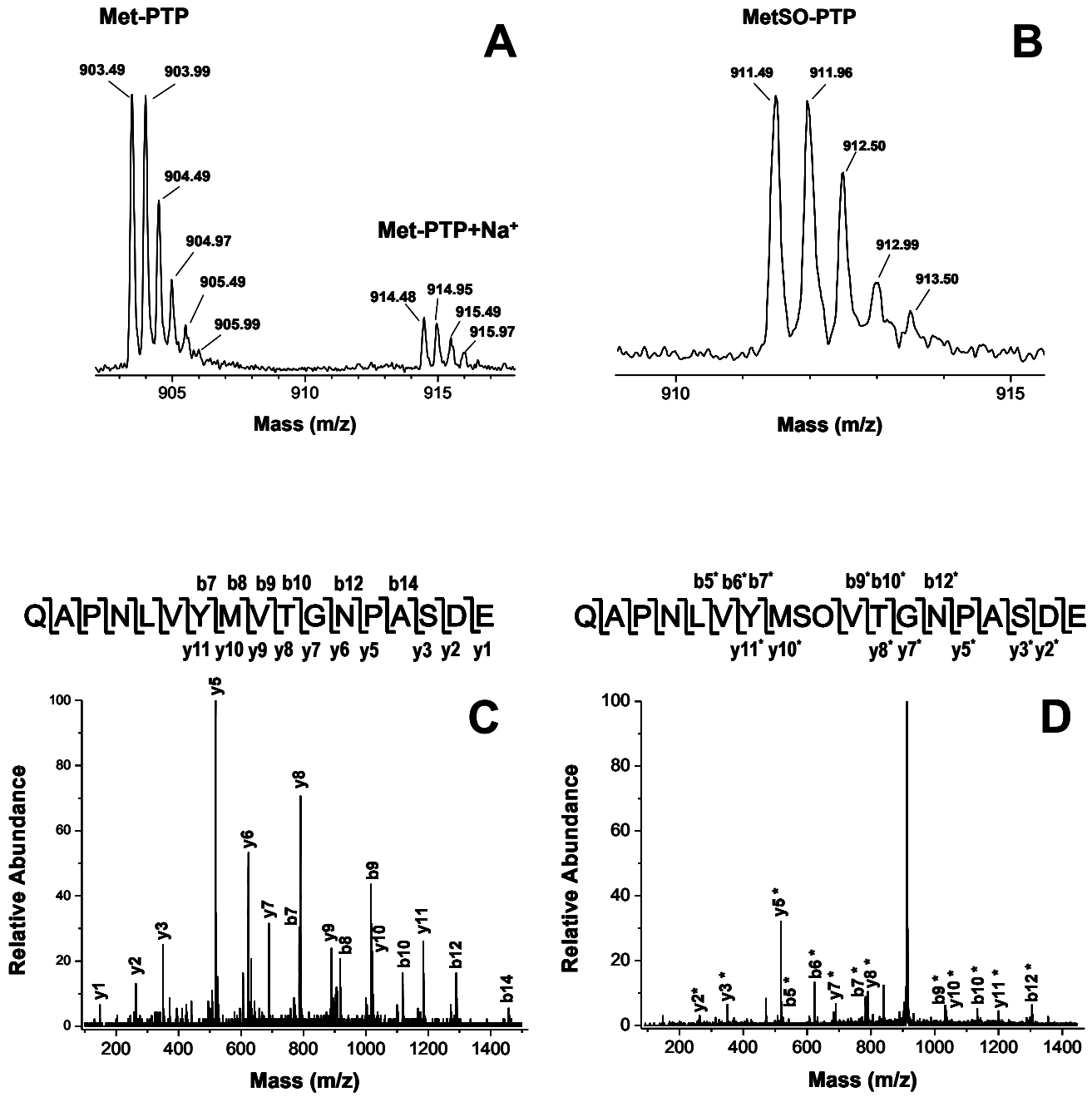
Met-PTP
A
903.49
903.99
904.49
904.97
905.49
905.99
Met-PTP+Na+
914.48
914.95
915.49
915.97
905
910
915
Mass (m/z)
MetSO-PTP
B
911.49
911.96
912.50
912.99
913.50
910
915
Mass (m/z)
b7 b8 b9 b10 b12 b14
Q A P N L V Y M V T G N P A S D E
y11 y10 y9 y8 y7 y6 y5 y3 y2 y1
C
Relative Abundance
Mass (m/z)
b5* b6* b7* b9* b10* b12*
Q A P N L V Y MSO V T G N P A S D E
y11* y10* y8* y7* y5* y3* y2*
D
Relative Abundance
Mass (m/z)

Fig. S2

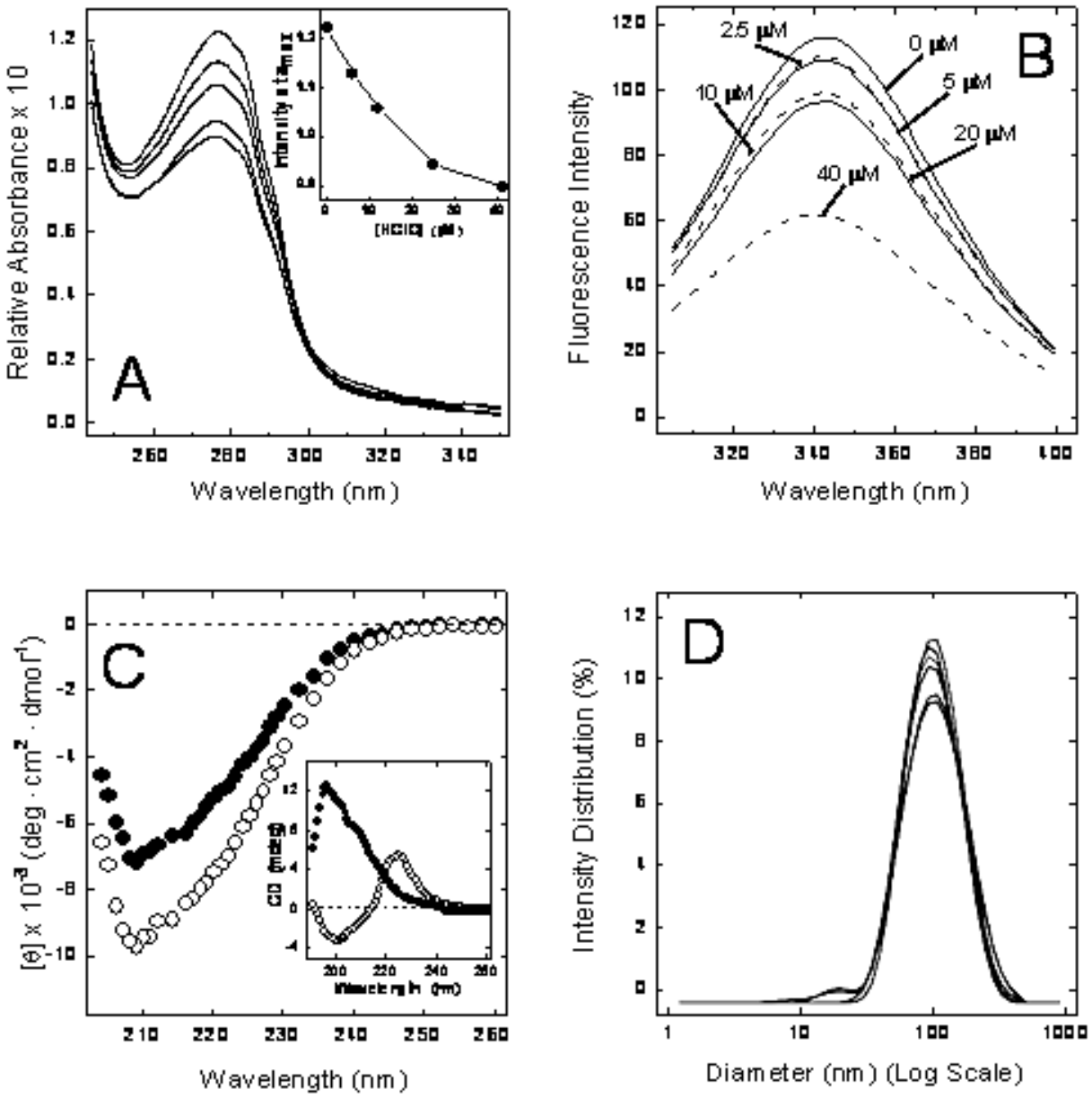
A
Relative Absorbance x 10
Wavelength (nm)
B
Fluorescence Intensity
Wavelength (nm)
2.5 μM
0 μM
10 μM
5 μM
20 μM
40 μM
C
[Θ] x 10^-3 (deg · cm^2 · dmol^-1)
Wavelength (nm)
D
Intensity Distribution (%)
Diameter (nm) (Log Scale)

Fig. S3

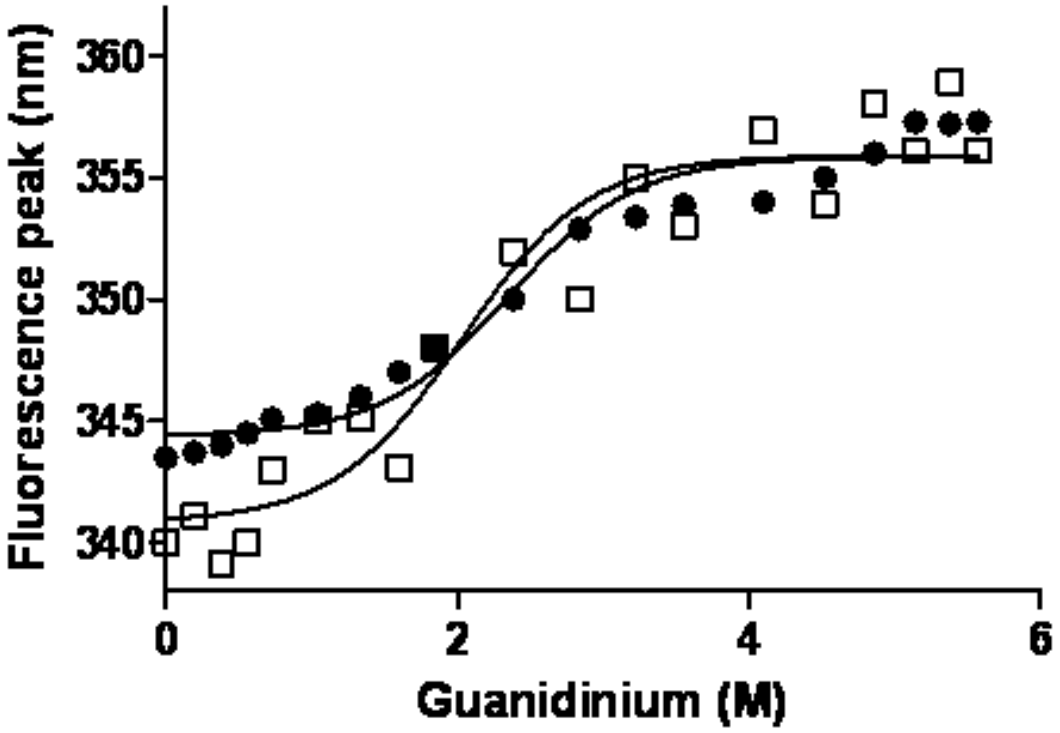


Fig. S4

Publication accepted by PLOS ONE on December 24th 2012

# THE OXIDATIVE MODIFICATION OF VON WILLEBRAND FACTOR IS ASSOCIATED WITH THROMBOTIC ANGIOPATHIES IN DIABETES MELLITUS

Laura Oggianu, PhD[1,2#], Stefano Lancellotti PhD[1#], Dario Pitocco, MD,[3], Francesco Zaccardi, MD[3], Paola Rizzo, PhD[1,3] , Francesca Martini, MD[3], Giovanni Ghirlanda, MD[3], and Raimondo De Cristofaro, MD[1,*]

[1]Institute of Internal Medicine and Geriatrics, and Haemostasis Research Centre, Catholic University School of Medicine, Rome, Italy; [2]Section of Biology Applied to Human Health, "Rome Tre" University, Rome, Italy; [3]Diabetes Care Unit, Department of Internal Medicine, Catholic University School of Medicine, Rome, Italy

# These Authors contributed equally to this study

*Correspondence to: Dr. R. De Cristofaro, MD

Haemostasis Research Centre, Institute of Internal Medicine and Geriatrics,

Catholic University School of Medicine, Largo F. Vito 1, 00168 Rome, Italy

Tel: +30 06 30154438; Fax: +39 06 30155915;

E-mail: rdecristofaro@rm.unicatt.it

**Abstract**

The thrombogenic activity of Von Willebrand factor (VWF) is proportional to its molecular size and inversely related to its proteolysis by ADAMTS-13. Oxidation of VWF severely impairs its proteolysis by the metalloprotease. This study was aimed at assessing in patients with type 1 and type 2 diabetes whether protein carbonyls, marker of oxidative stress, are associated with both the level and oxidation status of VWF as well as with micro- and macro-angiopathic complications. Eighty-three diabetic patients (41 type 1 and 42 type 2 diabetic subjects) and their respective eighty-three healthy controls were studied after verifying the availability, through institutional databases, of clinical biochemistry records spanning at least 3 years. VWF and protein carbonyls were measured by immunoassays, whereas VWF multimers were studied by SDS-agarose gel electrophoresis. Type 2 diabetic subjects had higher levels of VWF antigen (VWF:ag), VWF activity (VWF:act) and plasma proteins' carbonyls, compared to both their controls and type 1 diabetic subjects. Moreover, high molecular weight VWF multimers and specific VWF-bound carbonyls were significantly increased in subjects with micro- and macro-angiopathic complications. In both type 1 and type 2 diabetic subjects, ADAMTS-13 activity was in the normal range. In a multivariable analysis, only VWF-bound carbonyls were significantly associated with any form of thrombotic angiopathy in the entire group of T1 and T2 diabetic patients. These data provide first evidence that not only high VWF levels, but also its oxidation status and the presence of high molecular weight VWF multimers, that are not observed in SDS-agarose gel electrophoresis of normal subjects, are associated with thrombotic angiopathies in diabetes mellitus. These findings may help to identify diabetic patients particularly at risk for these complications and elucidate a new patho-physiological mechanism of thrombotic angiopathies in this clinical setting.

## Introduction

Diabetes mellitus (DM) is linked to tissues and organ damage through several pathological mechanisms, such as an increased polyol pathway, increased intracellular formation and activity of advanced glycation end-products, activation of protein kinase C isoforms and finally, over-activity of the hexosamine pathway. Altogether, these mechanisms were reported to be linked to an upstream overproduction of reactive oxygen (ROS) and nitrogen species (NOS). In particular, in the diabetic micro-circulation this is a direct consequence of intracellular high-glucose levels [1]. On the other hand, in the DM macrovasculature, ROS overproduction would stem from increased oxidation of fatty acids, main consequence of insulin resistance [1]. Moreover, hyperglycemia in DM promotes also an impairment of the antioxidant systems, such as glutathione reduced form (GSH) [2]. Oxidative stress is involved in the pathogenesis of endothelial dysfunction (ED), characterized, besides increased vascular stiffness and tone, by the presence of a prothrombotic and antifibrinolytic state [3]. The oxidative stress causes in these proteins formation of ROS- and NOS-modified amino acids, such as 3-nitrotyrosine (3-N-Tyr) and sulfoxy-methionine (Met-SO). The presence of these oxidized amino acids can affect functional properties of these proteins. In particular, both oxidized fibrinogen and VWF show pro-thrombotic tendency [4-6]. Moreover, oxidative stress may also induce accumulation of high molecular weight VWF multimers (UL-VWF), although at a minor extent than in thrombotic micro-angiopathies, where ADAMTS-13 is strongly reduced or absent, so that proteolytic processing of UL-VWF multimers is severely defective. Notably, UL-VWF multimers have the highest ability to recruit and activate platelets in the circulation. The formation of Met-SO at position 1606 in the A2 domain of VWF is indeed responsible for severe resistance to proteolysis by ADAMTS-13 [5,7], thus favoring an accumulation of UL-VWF multimers [5]. Although it is known that oxidative stress is present in subjects with diabetes, it is still debated how this condition is mechanistically linked to micro- and macro-vascular complications in this setting [8]. Thus, this study was aimed at assessing whether: i) the reported oxidative stress in DM involves also VWF, changing its levels and multimeric structure; ii) the proteolytic processing of VWF by ADAMTS-13 is altered by changes of either levels or function of ADAMTS-13; iii) the presence of oxidized VWF is associated with micro- and macro-angiopathic disorders in a set of both type 1 and type 2 diabetic patients.

## 2. Methods

*Subjects*

Diabetic subjects (n=83, 41 with type 1 diabetes (T1-DM), and 42 with type 2 diabetes (T2-DM)) were consecutively recruited from the outpatient diabetes clinic of the "A. Gemelli" hospital at the Catholic University School of Medicine of Rome. Inclusion criteria required that participants were adults (>18 yr old), did not have arrhythmia and abnormal serum electrolyte levels. An essential criterion for inclusion in the study was the availability, through databases, of HbA1c and other clinical biochemistry records spanning at least 3 years. Type 1 diabetes was diagnosed by the WHO guideline and informed written consent was obtained from each participant. No limits of disease duration were adopted to have a fully representative population of type 1 diabetic subjects, referring to a diabetes clinic. Recruited subjects with type 1 diabetes had a disease duration ranging from 3 to 42 years (mean 21.4±10.3 yr). Likewise, recruited type 2 diabetes subjects had disease duration of 2-55 years (mean 18±12 yr). The study was approved by the ethics committee of the Catholic University School of Medicine (EC n. A/493/2010, approved on 05/20/2010) and was conducted according to the recommendations of the Declaration of Helsinki. After the participants had given informed consent, we retrieved the sequential measurements of HbA1c and other clinical biochemistry parameters over the preceding 3 years. The main demographic and clinical characteristics of the study subjects are shown in Tables 1-2. All participants underwent a complete physical examination and completed questionnaires for diabetes duration, previous and current diseases, and use of medications. Subjects were all non-smokers. Ex-smokers were considered those who quit smoking for at least 3 years. Body weight, height, and waist circumference were measured in light clothing, and body mass index (BMI) was calculated. Hypertension was defined according to the current ESC/ESH guidelines [9]. The presence of diabetic micro-angiopathy was assessed by renal and retinal alterations. The

former were evaluated by calculation of the glomerular filtration rate (GFR) and microalbuminuria. The estimated GFR was calculated with the MDRD formula [10]. Direct fundoscopy was performed through dilated pupils by an experienced ophthalmologist, following the EURODIAB diabetic retinopathy scale [11]. Macroangiopathy was defined as any well documented case of ischemic heart disease (IHD), stroke and thrombotic peripheral artery disease (PAD) occurred and diagnosed 90±10 days prior to the enrolment visit. The diagnosis of IHD included coronary insufficiency and nonfatal myocardial infarction, while typical effort angina was excluded. All myocardial infarction case patients met the criteria of diagnostic ECG changes alone or two of the following criteria: typical chest pain of ≥20 minutes duration, abnormal troponin T levels at least twice the upper limit of normal, or characteristic ECG changes. Coronary insufficiency was considered if typical retrosternal chest pain of at least 15 minutes duration was associated with transient ischemic ECG changes but without significant elevation of troponin T or creatine-kinase levels. Diagnoses of myocardial infarction and coronary insufficiency were confirmed by hospital charts. The diagnosis of effort angina was based on symptoms of retrosternal squeezing or pressure-type discomfort occurring on exertion and relieved by rest or nitroglycerin. Exclusion criteria were left ventricular ejection fraction <30%, lung or liver failure, and known cause of anemia and thrombocytopenia (recent overt bleeding, congenital or acquired haematological disease, gastrointestinal disorder, and malignancy). Stroke diagnosis was confirmed by hospital charts and validated by tomographic examinations. Mild-to-moderate peripheral arterial disease (PAD) was diagnosed if the ankle brachial index (ABI) ranged from 0.41 to 0.90 or a history of limb revascularization was present. The mean ABI index in these patients was equal to 0.81±0.06. A complete list of drugs taken by each patient was carefully registered. Healthy subjects(n=41) among blood donors from the institutional blood bank of the "A. Gemelli" hospital of the Catholic University School of Medicine, Rome, Italy, were consecutively enrolled as controls for type 1 diabetes patients. They were between 38 and 55 years of age, were in good health, not smokers and had no risk factors for cardiovascular disease. Forty-two healthy, not smoking subjects between 40 and 79 years without signs of cardiovascular disorders were consecutively enrolled as controls for type 2 diabetes patients. The control group 1 and 2 were age- and sex-matched with type 1 and type 2 diabetic patients, respectively. The control groups were also blood group-matched with the patients, based on the known effect of blood group on the level of circulating VWF [12].

*Clinical biochemistry and haematological parameters*

Analyses of HbA1c, glucose and blood lipids were carried out at the Department of Clinical Biochemistry, A. Gemelli Hospital in Rome. HbA1c was measured in whole blood by ion exchange high performance liquid chromatography. Triglyceride and HDL cholesterol and LDL cholesterol were measured in serum, using an Olympus auto-analyzer. Microalbuminuria was measured by nephelometry (Behring Nephelometer, using reagents from Dade Behring Diagnostics, Marburg, Germany). Basic haematological and coagulation parameters were measured using an automatic blood cell cytometer (Sysmex SF-3000, Dasit, Milano, Italy) and ACL TOP coagulometers (Instrumentation Laboratory, Milano, Italy), respectively.

*Carbonyl group content of plasma proteins and purified VWF*

The protein carbonyl content was measured as a stable biomarker of oxidative modification of proteins. Carbonyl (CO) groups (aldehydes and ketones) are produced on protein side chains (especially of Pro, Arg, Lys, and Thr) when they are oxidized [13]. The plasma protein carbonyl content was measured according to the OxiSelect$^{TM}$ Protein Carbonyl ELISA (Cell Biolabs, Inc.,San Diego, CA, USA), which quantifies carbonyl groups by derivatizing proteins with dinitrophenylhydrazine (DNP). The sensitivity limit of the method was about 10 pmol carbonyls/mg of protein and the intra- and inter-assay CV was equal to 5.4% and 8.7%, respectively. In a subgroup of subjects (28 cases) from type 2 diabetes patients with the highest plasma protein carbonyls level (>200 pmol/mg), it was reliably possible to measure the specific carbonyl content of VWF, purified from plasma according to a previously described method, with some modifications [5]. Frozen plasma from each subject (20 ml) was thawed at room temperature, added with 0.2 g of PEG [poly(ethylene glycol)]-6000 (Sigma) to a final 1% (w/v) concentration, and gently stirred for

15 min. This solution was added with 1 mM PMSF (0.2 ml, 0.1 M) and 10 mM EDTA (0.4 ml, 0.5 M), as protease inhibitors and left overnight at 4°C under gentle magnetic stirring. The suspension was then centrifuged at 3000 rev./min for 1 h at 4°C. In each test tube, the supernatant was discarded and the pellet resuspended under gentle stirring with 0.2 ml of 110 mM sodium citrate buffer, pH 7.4, and 0.75 ml of 25 mM Tris/HCl, pH 6.8, containing 0.35 M NaCl and 2.6 M glycine. The suspension was centrifuged at 3000 rpm for 45 min at room temperature. The pellet was discarded, while the supernatant was added with solid NaCl to a final concentration of 1.55 M. The suspension was stirred for 30 min and then centrifuged at 6000 rpm for 30 min at 25°C. The supernatant was discarded, and the pellet (derived from the 20 ml plasma pool) was dissolved in citrate buffer (1 ml), divided into aliquots and stored at −80°C. Finally, the solution was fractionated by size exclusion HPLC (SE-HPLC), using a TSK gel Super SW3000 column equilibrated with 20 mM phosphate buffer, 0.15 M NaCl, pH 7.4, at a flow rate of 0.2 ml/min. The fractions contained in the void volume were collected and analyzed by SDS/PAGE and western blot, using a polyclonal anti-VWF Ab (Dako). No contaminating protein was observed in the SDS-PAGE gel. The concentration of purified VWF was determined spectrophotometrically by measuring the absorbance value at 280 nm, using a molar absorption coefficient of 0.846 $mg^{-1} \cdot cm^2$, calculated on the amino acid sequence of VWF monomer. The quality of VWF preparations was also assessed by measuring VWF concentration as antigen (VWF:Ag) and RiCof (ristocetin cofactor) (VWF:RiCof), according to the immunoturbidometric assays 'VWF antigen' and 'VWF activity' (Instrumentation Laboratory), as detailed previously [5]. The purified VWF was concentrated with a Sartorius Vivaspin 500 centrifugal disposable ultrafiltration device at 14000 rpm in a Thermo microfuge and its carbonyl content measured as detailed above.

*Measurement of plasma VWF:ag, VWF:act, and ADAMTS13 level*

Blood samples were collected in 3.8% citrate and rapidly stored at -80 °C. VWF:ag in plasma was measured using HemosIL von Willebrand Factor Antigen latex immunoassay kits (HemosIL, Instrumentation Laboratory, Milano, Italy) with ACL TOP coagulation system analyzers (Instrumentation Laboratory, Milano, Italy). VWF activity (VWF:act) was measured with a ristocetin cofactor assay using lyophilized platelets (BC VWF reagent kit, Siemens, Milano, Italy) with a BCS coagulation system analyzer (Siemens). The lower limit of normal level for both VWF:ag and VWF:act is 54 IU/dL. The validated normal range of the VWF:act/VWF:ag ratio (n. 200 normal donors) was from 0.71 to 1.35, with mean at 0.98±0.34. ADAMTS13 protease activity (expressed as percentage of normal) was measured by a fluorescence resonance energy transfer based assay using a VWF86 amino-acid peptide substrate (Instrumentation Laboratory, Milano, Italy) in a Varian Eclipse spectrofluorimeter. ADAMTS-13 antigen was measured by an EIA assay (ADAMTS-13 antigen, Instrumentation Laboratory, Milano, Italy).

*Plasma VWF multimer analysis*

Plasma VWF multimers were analyzed by discontinuous (0.8-1.2%) SDS-agarose electrophoresis and western blotting, as previously described [5]. Images were acquired and analyzed using a ChemiDoc™ XRS+ system (Bio-Rad, Richmond, CA, USA). The quantitative evaluation of UL-VWF multimers, was performed using the method proposed by Udvardy et al. [14]. UL-VWF was defined as high molecular weight multimers (>10000 kDa), not observed in multimer pattern of plasma VWF from healthy subject. The identification of these high molecular weight forms was also facilitated by comparing the electrophoretic pattern of recombinant VWF, a generous gift of Dr. Friedrich Scheiflinger (Baxter Innovations GmbH, Vienna, Austria), which does not contain any proteolyzed VWF band and includes multimers with molecular weight >10000 kDa. In particular, the amount of UL-VWF multimers was expressed with the $M_{MW}$ parameter [14]. Digital images of the membranes were obtained by a ChemiDoc MP calibrated densitometer and processed by its QuantityOne software (Bio-Rad Laboratories, Richmond, CA, USA). The background density of the membrane image was subtracted coarsely in a protein-free area. The resulting density (RD) of each VWF peak against relative mobility (RM) data was used for subsequent computations. The $M_{MW}$ parameter assesses the degree of multimerization. First, a curve of RD against RM values was constructed. The upper 25% of the total area under the densitogram peaks was calculated. The molecular weight corresponding to the lower boundary of the 25% of densitometric area was used to

calculate the $M_{MW}$ parameter. The molecular weight corresponding to this RM ($M_{MW}$) was estimated based on the correlation of the VWF peaks mobility and their molecular weight, estimated as 500 kDa for a homodimer unit corresponding to the lowest band at the bottom of the gel in each lane [14].

*Hydrolysis by ADAMTS-13 of VWF purified from clinical samples*

Von Willebrand factor, purified as detailed above from clinical samples, was used in these functional experiments. In particular, two fractions with the highest VWF-bound carbonyls (380 and 230 pmol/mg, respectively) were pooled. Purified VWF from normal subjects (n=2, carbonyl=40 pmol/mg) was also used as a control. The working solution contained VWF preparations at a final concentration of 4 μg/ml and incubated with 5 nM recombinant ADAMTS-13 (final concentration, CHO-derived, gene sequence from Gln34 to Trp688, with a C-terminal 10 His tag, purchased from R&D Sytem, Space Import-Export srl, Milano, Italy) in 1.2 mg/ml ristocetin (sulfate-free, used to unfold VWF under static conditions) [15], 5 mM Tris–HCl, 3 mM $CaCl_2$, pH 8.0, at 37 °C. An aliquot (50 μl) of this solution was sampled at 0 and 60 min and the reaction stopped by adding 10 mM EDTA. Hydrolysis of the samples was assessed by SDS–agarose electrophoresis in a 1.5% agarose gel and western blot, as detailed above.

*Statistical analysis*

All the biochemical parameters contained in the electronic database were monitored for a previous period of 3-5 years. The values pertaining to the biochemical variables (e.g. HbA1c, triglycerides etc.) used in the statistical analyses were expressed as mean one standard deviation of the 4-5 values measured in the year preceding the enrolment visit. The values of the oxidation markers and haemostatic parameters measured during the study and used in the statistical analyses were the mean of two measurements taken in two different occasions over a time interval of seven days, starting from the enrolment visit. In all cases, the two values differed by less than 10%. Previous studies showed that VWF levels are proportional to CV risk and that values >150% are associated with significant odds risk for both acute myocardial infarction and stroke. Assuming a) an expected difference of at least 30% between the mean values of some parameters such as VWF levels and carbonyls pertaining to each class of patients and controls, and b) a standard error of parameters of interest within 10%, we calculated that, enrolling about 40 subject/arm, the potency of the study was >0.95 with $\alpha$=0.05. Continuous variables with a normal distribution, according to the Kolmogorov-Smirnov test, were compared by t-test with Welch's and Bonferroni's correction to avoid biases arising from unequal variance and Type 1 errors, while skewed ones were compared by Mann-Whitney U test. Categorical variables were compared by Pearson's chi-square test. Multivariable logistic regression models were used to assess the significance of covariate-adjusted associations between continuous haemostatic and oxidation biomarkers and occurrence of any form of thrombotic angiopathy. Thus, a multivariable logistic backward regression analysis was performed using the data pertaining to both T1- and T2-DM patients. In this multivariable model, the occurrence of any vascular complication (micro- or macroangiopathies) was analyzed as a function of fibrinogen, VWF:act and VWF-bound carbonyls. These covariates were age- and sex-adjusted in the analysis. In the final model, total plasma protein carbonyls and D-dimer were excluded as independent variable to avoid the bias of multicollinearity [16], as in univariate analysis their values were correlated with the level of VWF-bound carbonyls ($p<0.001$, see also Fig. 1) and fibrinogen ($p=0.037$). Values of measured variables were reported as mean ± standard deviation, unless otherwise indicated. A two-sided p value <0.05 was required for statistical significance. Analyses were performed using SPSS software (version 13, SPSS, Chicago, IL, USA). Graphpad Prism software (version 5.00 for Windows, GraphPad Software, San Diego, CA, USA) was used to construct appropriate graphs.

## Results

*Clinical and biochemical characteristics of type 1 and type 2 diabetic patients*

The main characteristics of both T1- and T2-DM patients compared to respective controls are listed in Tables 1-3. In particular, only HbA1c in T1-DM subjects had a significantly higher value than in control subjects (see Table 1). The activity of ADAMTS-13, although significantly lower than in control subjects (83% vs 110.7%), was in the normal range (see Table 3). On the contrary, T2-DM subjects, though having comparable disease duration compared to T1-DM patients, showed higher levels of HbA1c, BMI, triglycerides and creatinine, with lower glomerular filtration rates (see Tables 1-2). Likewise, coagulation parameters and the protein oxidation biomarker (fibrinogen, VWF:activity, VWF:antigen, d-dimers and protein carbonyls) were higher in T2-DM subjects than in the relative controls and T1-DM patients (see Table 3). T2-DM patients, like T1-DM subjects, had ADAMTS-13 activity in the normal range (94.9±37.1, Table 3). However, the ADAMTS-13/VWF:act ratio was lower in both T1- and T2-DM patients compared with their respective controls, whereas no statistically significant difference was observed between the two groups of diabetic patients (see Table 3). The decreased ADAMTS-13/VWF:act ratio is not of unequivocal interpretation in the presence of normal levels of both ADAMTS-13 and VWF, although the decrease of this derived parameter might reflect a situation less favorable to an efficient ADAMTS-13/VWF interaction. APTT and prothrombin time were in the normal range for both T1- and T2-DM patients. It has to be remarked that treatment with aspirin (100 mg/day) and statins was applied in 52% and 55% of T2-DM subjects, respectively (see Table 2). Notably, all patients with previous macro- and diffuse micro-angiopathy (retinopathy plus renal impairment) were under treatment with aspirin.

*Univariate analyses of clinical, biochemical and haemostatic variables measured in diabetic and control subjects*

Individual results of univariate analysis of clinical, biochemical and haemostatic variables measured in all diabetics and control subjects showed that the level of plasma protein carbonyls was significantly and positively correlated with age ($p=0.039$), APTT ($p<0.001$), fibrinogen ($p=0.002$), VWF:ag ($p<0.001$), VWF:act ($p=0.003$) and any form of micro- ($p<0.001$) and macroangiopathy ($p<0.001$). The strong association between carbonyls and VWF levels with micro- and macroangiopathies prompted us to investigate the specific content of carbonyls in VWF. The removal capacity in the chromatographic procedure of VWF purification was equal to 4.43 $\log_{10}$. As shown in Figure 1, the carbonyl content of VWF purified from T2-DM patients was positively and logistically correlated with the overall carbonyl content of the plasma proteins contained in the same sample. Thus, although VWF is a minor component of plasma proteins, nevertheless it is sensitive to oxidative stress and undergoes oxidative modifications as in the case of much more abundant proteins, such as albumin and fibrinogen [4]. The non linear equation used to analyze the relationship between plasma protein carbonyls and VWF-bound carbonyls (see legend to Fig. 1) allowed also to calculate the latter for all T2-DM samples.

*Comparison between carbonyl content of plasma proteins, VWF and ADAMTS-13 in diabetic patients with and without micro- and macroangiopathic complications*

In T2-DM with microangiopathic complications (either renal or retinal or both), only total plasma protein carbonyls (384±170 pmol/mg vs 270±110 pmol/mg $p=0.023$) and VWF-bound carbonyls (92±20 vs 35±8 pmol/mg, $p=0.022$) were found significantly increased compared with not microangiopathic patients (Figure 2). On the other hand, in T2-DM patients with thrombotic macroangiopathies, VWF:act, plasma protein carbonyls and VWF-bound carbonyls were significantly higher than in patients not affected from these complications ($p=0.023$, 0.032 and 0.028, respectively; see Figure 3). Notably, although the values of fibrinogen was higher in T2-DM than in both controls and T1-DM subjects, no difference was found for this parameter between patients with macroangiopathies compared to diabetics without these complications ($p= 0.98$). Finally, Table 4 reports the values of haemostatic and oxidation biomarkers of T2-DM patients

with and without any form (micro- and/or macro-) of angiopathy. Globally, these results show that in angiopathic diabetics, UL-VWF multimers are more expressed and that their oxidative modifications are higher than in not angiopathic patients. On this basis, a multivariate logistic backward regression analysis was performed using the data pertaining to both T1- and T2-DM patients. In the final model, VWF-bound carbonyl level, adjusted for age and sex, was the only variable significantly associated with the development of any form of vascular complication in diabetic patients (OR=28.2, 5-95% CI= 1.2–658, p= 0.038, see Table 5). Instead, no significant association was found for VWF:act and fibrinogen levels (p=0.511 and 0.362, respectively).

*Association of plasma protein carbonyls with multimer size in type 2 diabetes patients*

As indicated above, the mean value of plasma protein carbonyls in type 2 DM patients with macroangiopathies was found equal to 309±37 pmol/mg, whereas in patients without macroangiopathies the same parameter value was equal to 270±25 pmol/mg (p=0.0023). Accordingly, the VWF-bound carbonyl levels were equal to 82±20 pmol/mg in macroangiopathic patients and 33±9 pmol/mg in not macroangiopathic diabetics (p=0.028). VWF:act was equal to 177±16% and 132±12% in macroangiopathic and not macroangiopathic patients, respectively (p=0.032). These findings were in agreement with the hypothesis that VWF of T2-DM patients undergoes oxidative modifications and changes its activity pattern. Hence, we investigated whether or not there was a relationship between the level of VWF-bound carbonyls and the amount of UL-VWF. This was the case, as shown by gels of SDS-agarose electrophoresis of VWF multimers. Figure 4 shows examples of typical cases of T2-DM patients with and without micro-and macro-angiopathies and VWF-bound carbonyls >100 pmol/mg. Under the experimental conditions used in the electrophoretic run, large VWF multimers were not resolved into single bands, but appeared as “smear” at the top of the gel. However, this feature was never present in the respective controls and diabetic patients without angiopathic complications, although the loaded VWF amount was the same. A positive linear association was found between VWF-bound carbonyls and the presence of UL-VWF, reflected by the $M_{MW}$ parameter (see Figure 5). Notably, this relationship was found in samples characterized by high carbonyl content of VWF (>100 pmol/mg) and occurrence of severe macrovascular complications. In this subset of T2-DM patients, no statistically significant difference was found between the patients with and without macrovascular complications for age (p=0.454), disease duration (p=0.347) and HbA1c levels (p=0.658).

*Hydrolysis by ADAMTS-13 of purified VWF samples from T2-DM and control subjects*

The results of the functional experiments testing the ability of ADAMTS-13 to proteolyze VWF purified from T2-DM and control subjects are shown in Fig. 6. The velocity of VWF hydrolysis was significantly lower in the case of VWF factor containing high level of carbonyl group (300 pmol/mg), compared to control VWF containing low amount of carbonyls (40 pmol/mg). After 60 min of incubation, VWF purified from normal controls was extensively hydrolyzed, whereas VWF with high oxidation status from T2-DM patients still contained VWF multimers with medium molecular weight.

## Discussion

The main novelty of this study is that not only the level but also the oxidative modification of VWF is strongly associated with both presence of high molecular weight multimers and thrombotic angiopathies in diabetes. Hyperglycemia is known to promote ROS production and impairment of antioxidant systems, such as generation of the reduced form of glutathione (GSH) and vitamin C [8,17,18]. Oxidative stress is involved in the pathogenesis of endothelial dysfunction (ED), which promotes a global prothrombotic and antifibrinolytic status [8]. ED plays a central role in the pathogenesis of atherosclerosis and its presence has been documented in patients with diabetes mellitus [19]. The occurrence of ED is associated with the elevation of several markers such as VWF, endothelin-1 (ET-1), vascular endothelial growth factor and vascular cell adhesion molecule-1. In particular, increased ET-1 and VWF levels were found in type 1 and type 2 diabetes patients [20,21]. Notably, in the Munich General Practitioner Project [22] and in the ARIC

study [23], increased levels of VWF:ag were identified as risk factors for macrovascular prevalence and mortality in type 2 diabetes. It is likely that oxidative stress is associated in type 2 diabetic patients with a systemic inflammatory status characterized by increased levels of cytokines as IL6 and TNF-α [24]. These inflammatory cytokines promote the release of VWF from endothelial cells and induce a defect of VWF proteolytic processing by ADAMTS-13 [25]. These effects may cause an increase of both level and size of VWF multimers, expressed by VWF:act. In this investigation, only a slight decrease of ADAMTS-13 level was found in diabetics, in agreement with previous reports [26,27]. However, only in the presence of severe ADAMTS-13 deficiency (level<6%), ultra-large VWF multimers accumulate, causing thrombotic microangiopathies [28]. Large VWF multimers are stored in the Weibel-Palade bodies (WPB) of endothelial cells (ECs) and are released into the bloodstream upon the interaction of several agonists with the respective receptors on ECs. A change in intracellular ROS can activate signal transduction pathways [29], driving in ECs the actin cytoskeleton assembly [30] and WPB mobilization. Hence, the increase of ROS production in diabetes can accelerate the secretion of VWF multimers from endothelial WPB, favoring the release of large VWF multimers (UL-VWF) into the circulation, as indeed shown in this study. The level of carbonyl content of purified VWF was found proportional to the same parameter measured in plasma proteins from diabetic patients. This phenomenon may arise in vivo from the exposure of VWF to oxidizing agents, as peroxynitrite, during the period of storage in the WPB of endothelial cells. In line with this hypothesis, our research group has recently demonstrated the specific oxidation of Met1606 in VWF purified from samples of patients with chronic kidney disease, another setting characterized by high oxidative stress [6]. A significant portion of the type 2 diabetes patients enrolled in this study was affected by diabetic nephropathy (see Table 2). This condition may have contributed to increase the oxidative stress, reflected by high levels of plasma protein carbonyls. However, it has to be remarked that the in our previous study, the oxidation of VWF was found elevated in patients with chronic renal failure under hemodialysis [6]. In the present study, the diabetic patients were characterized only by mild or moderate reduction of glomerular filtration rate, but none of them was under haemodialysis. Further studies are under way by our research group to investigate the possible presence and effects of oxidative stress on VWF in not diabetic patients with mild/moderate renal failure. Our research group and other investigators have shown that specific oxidation of Met1606 in VWF inhibits its proteolytic processing by ADAMTS-13 [5,7,31]. In particular, this effect was demonstrated in VWF purified from plasma of severe T2-DM patients [6].This mechanism may further contribute to favor the accumulation in the circulation of UL-VWF multimers, which have the highest pro-thrombotic activity. Previous studies showed indeed that UL-VWF multimers are present in severe type 2 diabetic patients with very high carbonyl content in VWF [5]. In the present study, we have investigated a larger and more representative diabetic population, in which the presence of UL-VWF multimers was found associated with occurrence of micro- and macro-angiopathic complications. The increased presence of UL-VWF multimers could not be attributed to ADAMTS-13 deficiency. In this clinical setting, ADAMTS-13 is present at a normal level (see Table 3), sufficient to proteolyze in part UL-VWF multimers, at variance with the situation observed in canonical forms of thrombotic microangiopathies, where ADAMTS-13 is <6%. In a subset of type 2 diabetes patients, we have indeed shown that the setting characterized by VWF-bound carbonyls >50 pmol/mg is significantly associated with micro- and macro-angiopathies. In a multivariate analysis, the level of VWF-bound carbonyls was the only parameter significantly associated in both T1- and T2-DM with occurrence of any kind of vascular complication with an OR equal to ≈28 ($p=0.038$). This finding supports the hypothesis that, beside the level, also the oxidation status and the multimeric pattern of this protein are associated with thrombotic vasculopathies. Recently, in an elegant study, Fu et al. have demonstrated that shear stress–induced unfolding of VWF exposes buried, oxidation-sensitive methionine residues, including Met1606, contained in the A1 and A2 VWF domain [32]. Conversion into methionine sulfoxide of these Met residues, buried in the coiled VWF conformation, is strongly facilitated by shear stress–induced unfolding of VWF multimers. Notably, methionine oxidation, besides reduced proteolysis by ADAMTS-13, results also in enhanced VWF binding to GpIb and platelet activation [5,32]. In addition, basic biophysical principles indicate that the higher the molecular size of the VWF, the higher is the sensitivity to shear stress [33]. Several studies have provided compelling evidence of the relevance of VWF levels in the pathogenesis of macrovascular thrombosis, especially in the brain circulation [34-36]. The findings of the present study emphasize also the relevance of the multimeric structure and especially of the oxidation status of VWF multimers, for their pro-thrombotic effects. This phenomenon, along with the documented intrinsic hyperactivity of platelets in type 2 diabetic patients [37,38], can contribute to intensify adhesion, activation, and aggregation of platelets,

favoring the occurrence of thrombotic complications in the arterial circulation. VWF has also other extra-haemostatic functions, including angiogenesis and leukocyte extravasation [39,40], which can cooperate in inducing thrombotic events. The effect of VWF oxidation on these biological functions is still unknown and needs to be investigated to assess its possible contribution to these phenomena. This study has several clinical implications and limits. The results of this pilot study would indicate the need of prospective and intervention studies on diabetic population to correlate the progression of oxidative modification of VWF with major adverse cardiovascular events and their pharmacological prevention. The use of aspirin for the primary prevention of cardiovascular events in diabetic individuals is a widely recommended practice in accordance with existing guidelines [41]. However, several prospective trials have shown that in diabetic patients, this drug shows a lower efficacy in protecting against thrombotic macroangiopathies than in not diabetic subjects [42-44]. This is likely a multifactorial phenomenon. However, it can be speculated that the lower pharmacological efficacy may be in part linked to lack of specificity of aspirin in inhibiting the VWF-platelet receptor interaction and signaling [45]. The use of novel anti-platelet agents as the inhibitors of the VWF-GpIb interaction [46-49] may ameliorate the outcome of antithrombotic therapy in T2-DM patients. Prospective studies are needed to assess whether the association of oxidative stress and VWF abnormalities is only a sustained epiphenomenon of thrombotic diseases or is causally related to macroangiopathic complications in diabetic patients. This conclusion cannot be unequivocally validated by the present study, since it is based on a post hoc analysis. Further work on the specificity and sensitivity of VWF:act and VWF-bound carbonyl level is therefore required to ascertain their role as prognostic biomarkers for thrombotic vasculopathies in type 2 diabetes mellitus. Even without a specific quantification of VWF-bound carbonyls, the measurement of overall level of carbonyls of plasma proteins may be used as a surrogate marker of oxidative modification of VWF, as shown in the present study. In conclusion, the emerging scenario shows that the oxidative stress in diabetes involves also VWF and is associated with increased presence of UL-VWF multimers that are involved in the genesis of major cardiovascular events in this clinical setting.

**Acknowledgments**: RDC thanks prof. V. De Filippis (University of Padua, Italy) for valuable suggestions and scientific discussions. The generous gift of recombinant VWF by Dr. Friedrich Scheiflinger (Baxter Innovations GmbH, Vienna, Austria) is gratefully acknowledged.

## References

1. Brownlee M (2005) The pathobiology of diabetic complications: a unifying mechanism. Diabetes 54: 1615-1625.
2. Lewis P, Stefanovic N, Pete J, Calkin AC, Giunti S, et al. (2007) Lack of the antioxidant enzyme glutathione peroxidase-1 accelerates atherosclerosis in diabetic apolipoprotein E-deficient mice. Circulation 115: 2178-2187.
3. Leopold JA, Loscalzo J (2009) Oxidative risk for atherothrombotic cardiovascular disease. Free Radic Biol Med 47: 1673-1706.
4. Parastatidis I, Thomson L, Burke A, Chernysh I, Nagaswami C, et al. (2008) Fibrinogen beta-chain tyrosine nitration is a prothrombotic risk factor. J Biol Chem 283: 33846-33853.
5. Lancellotti S, De Filippis V, Pozzi N, Peyvandi F, Palla R, et al. (2010) Formation of methionine sulfoxide by peroxynitrite at position 1606 of von Willebrand factor inhibits its cleavage by ADAMTS-13: A new prothrombotic mechanism in diseases associated with oxidative stress. Free Radic Biol Med 48: 446-456.
6. De Filippis V, Lancellotti S, Maset F, Spolaore B, Pozzi N, et al. (2012) Oxidation of Met1606 in von Willebrand factor is a risk factor for thrombotic and septic complications in chronic renal failure. Biochem J 442: 423-432.
7. Chen J, Fu X, Wang Y, Ling M, McMullen B, et al. (2011) Oxidative modification of von Willebrand factor by neutrophil oxidants inhibits its cleavage by ADAMTS13. Blood 115: 706-712.
8. Giacco F, Brownlee M (2010) Oxidative stress and diabetic complications. Circ Res 107: 1058-1070.

9. Mancia G, De Backer G, Dominiczak A, Cifkova R, Fagard R, et al. (2007) 2007 Guidelines for the management of arterial hypertension: The Task Force for the Management of Arterial Hypertension of the European Society of Hypertension (ESH) and of the European Society of Cardiology (ESC). Eur Heart J 28: 1462-1536.
10. Kemperman FA, Krediet RT, Arisz L (2002) Formula-derived prediction of the glomerular filtration rate from plasma creatinine concentration. Nephron 91: 547-558.
11. Stephenson JM, Fuller JH, Viberti GC, Sjolie AK, Navalesi R (1995) Blood pressure, retinopathy and urinary albumin excretion in IDDM: the EURODIAB IDDM Complications Study. Diabetologia 38: 599-603.
12. van Schooten CJ, Denis CV, Lisman T, Eikenboom JC, Leebeek FW, et al. (2007) Variations in glycosylation of von Willebrand factor with O-linked sialylated T antigen are associated with its plasma levels. Blood 109: 2430-2437.
13. Stadtman ER, Levine RL (2000) Protein oxidation. Ann N Y Acad Sci 899: 191-208.
14. Udvardy ML, Szekeres-Csiki K, Harsfalvi J (2009) Novel evaluation method for densitometric curves of von Willebrand factor multimers and a new parameter (M(MW)) to describe the degree of multimersation. Thromb Haemost 102: 412-417.
15. De Cristofaro R, Peyvandi F, Palla R, Lavoretano S, Lombardi R, et al. (2005) Role of chloride ions in modulation of the interaction between von Willebrand factor and ADAMTS-13. J Biol Chem 280: 23295-23302.
16. Katz M (2011) Multivariable Analysis. A Practical Guide for Clinicians and Public Health Researchers. Cambridge, UK: Cambridge University Press. 89 p.
17. Sinclair AJ, Taylor PB, Lunec J, Girling AJ, Barnett AH (1994) Low plasma ascorbate levels in patients with type 2 diabetes mellitus consuming adequate dietary vitamin C. Diabet Med 11: 893-898.
18. Gandhi CR, Roy Chowdhury D (1979) Effect of diabetes mellitus on sialic acid & glutathione content of human erythrocytes of different ages. Indian J Exp Biol 17: 585-587.
19. Avogaro A, Albiero M, Menegazzo L, de Kreutzenberg S, Fadini GP (2011) Endothelial dysfunction in diabetes: the role of reparatory mechanisms. Diabetes Care 34 Suppl 2: S285-290.
20. Morise T, Takeuchi Y, Kawano M, Koni I, Takeda R (1995) Increased plasma levels of immunoreactive endothelin and von Willebrand factor in NIDDM patients. Diabetes Care 18: 87-89.
21. Seligman BG, Biolo A, Polanczyk CA, Gross JL, Clausell N (2000) Increased plasma levels of endothelin 1 and von Willebrand factor in patients with type 2 diabetes and dyslipidemia. Diabetes Care 23: 1395-1400.
22. Standl E, Balletshofer B, Dahl B, Weichenhain B, Stiegler H, et al. (1996) Predictors of 10-year macrovascular and overall mortality in patients with NIDDM: the Munich General Practitioner Project. Diabetologia 39: 1540-1545.
23. Adeniyi A, Folsom AR, Brancati FL, Desvorieux M, Pankow JS, et al. (2002) Incidence and risk factors for cardiovascular disease in African Americans with diabetes: the Atherosclerosis Risk in Communities (ARIC) study. J Natl Med Assoc 94: 1025-1035.
24. Hajer GR, van Haeften TW, Visseren FL (2008) Adipose tissue dysfunction in obesity, diabetes, and vascular diseases. Eur Heart J 29: 2959-2971.
25. Bernardo A, Ball C, Nolasco L, Moake JF, Dong JF (2004) Effects of inflammatory cytokines on the release and cleavage of the endothelial cell-derived ultralarge von Willebrand factor multimers under flow. Blood 104: 100-106.
26. Skeppholm M, Kallner A, Kalani M, Jorneskog G, Blomback M, et al. (2009) ADAMTS13 and von Willebrand factor concentrations in patients with diabetes mellitus. Blood Coagul Fibrinolysis 20: 619-626.
27. Taniguchi S, Hashiguchi T, Ono T, Takenouchi K, Nakayama K, et al. (2010) Association between reduced ADAMTS13 and diabetic nephropathy. Thromb Res 125: e310-316.
28. George JN (2006) Clinical practice. Thrombotic thrombocytopenic purpura. N Engl J Med 354: 1927-1935.
29. Suzukawa K, Miura K, Mitsushita J, Resau J, Hirose K, et al. (2000) Nerve growth factor-induced neuronal differentiation requires generation of Rac1-regulated reactive oxygen species. J Biol Chem 275: 13175-13178.

30. Vepa S, Scribner WM, Parinandi NL, English D, Garcia JG, et al. (1999) Hydrogen peroxide stimulates tyrosine phosphorylation of focal adhesion kinase in vascular endothelial cells. Am J Physiol 277: L150-158.
31. Pozzi N, Lancellotti S, De Cristofaro R, De Filippis V (2012) Modeling ADAMTS13-von Willebrand factor interaction: Implications for oxidative stress-related cardiovascular diseases and type 2A von Willebrand disease. Biophys Chem 160: 1-11.
32. Fu X, Chen J, Gallagher R, Zheng Y, Chung DW, et al. (2011) Shear stress-induced unfolding of VWF accelerates oxidation of key methionine residues in the A1A2A3 region. Blood 118: 5283-5291.
33. Di Stasio E, De Cristofaro R (2010) The effect of shear stress on protein conformation: Physical forces operating on biochemical systems: The case of von Willebrand factor. Biophys Chem 153: 1-8.
34. van Schie MC, Wieberdink RG, Koudstaal PJ, Hofman A, Ikram MA, et al. (2012) Genetic Determinants of Von Willebrand Factor Plasma Levels and the Risk of Stroke: The Rotterdam Study. J Thromb Haemost 10: 550-556.
35. Frankel DS, Meigs JB, Massaro JM, Wilson PW, O'Donnell CJ, et al. (2008) Von Willebrand factor, type 2 diabetes mellitus, and risk of cardiovascular disease: the framingham offspring study. Circulation 118: 2533-2539.
36. De Meyer SF, Stoll G, Wagner DD, Kleinschnitz C (2012) Von Willebrand factor: an emerging target in stroke therapy. Stroke 43: 599-606.
37. Ferreiro JL, Angiolillo DJ (2011) Diabetes and antiplatelet therapy in acute coronary syndrome. Circulation 123: 798-813.
38. Vera RH, Vilahur G, Ferrer-Lorente R, Pena E, Badimon L (2012) Platelets Derived From the Bone Marrow of Diabetic Animals Show Dysregulated Endoplasmic Reticulum Stress Proteins That Contribute to Increased Thrombosis. Arterioscler Thromb Vasc Biol 32: 2141-2148.
39. Starke RD, Ferraro F, Paschalaki KE, Dryden NH, McKinnon TA, et al. (2011) Endothelial von Willebrand factor regulates angiogenesis. Blood 117: 1071-1080.
40. Petri B, Broermann A, Li H, Khandoga AG, Zarbock A, et al. (2010) von Willebrand factor promotes leukocyte extravasation. Blood 116: 4712-4719.
41. Nicolucci A, De Berardis G, Sacco M, Tognoni G (2007) AHA/ADA vs. ESC/EASD recommendations on aspirin as a primary prevention strategy in people with diabetes: how the same data generate divergent conclusions. Eur Heart J 28: 1925-1927.
42. Ridker PM, Cook NR, Lee IM, Gordon D, Gaziano JM, et al. (2005) A randomized trial of low-dose aspirin in the primary prevention of cardiovascular disease in women. N Engl J Med 352: 1293-1304.
43. Ogawa H, Nakayama M, Morimoto T, Uemura S, Kanauchi M, et al. (2008) Low-dose aspirin for primary prevention of atherosclerotic events in patients with type 2 diabetes: a randomized controlled trial. Jama 300: 2134-2141.
44. Belch J, MacCuish A, Campbell I, Cobbe S, Taylor R, et al. (2008) The prevention of progression of arterial disease and diabetes (POPADAD) trial: factorial randomised placebo controlled trial of aspirin and antioxidants in patients with diabetes and asymptomatic peripheral arterial disease. BMJ 337: a1840.
45. Hawiger J (1991) Adhesive interactions of platelets and their blockade. Ann N Y Acad Sci 614: 270-278.
46. Gilbert JC, DeFeo-Fraulini T, Hutabarat RM, Horvath CJ, Merlino PG, et al. (2007) First-in-human evaluation of anti von Willebrand factor therapeutic aptamer ARC1779 in healthy volunteers. Circulation 116: 2678-2686.
47. Ulrichts H, Silence K, Schoolmeester A, de Jaegere P, Rossenu S, et al. (2011) Antithrombotic drug candidate ALX-0081 shows superior preclinical efficacy and safety compared with currently marketed antiplatelet drugs. Blood 118: 757-765.
48. Markus HS, McCollum C, Imray C, Goulder MA, Gilbert J, et al. (2011) The von Willebrand inhibitor ARC1779 reduces cerebral embolization after carotid endarterectomy: a randomized trial. Stroke 42: 2149-2153.
49. Navarrete AM, Casari C, Legendre P, Marx I, Hu JR, et al. (2012) A murine model to characterize the anti thrombotic effect of molecules targeting human von Willebrand factor. Blood 120: 2723-2732.

**Table 1**

**Clinical and biochemical characteristics of T1- , T2-DM patients and respective controls**

| Parameter | T1-DM (n =41) | Controls for T1-DM patients (n = 41) | P* | T2-DM (n = 42) | Controls for T2-DM patients (n = 42) | P* | P** |
|---|---|---|---|---|---|---|---|
| Age (yrs) | 41±14[§] | 42±13 | 0.66 | 63.8 ±9.9 | 59.9 ±11.9 | 0.106 | **<0.001** |
| Sex (M/F) | 16/19 | 15/20 | 0.92 | 19/23 | 29/13 | 0.71 | 0.456 |
| Disease duration (yrs) | 21.4 ±10.3 | null | n.a. | 18 ±12 | null | n.a. | 0.303 |
| BMI | 27.2±2.1 | 27 ±2 | 0.23 | **28 ±4** | **25 ±1.7** | **<0.001** | 0.67 |
| **HbA1c (%)*** | **7.6 ±1.1** | **5.1±10.4** | **<0.001** | **7.7 ±1.2** | **5.1 ±0.4** | **<0.001** | 0.134 |
| Cholesterol total (mg/dl) | 184±29 | 179 ±30 | 0.49 | 170±37 | 167±35 | 0.704 | 0.234 |
| Cholesterol (HDL) (mg/dl) | 60±11 | 52±10 | 0.16 | **46±10** | **58±11** | **0.065** | **0.026** |
| Cholesterol (LDL) (mg/dl) | 108±27 | 106±29 | 0.55 | 101±38 | 103±37 | 0.6 | 0.12 |
| Triglycerides (mg/dl) | 85±148 | 83±29 | 0.87 | **133±50** | **86 ±30** | **<0.001** | **<0.001** |
| Blood group “0” vs “non-0” | 37% vs 63% | 37% vs 63% | n.a. | 38% vs. 62% | 38% vs. 62% | n.a. | 0.987 |

Legend: § The values of mean±SD are listed;
* Comparison with respective controls;
**Comparison between type 1 and type 2 patients.
The parameters with significantly different ($p<0.05$) values are listed in bold

**Table 2**

**Biochemical characteristics and therapy of T1- and T2-DM patients and respective controls**

| Parameter | T1-DM (n =41) | Control subjects for T1-DM patients (n = 41) | P* | T2-DM (n = 42) | Control for T2-DM patients (n = 42) | P* | P** |
|---|---|---|---|---|---|---|---|
| **Hypertension** | 9/41 (22.9%) | null | n.a. | 29/42 (59.5%) | Null | n.a. | **<0.001** |
| **Creatinine (mg/dl)** | **1.04±0.17** | **0.93±0.1** | **0.002** | **2.4±2.3** | **0.9±0.3** | **<0.001** | **<0.001** |
| Microalbuminuria (mg/L, v.n. <25 mg/L) | 12±16 | 6±2 | n.a. | **145±240** | **15±10** | **<0.001** | **<0.001** |
| GFR calculated ($ml/m^2$ min) | 88±16 | 90±18 | 0.592 | **51±25** | **85±16** | **<0.001** | **<0.001** |
| **Macroangiopathies (AMI. Stroke, PAD)** | **3/41 (7%)** | null | n.a. | **21/42 (50%)** | null | n.a. | **<0.001** |
| **Therapy:** | | | | | | | |
| **Oral hypoglycemic** | **12/41(29%)** | Null | n.a. | **26/42 (62%)** | Null | n.a. | **<0.001** |
| **Insulin** | **41/41(100%)** | Null | n.a. | **10/42 (24%)** | Null | n.a. | **<0.001** |
| **Anti-hypertensive (ACE inhibitors)** | **6/42 (14%)** | Null | n.a. | **21/42 (50%)** | Null | n.a. | **<0.001** |
| **Statins** | **6/42 (14%)** | Null | n.a. | **23/42 (55%)** | Null | n.a. | **<0.001** |
| **Aspirin** | **4/42 (10%)** | null | n.a. | **22/42(52%)** | Null | n.a. | **<0.001** |

Legend: § The values of mean±SD are listed;
* Comparison with respective controls;
** Comparison between type 1 and type 2 patients.
The parameters with significantly different ($p<0.05$) values are listed in bold

**Table 3**

**Haemostatic and oxidative biomarker levels in T1- and T2-DM patients and respective controls**

| Parameter | T1-DM (n =41) | Controls for T1-DM patients (n =41) | P* | T2-DM (n = 42) | Controls for T2-DM patients (n =42) | P* | P** |
|---|---|---|---|---|---|---|---|
| Fibrinogen (mg/dl) | 250±31[§] | 245±34 | 0.546 | **352±118** | **264±50** | **<0.001** | **0.0169** |
| D-dimer | 196±187 | 160±57 | 0.289 | **306±243** | **171±59** | **<0.001** | **0.0008** |
| VWF:ag (%) | 110±42 | 108±24 | 0.789 | **165±65** | **115±26** | **<0.001** | **<0.001** |
| VWF:act (%) | 108±41 | 97±18 | 0.156 | **148±72** | **102±22** | **<0.001** | **0.0056** |
| VWF-R (Act/Ag) | 0.92±0.2 | 0.91±0.1 | 0.051 | 0.94±0.5 | 0.9 ±0.13 | 0.618 | 0.589 |
| ADAMTS13 antigen (ng/ml) | 595±157 | 629±143 | 0.292 | 592±198 | 589±185 | 0.936 | 0.976 |
| **ADAMTS-13 activity (%)** | **83±21** | **111±25** | **<0.001** | 95±37 | 100±32 | 0.8243 | 0.332 |
| **ADAMTS13 / VWF:act ratio** | **0.8±0.5** | **1.14±0.5** | **0.038** | **0.6±0.5** | **0.98±0.5** | **0.021** | 0.214 |
| Log $M_{MW}$ | 6.1±0.7 | 6.1±0.6 | 0.63 | **7.3±0.8** | **6.2±0.7** | **0.0062** | **0.0065** |
| Protein carbonyls (pmol/mg) | 167±9 | 140±13 | 0.35 | **340±170** | **128±7** | **<0.001** | **<0.001** |

§ The values of mean±SD are listed in the table

**Table 4**

**Haemostatic and oxidative biomarker parameters of T2-DM patients with and without any form of angiopathies**

| Parameter | T2-DM<br>No angiopathies<br>(n =20) | T2-DM<br>With angiopathies<br>(n =22) | P<br>(two-tailed) |
|---|---|---|---|
| Fibrinogen (mg/dl) | 251±77[§] | 392±107 | 0.0023 |
| D-dimer | 227±133 | 378±297 | 0.043 |
| VWF:ag (%) | 145±54 | 182±71 | 0.061 |
| VWF:act (%) | 132±75 | 193±68 | 0.022 |
| ADAMTS-13 activity (%) | 66±34 | 111±28 | 0.0005 |
| Log $M_{MW}$ | 6.1±0.6 | 7.4±1.3 | 0.0002 |
| Protein carbonyls (pmol/mg) | 312±80 | 370±100 | 0.035 |
| VWF-bound carbonyls (pmol/mg) | 182±134 | 364±205 | 0.002 |

§ The values of mean±SD are listed in the table

**Table 5**

**Multivariable-adjusted* logistic regression for thrombotic angiopathies with haemostatic and oxidation variables in T1- and T2-DM patients (n=83)**

| Variables | OR (5-95% confidence interval) | | P |
|---|---|---|---|
| VWF-bound carbonyls | 28.2 | (1.2–658) | 0.038 |
| VWF:act | 1.003 | (0.995-1.011) | 0.511 |
| Fibrinogen | 1.003 | (0.997-1.008) | 0.362 |

* Adjusted for age and sex

## Figure legends

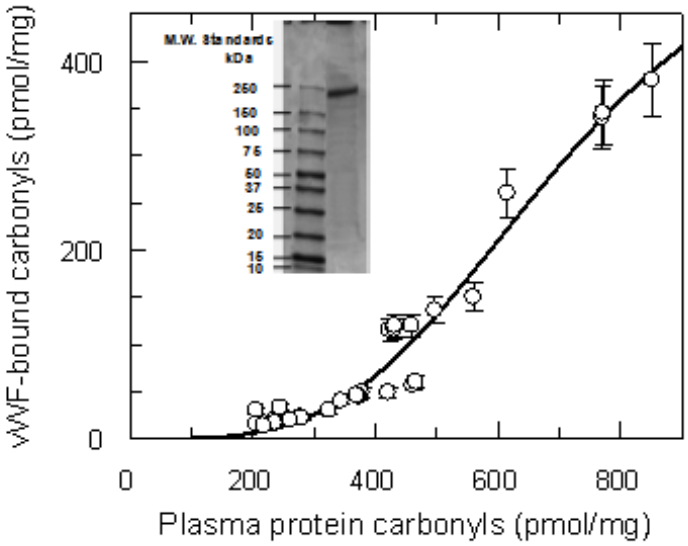


**Figure 1**

**Figure 1. Correlation between total carbonyl content of plasma proteins and that of VWF purified from plasma samples of type 2 diabetes patients**. The continuous line was drawn according to this phenomenological equation $VWF_{carb} = (VWF_{carb})_{max} \times (P_{carb})_h / (P_{50h} + P_{carbh})$, where $(VWF_{carb})_{max}$ is the asymptotic value of VWF carbonyls (best fit value: 587±146 pmol/mg), $P_{carb}$ is the carbonyl content of plasma proteins, h is an exponential parameter (best fit= 3.6±0.6) and $P_{50}$ is the concentration of plasma proteins carbonyls equal to $(VWF_{carb})_{max}/2$ (best fit: 706±107 pmol/mg). The vertical bars are the standard errors. In the inset, the SDS-PAGE gel (4-12%) of the purified and reduced VWF preparation is shown. On the left the molecular weight standards are also shown.

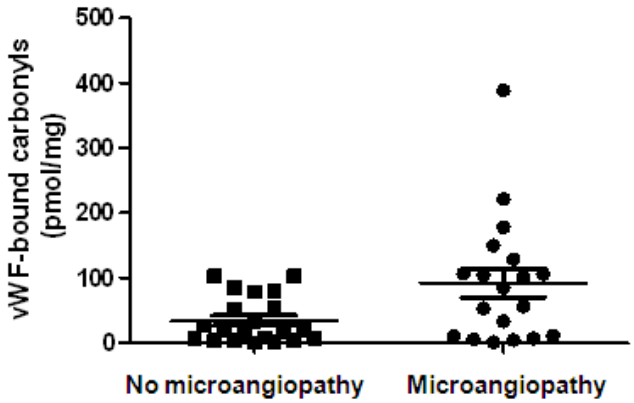


**Figure 2**

**Figure 2. Statistical comparison between calculated VWF-bound-carbonyl levels in type 2 diabetic patients with and without microangiopathic complications (renal and retinal).** According to Mann-Whitney test, VWF-bound carbonyls had higher values in microangiopathic subjects than in non macroangiopathic diabetics (mean values ± SD: 92±22 vs 35±8 pmol/mg, respectively, p=0.022).

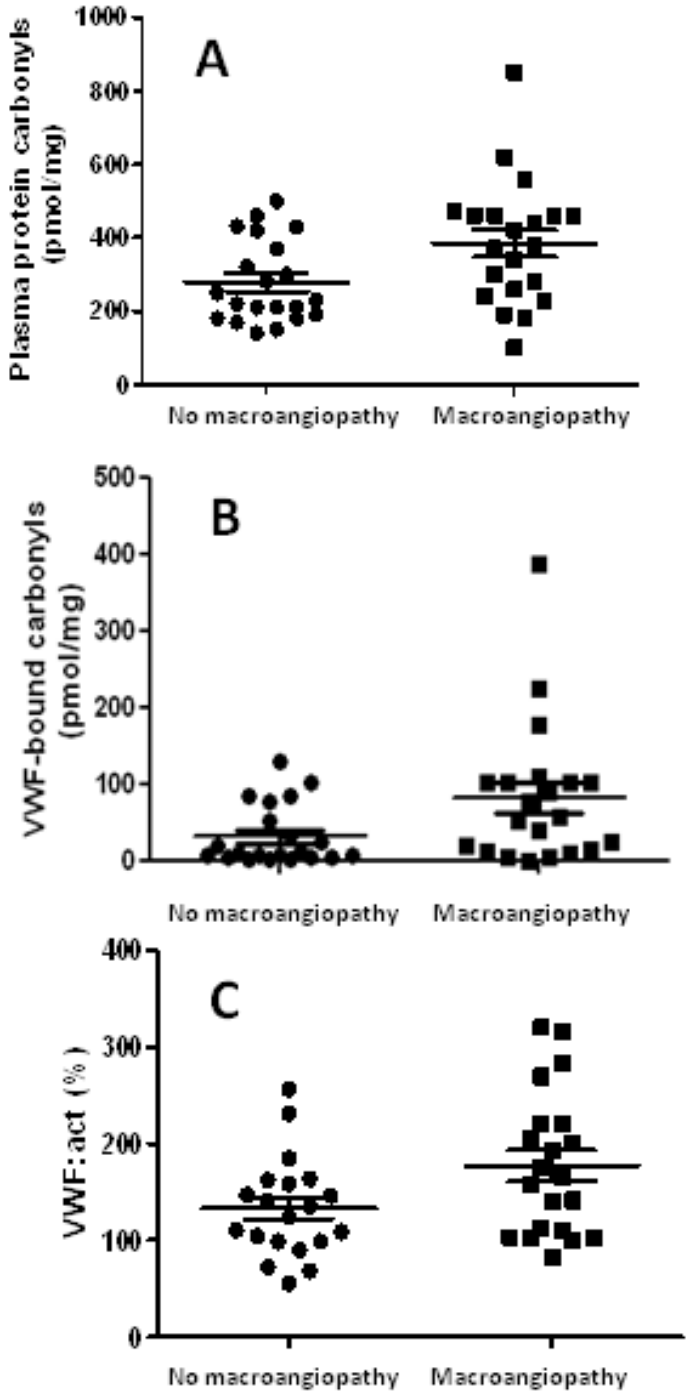


**Figure 3**

**Figure 3. Statistical comparison between (A) carbonyl content of plasma proteins, (B) VWF-bound carbonyls and (C) VWF:act in type 2 diabetic patients with and without macroangiopathies (AMI, stroke and PAD).** According to Mann-Whitney test, these parameters showed higher values in macroangiopathic s than in non macroangiopathic diabetics (mean values ± SD**:** 380±37 pmol/mg vs 270±25 pmol/mg, p=0.0234, 82±20 vs 33±9 pmol/mg, p=0.028 and 177±16% vs 132±12%, p=0.032, respectively.

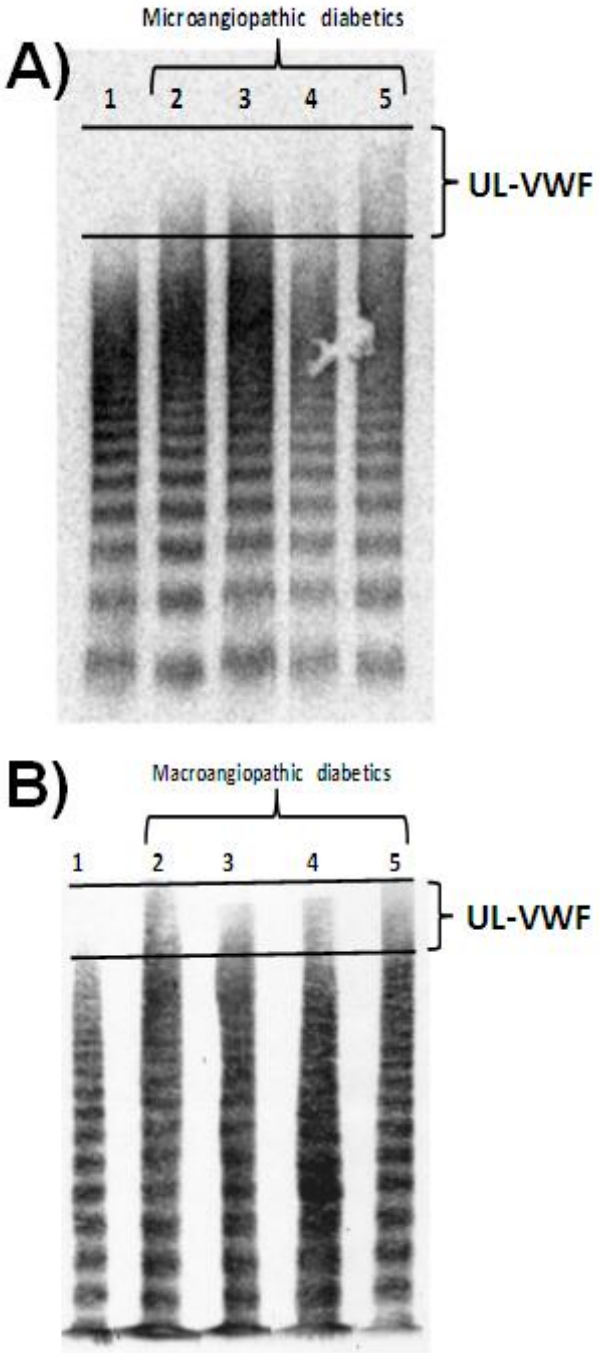


**Figure 4**

**Figure 4. Comparison of SDS-agarose gel electrophoresis and western blot of VWF multimers between type 2 diabetic patients with low VWF-bound carbonyls without microangiopathy and and those with high levels of VWF-bound carbonyls and several forms of microangiopathies.**
**A)** SDS-agarose gel electrophoresis and western blot of VWF multimers from a pool (n=10) of type 2 diabetic patients without microangiopathy and low VWF-bound carbonyls (<50 pmol/mg) (1) and with high levels of VWF-bound carbonyls (>100 pmol/mg) and several forms of microangiopathies (2: nefropathy; 3: nefropathy + grade 3 retinopathy; 4: nefropathy + retinopathy + autonomic neuropathy; 5: nefropathy + grade 3 retinopathy; autonomic neuropathy + coronary microangiopathy). The agarose gel was discontinuous (0.4% agarose in stacking gel and 1.2 % agarose in running gel. The amount of loaded VWF was similar in all samples (about 2 μg). **B)** SDS-agarose gel electrophoresis and western blot of VWF multimers from type 2 diabetic patients without macroangiopathy (1) and with several forms of macroangiopathies (2-4: coronaropathy; 5: coronaropathy + PAD). The presence of UL-VWF in samples is indicated between the dashed lines.

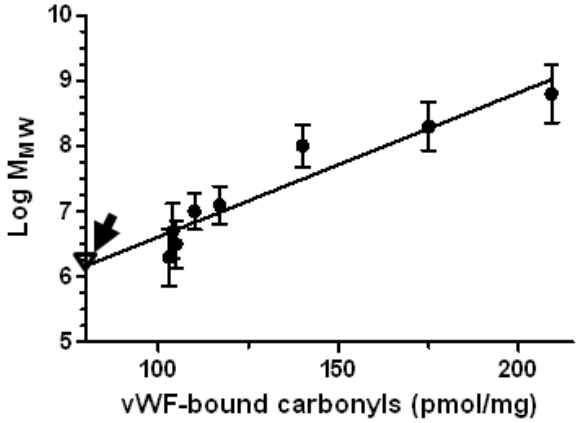


**Figure 5**

**Figure 5. Association of carbonyl content of purified VWF with the $M_{MW}$ parameter for T2-DM patients with macrovascular complications**. The continuous line represents the linear regression ($R^2$=0.908, p=0.0002). The arrow shows the mean value of the parameter in age- and sex- matched healthy controls ($M_{MW}$ =6.2±0.7), all having carbonyl content of VWF<20 pmol/mg (Δ). Notably, all the patients with VWF-bound carbonyls>100 pmol/mg suffered from both micro- and macrovascular complications.

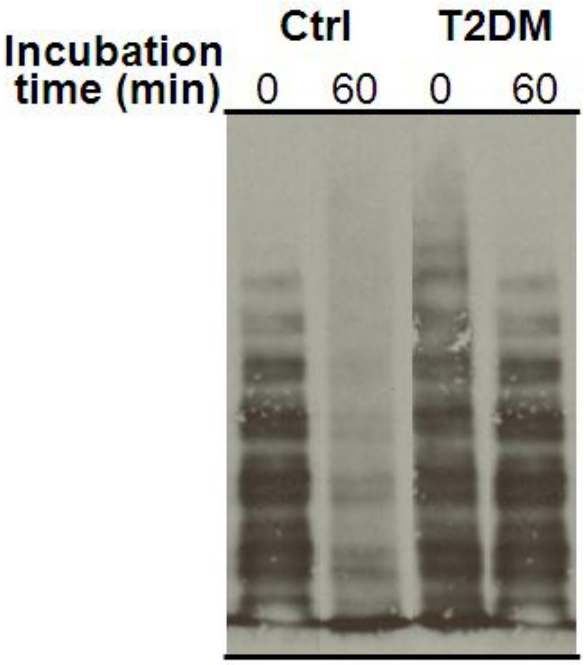


**Figure 6**

**Figure 6. Cleavage by ADAMTS-13 of VWF multimers in a pool obtained from two T2-DM patients and two healthy subjects (Ctrl).** Purified VWF multimers were digested by 5 nM ADAMTS-13 for 60 min in the presence of 1.2 mg/ml ristocetin under the experimental conditions detailed in the text. The same protein amounts were loaded on the gels. The samples from diabetic patients had the highest VWF carbonyl content (380 pmol/mg), whereas the controls had a lower carbonyl content (40 pmol/mg).

BJ www.biochemj.org



BJ Structure

Biochem. J. (2012) **442**, 423–432 (Printed in Great Britain) doi:10.1042/BJ20111798





# Oxidation of Met[1606] in von Willebrand factor is a risk factor for thrombotic and septic complications in chronic renal failure

Vincenzo DE FILIPPIS*[1], Stefano LANCELLOTTI†, Fabio MASET*, Barbara SPOLAORE*, Nicola POZZI*[2], Giovanni GAMBARO‡, Laura OGGIANU†§, Lorenzo A. CALÒ‖ and Raimondo DE CRISTOFARO†[1]

*Laboratory of Protein Chemistry, Department of Pharmaceutical Sciences, University of Padova, Padova, Italy, †Haemostasis Research Centre, Institute of Internal Medicine and Geriatrics, Catholic University School of Medicine, Rome, Italy, ‡Division of Nephrology and Dialysis, Department of Internal Medicine and Medical Specialties, Renal Program, Columbus-Gemelli University Hospital, Catholic University, Rome, Italy, §Section of Biology Applied to Human Health, 'Roma Tre' University, Rome, Italy, and ‖Department of Clinical and Experimental Medicine and Postgraduate School of Nephrology, University of Padova, Padova, Italy

CKD (chronic kidney disease) is a life-threatening pathology, often requiring HD (haemodialysis) and characterized by high OS (oxidative stress), inflammation and perturbation of vascular endothelium. HD patients have increased levels of vWF (von Willebrand factor), a large protein (~240 kDa) released as UL-vWF (ultra large-vWF polymers, molecular mass ~20000–50000 kDa) from vascular endothelial cells and megakaryocytes, and responsible for the initiation of primary haemostasis. The pro-haemostatic potential of vWF increases with its length, which is proteolytically regulated by ADAMTS-13 (a disintegrin and metalloproteinase with thrombospondin motifs 13), a zinc-protease cleaving vWF at the single Tyr[1605]–Met[1606] bond, and by LSPs (leucocyte serine proteases), released by activated PMNs (polymorphonuclear cells) during bacterial infections. Previous studies have shown that *in vitro* oxidation of Met[1606] hinders vWF cleavage by ADAMTS-13, resulting in the accumulation of UL-vWF that are not only more pro-thrombotic than shorter vWF oligomers, but also more efficient in binding to bacterial adhesins during sepsis. Notably, HD patients have increased risk of developing dramatic cardiovascular and septic complications, whose underlying mechanisms are largely unknown. In the present study, we first purified vWF from HD patients and then chemically characterized its oxidative state. Interestingly, HD-vWF contains high carbonyl levels and increased proportion of UL-vWF polymers that are also more resistant to ADAMTS-13. Using TMS (targeted MS) techniques, we estimated that HD-vWF contains >10 % of Met[1606] in the sulfoxide form. We conclude that oxidation of Met[1606], impairing ADAMTS-13 cleavage, results in the accumulation of UL-vWF polymers, which recruit and activate platelets more efficiently and bind more tightly to bacterial adhesins, thus contributing to the development of thrombotic and septic complications in CKD.

Key words: a disintegrin and metalloproteinase with thrombospondin motifs 13 (ADAMTS-13), chronic renal failure, mass spectrometry, oxidative stress sepsis, von Willebrand factor (vWF).

## INTRODUCTION

CKD (chronic kidney disease), often requiring HD (haemodialysis) treatment, is a life-threatening disease of outstanding clinical relevance and dramatic social and economic burden [1,2]. Available data conclusively demonstrate that CKD is characterized by high OS (oxidative stress) [3–5], with increased production of ROS (reactive oxygen species) and RNS (reactive nitrogen species), including $H_2O_2$ (hydrogen peroxide), superoxide radical ($O_2^{\bullet -}$) and PN (peroxinitrite; $ONOO^-$) [6,7]. CKD is also associated with a pro-inflammatory state [8] and perturbation of vascular endothelium [9], whereby CKD can be ultimately regarded as a vasculopathic state [10]. Markedly increased expression of NADPH oxidase (a key enzyme in ROS generation) has been observed in the vascular endothelium of HD patients, together with high levels of the pro-inflammatory cytokine IL-6 (interleukin 6) and acute-phase CRP (C-reactive protein) [3]. Extracellular reduced thiols (e.g. free cysteine and homocysteine and albumin-bound cysteine), constituting an important component of the natural antioxidant defence [11,12], are depleted in HD patients, whereas the corresponding oxidized thiols accumulate, with a resulting pro-thrombotic effect [3,13]. Many other oxidation end-products of lipids, carbohydrates, and proteins accumulate in the plasma of HD patients primarily as a result of their concomitant increased production and diminished renal clearance in CKD [3], but also due to the enhanced release of myeloperoxidase from phagocytes that are activated during HD treatment [14]. Noteworthy, increased plasma levels of the haemostatic vWF (von Willebrand factor) have been found in uremic patients and represents a key marker of vascular endothelium perturbation occurring in CKD [15,16].

vWF is a large (molecular mass of monomers ~240 kDa) multidomain protein [17,18] released as UL-vWF [ultra large-vWF polymers, $(20–50)\times10^3$ kDa] from endothelial cells and platelets upon stimulated and basal secretion [19]. Under conditions of normal blood flow, UL-vWF is in a globular/collapsed state and exerts only poor haemostatic activity [20]. Conversely, under

Abbreviations used: ADAMTS-13, a disintegrin and metalloproteinase with thrombospondin motifs 13; a.m.u., atomic mass unit; CKD, chronic kidney disease; CVD, cardiovascular disease; DNP, dinitrophenylhydrazine; ESI–TOF, electrospray ionization–time-of-flight; ESRD, end-stage renal disease; HD, haemodialysis; HRP, horseradish peroxidase; LC-MS, liquid chromatography-MS; LSP, leucocyte serine protease; MetSO, methionine sulfoxide; MS/MS, tandem MS; NT, 3-nitrotyrosine; OS, oxidative stress; PMN, polymorphonuclear cell; PN, peroxynitrite; PTP, proteotypic peptide; RCM, reduced and carboxamidomethylated; RiCof, ristocetin cofactor; ROS, reactive oxygen species; RP-HPLC, reverse-phase-HPLC; TFA, trifluoroacetic acid; TIC, total ion current; TMS, targeted MS; T2D, Type 2 diabetes; vWF, von Willebrand factor; UL-vWF, ultra large-vWF; vWF-Ox, oxidized vWF.

[1] Correspondence may be addressed to either of these authors (email vincenzo.defilippis@unipd.it or rdecristofaro@rm.unicatt.it).
[2] Present address: Department of Biochemistry and Molecular Biology, Doisy Research Center, Saint Louis University, 1100 South Grand Blvd, St. Louis, MO, 63104, U.S.A.

the high shear forces generated at sites of vascular injury, UL-vWF multimers elongate [21] and initiate primary haemostasis by exposing specific regions responsible for the interaction with collagen in the damaged subendothelium and for platelet recruitment and activation [22,23]. Notably, the platelet-aggregating potential of vWF is crucially dependent on its length [23]. Indeed, longer UL-vWF multimers are intrinsically more sensitive to shear-induced unfolding [24] and therefore are more prothrombotic than shorter vWF species [22,23]. The length of UL-vWF is regulated proteolytically by ADAMTS-13 (a disintegrin and metalloproteinase with thrombospondin motifs 13), a zinc-dependent plasma protease that exclusively cleaves vWF at the single peptide bond $Tyr^{1605}$–$Met^{1606}$ [25] that is recognized by the protease only after shear-induced partial unfolding of vWF [26]. Remarkably, apart from its key role in haemostasis, UL-vWF also participates in bacterial infection [27]. Many bacterial pathogens express on their surface adhesin molecules, such as staphylococcal Protein A, that preferentially engage UL-vWF polymers to adhere to vascular vessels and transmigrate into tissues, thus expanding infection [27]. Bacterial adhesion also triggers recruitment, activation and extravasation of PMNs (polymorphonuclear cells) [27,28], secreting ROS and LSPs (leucocyte serine proteases: elastase, proteinase-3 and cathepsin-G) [29] that efficiently cleave UL-vWF multimers at or near the same peptide bond hydrolysed by ADAMTS-13 [30,31]. Hence, the haemostatic potential of vWF is the result of a dynamic equilibrium existing between the concentration of bioactive UL-vWF released from vascular endothelial cells and the proteolytic efficiency of circulating ADAMTS-13 and LSPs in different clinical settings.

Recently, we have shown that vWF purified from the plasma of patients with T2D (Type 2 diabetes), a severe metabolic disease characterized by OS and complicated by dramatic thrombotic microangiopathies [32], contains higher carbonyl levels, taken as reliable markers of protein oxidative damage [33], than those found in vWF from healthy subjects and higher proportion of UL-vWF polymers that were more resistant to proteolysis by ADAMTS-13 and retained the capacity of interacting with platelets [34]. Interestingly, similar results were obtained after *in vitro* oxidation of normal vWF with physiological concentrations of PN. Hence we proposed that impairment of ADAMTS-13-mediated proteolytic shortening of vWF by oxidation of the vulnerable $Tyr^{1605}$–$Met^{1606}$ bond might represent a novel prothrombotic mechanism contributing to the pathogenesis of microangiopathic complications in T2D [34]. Due to the exceedingly low amounts of T2D-vWF available and the complexity of the vWF molecule, containing many oxidant-sensitive amino acids, our hypothesis was tested on the synthetic vWF peptide vWF74 (i.e. the minimal peptide sequence, residues 1596–1669, of vWF that can be efficiently cleaved by ADAMTS-13) and its analogues vWF74-NT (3-nitrotyrosine) and vWF74-MetSO (methionine sulfoxide), where $Tyr^{1605}$ and $Met^{1606}$ were replaced by their corresponding nitro-oxidation products NT and MetSO respectively. Remarkably, vWF74-MetSO was almost fully resistant to proteolysis by ADAMTS-13, whereas vWF74-NT was hydrolysed as efficiently as the unmodified peptide vWF74 [34], indicating that $Met^{1606}$ oxidation (but not $Tyr^{1605}$ nitration) hinders vWF cleavage. This finding is unique to ADAMTS-13 and opposes the general trend whereby oxidative modifications destabilize proteins and enhance their susceptibility to proteolytic attack [29]. The molecular basis of this behaviour has been recently revealed by modelling and docking simulations, showing that the resistance of the $Tyr^{1605}$–$MetSO^{1606}$ bond to ADAMTS-13 hydrolysis is caused by loss of hydrophobic interactions and steric clashes introduced in the protease-active site upon methionine oxidation [35].

Notably, HD patients have a greatly increased risk of CVD (cardiovascular disease) that accounts for up to 60 % of deaths in CKD [1,36]. The excess incidence of CVD has been rationalized taking into account 'non-traditional' risk factors for CVD, including OS, inflammation and endothelial dysfunction [9]. Notwithstanding, the biochemical root linking high OS to CVD in HD patients is largely unknown [3,4]. Another major clinical issue in CKD entails the high frequency with which these patients develop sepsis (i.e. in 56 % of cases) that may even double the mortality rate [37]. Again, the underlying molecular mechanism leading to septic complications is still elusive [37]. These considerations and the concomitant presence in HD patients of high OS and elevated vWF concentrations, prompted us to chemically characterize the oxidative state of vWF purified from HD patients. Our data show that HD-vWF contains high carbonyl levels and increased proportion of UL-vWF polymers that are also more resistant to ADAMTS-13. Using TMS (targeted MS) techniques, we estimate that $>10$ % of $Met^{1606}$ in vWF from HD patients is oxidatively modified to MetSO. Hence we conclude that accumulation of UL-vWF, ultimately caused by oxidation of $Met^{1606}$ occurring under high OS, may contribute to the development of cardiovascular and septic complications in CKD.

## EXPERIMENTAL

### Human blood samples

Blood samples were supplied by the institutional blood bank of the 'A. Gemelli' Hospital (Catholic University School of Medicine, Rome, Italy) and of the University Hospital (University of Padua, Padua, Italy), while the protocols for all clinical studies were scrutinized and approved by the corresponding Institutional Review Boards. All subjects gave their informed consent to the present study. Healthy subjects ($n = 39$) were blood donors from the institutional blood bank. They were between 38 and 58 years of age, were in good health, non-smokers and had no risk factors for CVD. Patients ($n = 39$) with ESRD (end-stage renal disease), treated with HD three times/week for 1–18 years, without malignant neoplasms, were age- and sex-matched with controls. Considering the known effect of blood group on the level of circulating vWF, the control subjects were also blood group-matched with the HD patients [38]. Blood samples were collected in 3.8 % citrate, then centrifuged at 5000 rev./min for 20 min at 20 °C. The plasma samples were then stored at − 80 °C. Frozen blood samples from healthy or HD patients were thawed at 37 °C.

### Purification of vWF from HD patients

vWF from the plasma pool of healthy subjects and of HD patients with CKD was purified, essentially following the cryoprecipitation method [39], as described previously [34,40]. EDTA-anti-coagulated blood samples were collected from 30 patients of the Padova University Hospital, under chronic dialysis treatment (i.e. 210–240 min/dialysis session, three times a week, using polysulfone dialysers) for at least 1 year (1–15 years range). Five samples (200 ml) of pooled plasma, obtained after blood centrifugation (5000 rev./min for 20 min at 20 °C), were stored at − 80 °C until use. Patients were selected on the basis of lack of malignancy, heart failure, chronic pulmonary diseases and hospitalization in the preceding 6 months.

Briefly, the frozen plasma pool (200 ml) was thawed at room temperature, added with 2 g of PEG [poly(ethylene glycol)]-6000 (Sigma) to a final 1 % (w/v) concentration, and gently stirred for

15 min. This solution was added with 1 mM PMSF (2 ml, 0.1 M) and 10 mM EDTA (4 ml, 0.5 M), as protease inhibitors and left overnight at 4 °C under gentle magnetic stirring. The suspension was then centrifuged in 50 ml Falcon tubes at 3000 rev./min for 1 h at 2 °C. In each Falcon tube, the supernatant was discarded and the pellet resuspended under gentle stirring with 2 ml of 110 mM sodium citrate buffer, pH 7.4, and 6.5 ml of 25 mM Tris/HCl, pH 6.8, containing 0.35 M NaCl and 2.6 M glycine. The suspension was centrifuged at 3000 rev./min for 45 min at 25 °C. The pellet was discarded, while the supernatant was added with solid NaCl to a final concentration of 1.55 M. The suspension was stirred for 30 min and then centrifuged at 6000 rev./min for 30 min at 25 °C. The supernatant was discarded, and the pellet (derived from the 200 ml plasma pool) was dissolved in citrate buffer (1 ml), divided into aliquots and stored at − 80 °C. Finally, the solution was fractionated by gel-filtration chromatography. The citrate solution was thawed, centrifuged at 13 000 rev./min for 5 min, filtered at 0.45 $\mu$m and then loaded on to an in-house packed (2×50 cm) Sephacryl S-400 column eluted with 10 mM Hepes, pH 7.5, and 150 mM NaCl at a flow rate of 0.5 ml/min. Fractions (0.5 ml) were collected and analysed by SDS/PAGE on a Bio-Rad (Hercules) TGX 4–15 % gradient gel, under reducing conditions. The gel was run at 12 mA constant current and Coomassie Blue stained. The high-molecular-mass standards (Sigma, catalogue number 17-0615-01) were used as protein markers. Fractions containing a single band at molecular mass compatible with that of intact vWF were collected, pooled and the concentration of the final solution was determined spectrophotometrically by measuring the absorbance value at 280 nm, using a molar absorption coefficient ($\varepsilon$) of 0.846 $mg^{-1} \cdot cm^2$, calculated on the amino acid sequence of vWF monomer. The quality of vWF preparations was assessed by measuring vWF concentration as antigen (vWF:Ag) and RiCof (ristocetin cofactor) (vWF:RiCof), according to the immunoturbidometric assays 'vWF antigen' and 'vWF activity' (Instrumentation Laboratory), as detailed previously [34,40].

### Determination of the carbonyl content of vWF purified from HD patients

vWF from HD patients of the 'A. Gemelli' University Hospital (Rome, Italy) was micropurified by immunoaffinity chromatography, as detailed previously [34]. Briefly, rabbit polyclonal anti-vWF antibody (2 mg) (Dako) was covalently coupled to Affi-Gel-10 agarose beads (1 ml) (Bio-Rad Laboratories). For each HD patient, the plasma sample (1 ml) was added to the anti-vWF antibody-conjugated beads (0.1 ml). After 1 h of incubation, the suspension was centrifuged (1 min at 1000 rev./min), the supernatant discarded and the gel washed three times with 1 ml of 10 mM Hepes, pH 7.4, 0.15 M NaCl. vWF was recovered by incubating the settled gel beads with a 6 M guanidine hydrochloride solution (0.1 ml) for 15 min under mild agitation. The total protein content was measured by the BCA (bicinchoninic acid) method, using the Bio-Rad Laboratories protein assay, and the carbonyl content of purified vWF samples was measured using the OxiSelect™ Protein Carbonyl ELISA Kit (Cell Biolabs), as reported previously [34]. In this assay, carbonyls were quantified by reaction with DNP (dinitrophenylhydrazine), to form phenylhydrazone derivatives [33], and subsequent incubation with biotinylated anti-DNP antibody followed by strepdavidin-linked HRP (horseradish peroxidase). A calibration curve was obtained with BSA at known content of carbonyl groups. The assay allowed us to obtain a reproducible sensitivity down to 10 pmol carbonyl/mg of protein, with an inter-assay variation of 13 %.

### Hydrolysis by ADAMTS-13 of vWF purified from HD patients

Normal vWF and vWF samples (100 $\mu$l and 20 $\mu$g/ml) from HD patients were incubated with recombinant ADAMTS-13 (5 nM) at 37 °C in 5 mM Tris/HCl, pH 8.0, and 3 mM $CaCl_2$ in the presence of sulfate-free ristocetin (1.5 mg/ml). After 0, 1 and 2 h, aliquots (50 $\mu$l) were sampled and the reaction stopped by adding EDTA (10 mM final concentration). The samples were analysed by SDS-agarose electrophoresis on a 1.2 % agarose gel, followed by immunoblotting with rabbit anti-human vWF polyclonal antibody and HRP-conjugated secondary anti-rabbit antibody (Dako), as detailed previously [31,34].

### *In vitro* oxidation of vWF from healthy subjects

The concentration of sodium PN (Cayman Chemical), was determined spectrophotometrically by measuring the absorbance of the solution at 302 nm, using a molar absorptivity value of 1670 $M^{-1} \cdot cm^{-1}$ [34]. The stock solution was stored at − 80 °C and remained stable for at least 4 weeks. Immediately before use, the stock solution was diluted in 0.1 M NaOH and, during the experiments, was maintained in an ice bath. This vWF preparation (200 $\mu$l, 0.4 mg/ml) was subjected to 'pulsed oxidation' reaction with PN (10 $\mu$M) by multiple additions of oxidant solution (2 $\mu$l, 0.1 M stock solution in 0.1 M NaOH) for 60 min at a rate of one addition per minute. As a control, the reference vWF solution was treated with NaOH alone under identical experimental conditions.

### Production of PTPs (proteotypic peptides)

PTPs of vWF are peptides representative of vWF containing $Met^{1606}$ in the unmodified (Met-PTP) or sulfoxide (MetSO-PTP) form, were produced by proteolysis of the synthetic peptides vWF74 or vWF74-MetSO, with Glu-C protease from *Staphylococcus aureus* (Calbiochem). The pseudo-wild-type peptide vWF74 ($D^{1596}$REQAPNLVYMVTGNPASDEIKRLPGD-IQVVPIGVGPNANVQELERIGWPNAPILIQDFETLPREAPD-LVLQR$A^{1669}$), in which the C-terminal $Cys^{1669}$ was replaced by alanine, and its MetSO derivative (vWF74-MetSO) were obtained by stepwise solid-phase synthesis, as detailed previously [34]. Proteolysis of vWF74 or vWF74-MetSO (220 $\mu$l, 0.34 mg/ml) in 0.1 M Hepes buffer, pH 7.4, containing 0.15 M NaCl, was conducted for 23 h at 37 °C at a protease/substrate ratio of 1:20 (w/w). The reaction was stopped by the addition of TFA (trifluoroacetic acid) and fractionated on a Grace-Vydac (Hesperia) $C_{18}$ analytical column (0.46×25 cm; 5 $\mu$m granulometry) equilibrated in 0.1 % aqueous TFA and eluted with a linear acetonitrile–0.078 % TFA gradient at a flow rate of 0.8 ml/min. The peptide material eluted in correspondence with the chromatographic peaks was collected and analysed by MS on a model Mariner ESI–TOF (electrospray ionization–time-of-flight) spectrometer (PerSeptive BioSystems). The two PTPs Met-PTP and MetSO-PTP, identified by MS analysis, were micropurified (∼100 $\mu$g) by RP-HPLC (reverse-phase-HPLC) and subsequently used for MS analysis.

### TMS analysis

vWF (125 $\mu$l, 0.4 mg/ml) in 0.1 M Tris/HCl buffer, pH 7.5, and 0.15 M NaCl was first reduced for 20 min at 80 °C with 4 mM DTT (dithiothreitol) (5 $\mu$l, 120 mM stock solution) and then alkylated with 10 mM iodoacetamide (5 $\mu$l, 280 mM stock solution) for 15 min at 37 °C in the dark, keeping the solution pH constant at 7.5 by adding Tris base (1 M). The reaction mixture (135 $\mu$l),

containing the RCM (reduced and carboxamidomethylated) vWF, was treated with 250 $\mu$M PN in a 'single-shot' addition (25 $\mu$l of a 1.6 mM stock solution), to yield the corresponding oxidized species, RCM-vWF-Ox (oxidized vWF). Samples of RCM-vWF-Ox were also obtained by 'multiple-shot' addition of PN (10 $\mu$M final concentration) for 60 min at a rate of one shot per min, as detailed above. Samples of RCM-vWF and RCM-vWF-Ox were digested in parallel for 24 h at 37 °C by adding to the reaction mixture Glu-C endoprotease (11 $\mu$l, 0.234 mg/ml stock solution) at a protease/RCM-vWF ratio of 1:20 (w/w). Alternatively, vWF was first oxidized with PN, according to the single- or multiple-shot procedure, under continuous vortexing, subjected to reduction and carboxamidomethylation reaction and finally to proteolysis with Glu-C protease.

Proteolysis mixtures were directly analysed by LC-MS (liquid chromatography-MS) using a micropump-200 HPLC system from PerkinElmer connected to a Mariner mass spectrometer. Samples (25 $\mu$l) of digested RCM-vWF and RCM-vWF-Ox (8 $\mu$g $\approx$ 32 pmols) were added with an acidic solution (60 $\mu$l) of 6 M GdmCl (guanidinium chloride) in 1 % (v/v) aqueous HCOOH (formic acid) and loaded on to a Grace-Vydac $C_{18}$ microbore column (1 × 100 mm, 5 $\mu$m granulometry) equilibrated for 20 min with 1 % aqueous HCOOH, containing 1 % acetonitrile, and eluted with an exponential acetonitrile–1 % HCOOH gradient from 1 to 80 % in 50 min at a flow rate of 10 $\mu$l/min. Spray tip potential was set at 4.0 kV, while the nozzle potential and temperature were set at 200 V and 140 °C respectively. The resulting chromatographic trace was obtained by recording the TIC (total ion current) produced at the microchannel plate detector as a function of time. The reference PTPs Met-PTP and MetSO-PTP were analysed by LC-MS under identical conditions.

MS/MS (tandem MS) measurements were performed on a Micro Q-TOF mass spectrometer from Micromass equipped with a Z-spray nanoflow electrospray ionization interface and connected to a model CapLC capillary HPLC system from Waters. Mass spectra of the peptide digests of RCM-vWF and RCM-vWF-Ox were acquired using the nanoelectrospray source operating at capillary, cone and extractor voltages of 2700, 35 and 1 V respectively (positive ion mode). Digested vWF samples (7 $\mu$l $\approx$ 2 $\mu$g) were loaded on to a $C_{18}$ (75 $\mu$m × 150 mm, 3.5 $\mu$m granulometry) NanoEase column (Waters), eluted with a linear acetonitrile–0.1 % HCOOH gradient from 5 to 70 % in 42 min at a flow rate of 0.2 $\mu$l/min. MS/MS analyses were performed selectively for the proteolytic peptides having monoisotopic *m/z* values identical, within the error of mass determination (i.e. <20 ppm), with those of the reference PTPs Met-PTP [i.e. *m/z* 903.49($2^+$)] and MetSO-PTP [i.e. *m/z* 911.48($2^+$)].

## RESULTS

### Purification of vWF from healthy subjects and from HD patients

Blood samples from healthy subjects or from patients with CKD and a history of HD treatment were pooled, centrifuged and the resulting plasma samples were stored at −80 °C. After thawing, vWF was purified from normal and CKD plasma following essentially the cryoprecipitation method (see the Experimental section) [39]. The cryoprecipitate was finally fractionated on a Sephacryl S-400 gel-filtration column (Figure 1). The purity and integrity of our vWF preparations were assessed by reducing SDS/PAGE (Figure 1, inset), showing a single band at approximately 250 kDa for vWF purified from either healthy subjects or HD patients. From 200 ml of plasma, approximately 200 $\mu$g of highly homogeneous and intact vWF

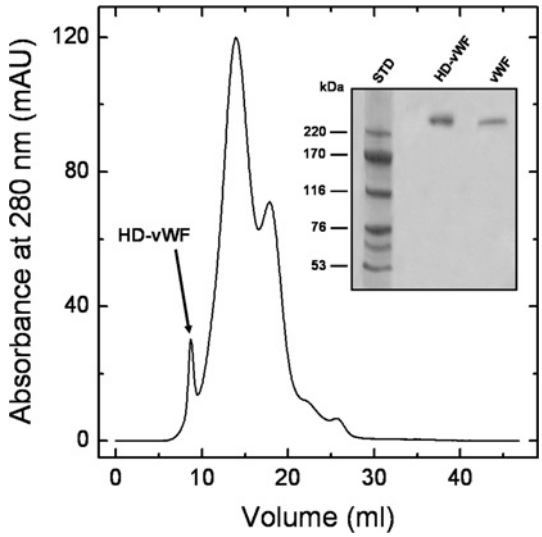


**Figure 1 Purification and analysis of HD-vWF by gel-filtration chromatography and SDS/PAGE**

An aliquot (500 $\mu$l) of the citrate solution deriving from the cryoprecipitated plasma of HD patients was loaded on to a Sephacryl S-400 column (see the Experimental section). vWF multimers were eluted with the void volume, as indicated. Inset: an aliquot (10 $\mu$g) of purified HD-vWF was analysed by SDS/PAGE on a gradient 4–15 % gel, under reducing conditions. As a control, normal vWF, purified by the same procedure, was also loaded. STD, high-molecular mass protein standard; vWF, normal von Willebrand factor purified from healthy subjects; HD-vWF, von Willebrand factor purified from HD patients.

were obtained. The concentration of the final purified vWF solutions was determined spectrophotometrically, and the quality of vWF preparations was assessed by immunoturbidometric assays that measure vWF:Ag and vWF:RiCof [34,40]. Our vWF preparations displayed good protein quality and function, with a vWF:RiCof/vWF:Ag ratio of 0.81 ± 0.15.

### Determination of the carbonyl content and proteolysis by ADAMTS-13 of vWF purified from HD patients

vWF samples from patients ($n = 39$) with ESRD were micropurified by immunoaffinity chromatography (see the Experimental section) and the carbonyl content was determined as a reliable marker of oxidative modifications in proteins [33]. Under oxidizing conditions, sensitive amino acid side chains (i.e. serine, threonine and tyrosine) are converted into their corresponding formyl/ketonic derivatives, with a resulting increase in the protein carbonyl groups. Notably, the carbonyl content (Figure 2A) of HD-vWF was appreciably higher than in normal vWF (i.e. 1.17 ± 0.97 compared with 0.12 ± 0.10 nmol/mg of protein respectively; $P < 0.0001$). SDS-agarose gel electrophoresis, followed by Western-blot analysis, showed that HD-vWF contains a higher proportion of ultra-large multimers (UL-vWF) than normal vWF (Figure 2B). Furthermore, Figure 2(B) showed also that HD-vWF is significantly more resistant to proteolysis by ADAMTS-13 than normal vWF after 1 and 2 h of incubation.

### Mass spectrometric identification of MetSO at position 1606 of normal vWF oxidized *in vitro* with PN

Oxidation of plasma purified UL-vWF was carried out *in vitro* with PN (10 $\mu$M) for 60 min using the 'pulsed oxidation' procedure (see the Experimental section) developed previously for the synthetic vWF74 peptide [34]. This procedure aimed to possibly mimic the continuous flow of oxidant (1–10 $\mu$M) that

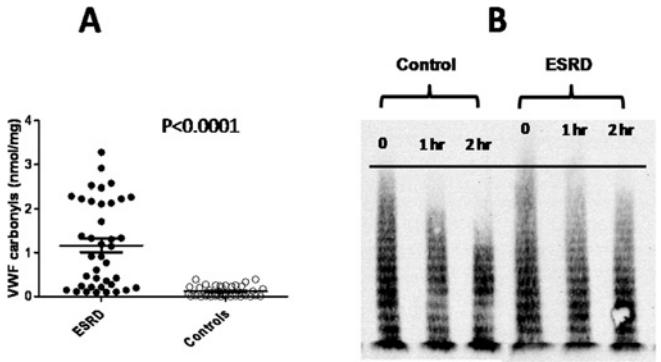


**Figure 2 Analysis of vWF from patients with ESRD**

(**A**) Determination of the carbonyl content in vWF from patients with ESRD and from healthy subjects. The horizontal lines represent the means of the corresponding data set. (**B**) Western blot electrophoretic analysis of vWF multimers from a patient with ESRD and a pool of 10 normal subjects. The samples were analysed by SDS-agarose electrophoresis on a 1.2 % agarose gel, followed by immunoblotting with anti-human vWF polyclonal antibody (see the Experimental section). The horizontal line delimits the form with very high-molecular mass (up), which is more represented in the ESRD patients. The same immunoelectrophoretic run was used to investigate the sensitivity of purified vWF to cleavage by ADAMTS-13. vWF samples (100 $\mu$l, 20 $\mu$g/ml) were incubated for 1 and 2 h at 37 °C with ADAMTS-13 (5 nM) in the presence of ristocetin (1.5 mg/ml) and then analysed by SDS-agarose electrophoresis and Western blotting.

may be produced, even for hours, at inflammatory sites *in vivo* [41]. The strategy we used in the present study for identifying MetSO at position 1606 of vWF-Ox is based on the TMS approach [42] and involves the following steps: (i) selection and production of PTPs with known physico-chemical properties (e.g. retention time in RP-HPLC, *m*/*z* ratio and fragmentation pattern in MS) that are unique to vWF with Met[1606] in the unmodified (Met-PTP) or sulfoxide (MetSO-PTP) forms, to be used as reference peptides in targeted LC-MS experiments; (ii) production of vWF-Ox; (iii) enzymatic fragmentation of vWF and vWF-Ox with Glu-C protease; (iv) LC-MS analysis of the proteolysis mixture and identification of PTPs by TMS; and (v) determination of the amino acid sequence of PTPs in the proteolysis mixture by MS/MS analysis.

From the analysis of the theoretical fragmentation pattern of vWF with Glu-C endoprotease, the peptide sequence Q[1599]APNLVYMVTGNPASDE[1615] was selected as a suitable PTP, representative of vWF with unmodified or oxidized Met[1606]. This peptide, in fact, apart from tyrosine and methionine, does not contain any other oxidizable amino acid that might otherwise complicate the interpretation of the resulting MS spectra. Using this approach, we showed that only Met[1606] (but not Tyr[1605]) was modified. To prepare Met-PTP and MetSO-PTP, the synthetic peptides vWF74 and vWF74-MetSO, produced as detailed previously [34], were treated with Glu-C protease and the corresponding reaction mixtures fractionated by RP-HPLC (Figures 3A and 3B). All fragments were identified by MS analysis (see Figure 3C and Supplementary Table S1 at http://www.BiochemJ.org/bj/442/bj4420423add.htm), whereas the PTPs, Met-PTP [*m*/*z* 903.49($2^+$)] and MetSO-PTP [*m*/*z* 911.48($2^+$)], were purified on a microgram scale and then used as reference peptides in TMS analysis (Figure 4). Proteolysis reactions of unmodified and PN-treated vWF were analysed by LC-MS on a Mariner ESI–TOF spectrometer or on a Micro Q-TOF mass spectrometer (Figures 4A and 4B). The presence of the monoisotopic peptide species at *m*/*z* values 903.12($2^+$) and 911.51($2^+$) (Figures 4C and 4D), eluting in correspondence with the reference PTPs, allowed us to unequivocally identify Met-PTP and MetSO-PTP in the TIC

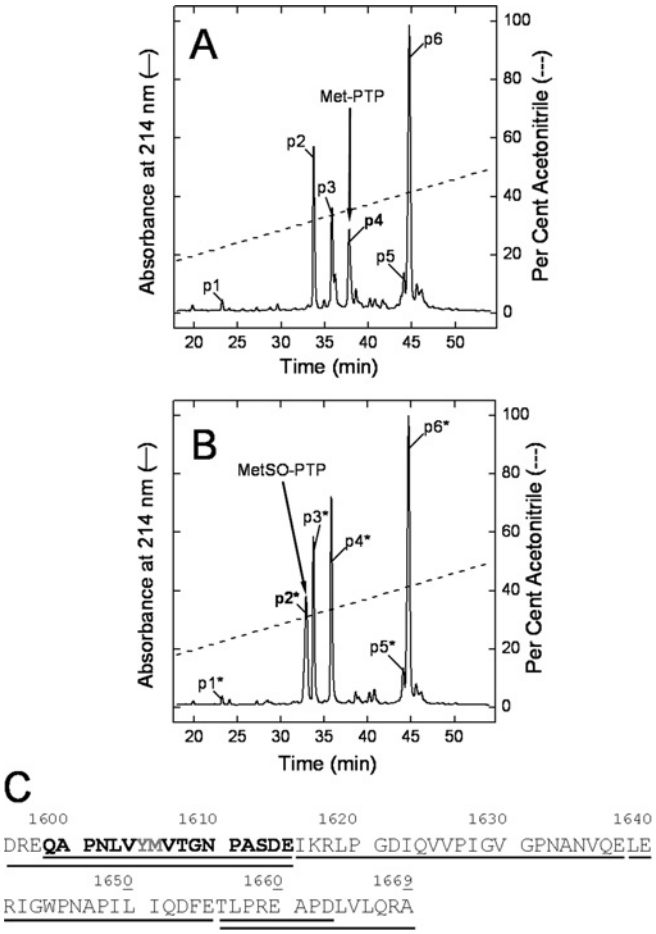


**Figure 3 Production of the PTPs Met-PTP and MetSO-PTP**

RP-HPLC analysis of the proteolysis reaction of vWF74 (**A**) and vWF74-MetSO (**B**) with Glu-C protease. The chemical identity of the proteolytic fragments, deriving from vWF74 (p1, p2, p3, etc.) or vWF74-MetSO (p1*, p2*, p3*, etc.), was established by MS analysis and is reported in Supplementary Table S1 at http://www.BiochemJ.org/bj/442/bj4420423add.htm. The peptides p4 and p2* were identified as the PTPs Met-PTP and MetSO-PTP respectively. As expected from the polar nature of MetSO, MetSO-PTP elutes at retention times much shorter than Met-PTP. (**C**) Amino acid sequence of the synthetic peptide vWF74. The identified fragments are underlined, while the PTP (i.e. Met-PTP or MetSO-PTP) is in bold. For clarity, the scissile tyrosine–methionine bond is in grey.

trace of the proteolysis reaction of untreated and PN-treated UL-vWF. The mass difference between MetSO-PTP [1821.18 a.m.u. (atomic mass unit)] and Met-PTP (1805.10 a.m.u.) is 16 a.m.u., compatible with Met→MetSO oxidation. Notably, we could not identify any other peptide matching the mass of PTP nitrated at Tyr[1605], in agreement with our previous results obtained with vWF74, showing that Tyr[1605] remains unmodified [34]. In the final step, the chemical identity of Met-PTP and MetSO-PTP in the proteolysis reactions was confirmed by MS/MS sequence analysis (Figures 4E and 4F), whereby only peptide species with *m*/*z* values corresponding to those of Met-PTP and MetSO-PTP were selected (Figures 4C and 4D). The mass values of the peptides belonging to the *b*- and *y*-series and in particular the identification of eight fragment ion pairs (Supplementary Table S2 at http://www.BiochemJ.org/bj/442/bj4420423add.htm), differ on average by $16.00 \pm 0.01$ a.m.u., provided clear-cut evidence for the presence of MetSO at position 1606 of vWF-Ox.

Noteworthy, at variance with the conventional 'shotgun' MS approach recently used for analysing HClO (hypochlorous acid)-mediated vWF oxidation [43], our TMS method only

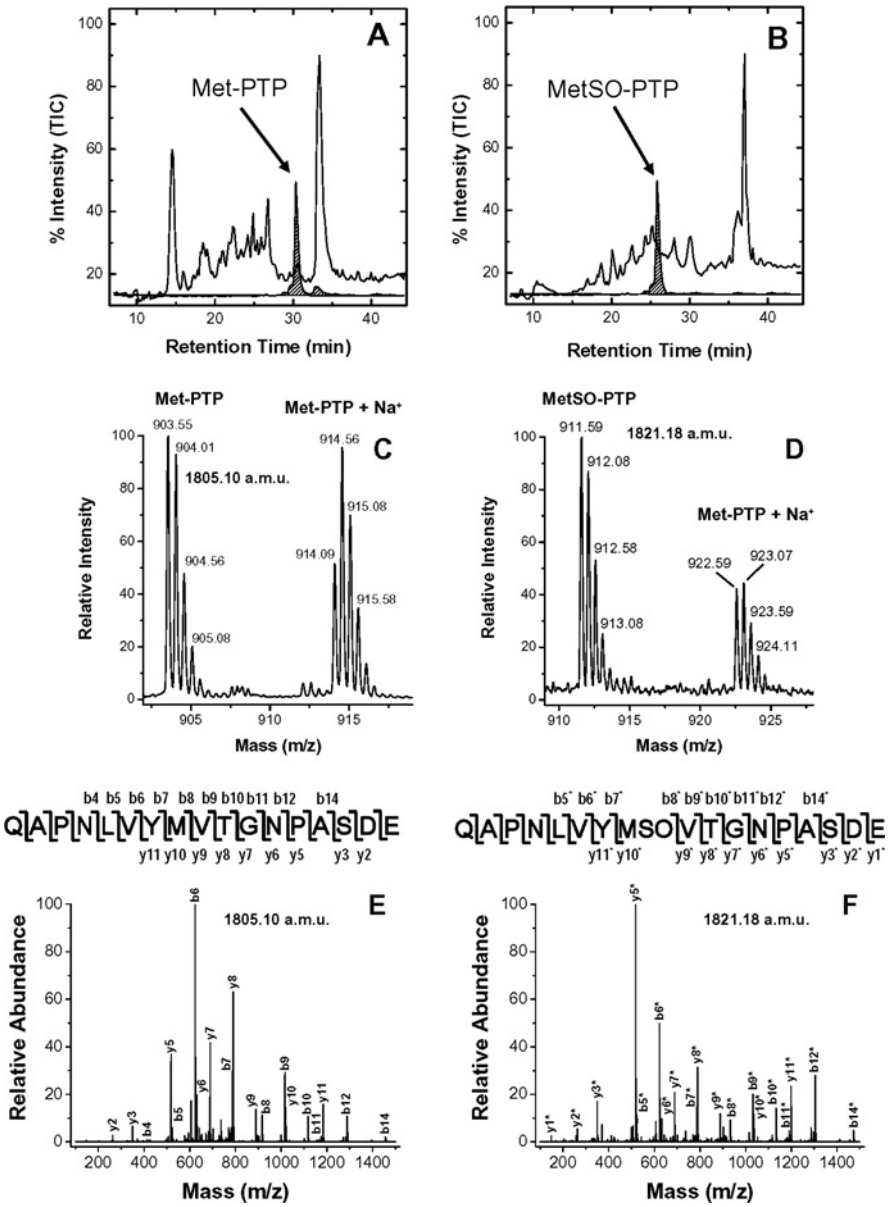


**Figure 4 LC-MS/MS identification of MetSO at position 1606 of normal vWF oxidized *in vitro* with PN (Ox-vWF)**

(**A** and **B**) LC-MS analysis of the proteolysis reaction of vWF (**A**) and Ox-vWF (**B**) with Glu-C protease. Intact (RCM-vWF) and oxidized (RCM-Ox-vWF) vWF samples (8 $\mu$g) with cysteines reduced and carboxamidomethylated were digested with Glu-C protease and analysed by LC-MS on a Mariner ESI–TOF spectrometer, using a microbore $C_{18}$ column (see the Experimental section). The TIC traces of the reference peptides Met-PTP and MetSO-PTP (shaded peaks) are superimposed to those of the corresponding proteolytic mixtures of untreated and PN-oxidized vWF. (**C**–**F**) MS and MS/MS spectra of the PTPs Met-PTP and MetSO-PTP selected in the proteolysis mixture of vWF (**C** and **E**) and Ox-vWF (**D** and **F**). Reaction samples (2 $\mu$g) were analysed by LC-MS on a Micro Q-TOF mass spectrometer, using a capillary $C_{18}$ column. The peptide species with *m*/*z* values identical with those of Met-PTP and MetSO-PTP were selected and subjected to sequence analysis. The mass values and the amino acid sequence of the fragment ions identified in the *b*- and *y*-series are reported in Supplementary Table S2 at http://www.BiochemJ.org/bj/442/bj4420423add.htm.

requires identification of the PTP MetSO-PTP in the LC-MS trace of proteolysed vWF, neglecting all other oxidative modifications that might occur at a variable extent in vWF sequence at sensitive amino acids (i.e. there are 169 cysteine, 56 phenylalanine, 53 histidine, 49 tyrosine, 41 methionine and 18 tryptophan residues in the vWF sequence) in different oxidant milieu (e.g. $H_2O_2$, $O_2\cdot^-$, $ONOO^-$ and HClO).

### Mass spectrometric identification of MetSO at position 1606 of vWF purified from HD patients

vWF purified from the plasma of HD patients was treated according to the TMS procedure set up for normal vWF samples oxidized *in vitro* with PN (see above). The LC-MS analysis of the proteolysis reaction of HD-vWF with Glu-C endoprotease is shown in Figure 5(A). At retention times compatible with those of the reference PTPs Met-PTP and MetSO-PTP, two doubly charged monoisotopic species could be detected at *m*/*z* values of 903.49($2^+$) (Figure 5B) and 911.49($2^+$) (Figure 5C). These values are identical with those of the reference PTPs Met-PTP [*m*/*z* 903.47($2^+$)] and MetSO-PTP [*m*/*z* 911.50($2^+$)] and account for a mass difference of 16 a.m.u. Peptide sequencing by MS/MS measurements allowed us to confirm the presence of Met-PTP and MetSO-PTP in the proteolysis mixture of HD-vWF (Figures 5D and 5E). Even in this case, eight fragment ion pairs of the *b*- and

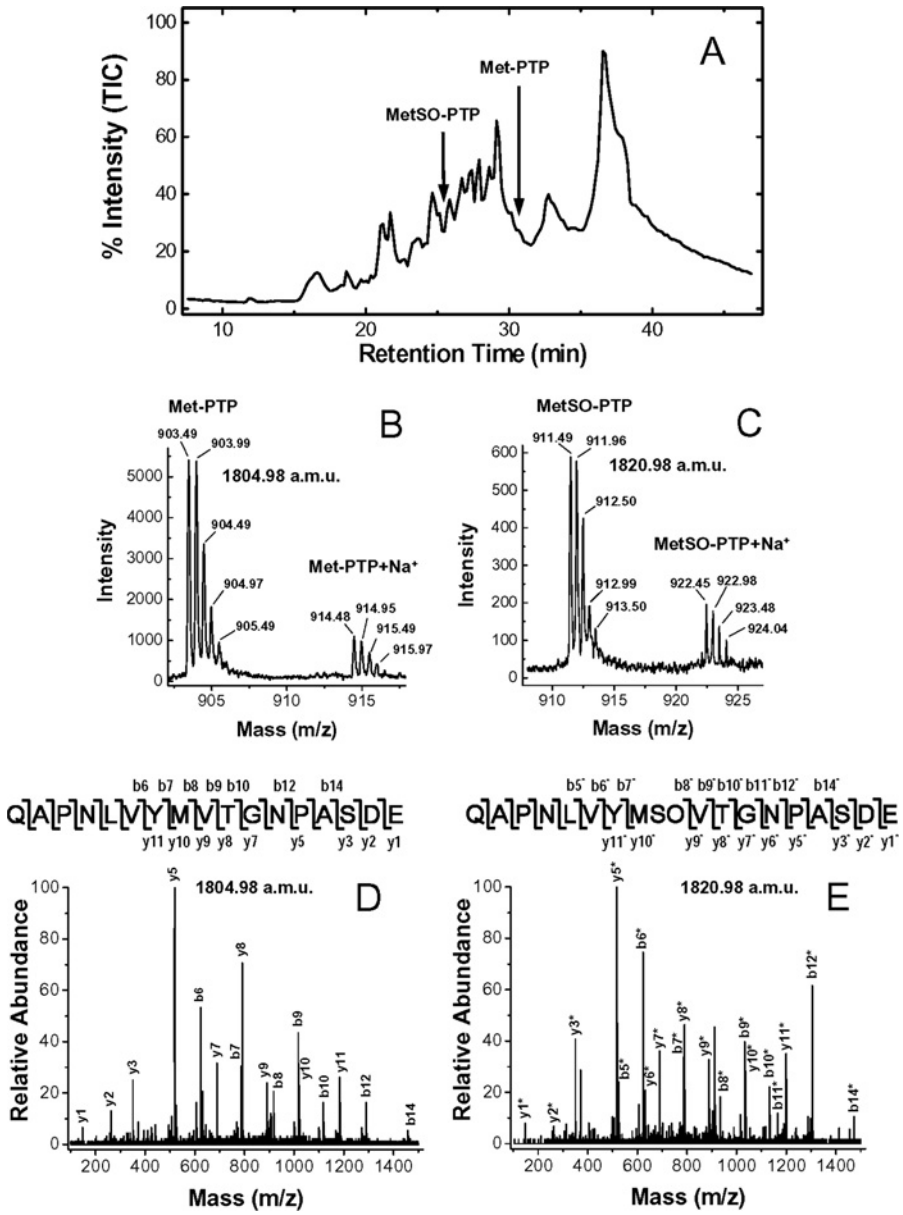


**Figure 5 LC-MS/MS identification of MetSO at position 1606 in vWF purified from HD patients**

(**A**) LC-MS analysis of the proteolysis reaction of HD-vWF with Glu-C protease. A sample (10 $\mu$g) of purified HD-vWF with cysteines reduced and carboxamidomethylated was digested with Glu-C protease and analysed by LC-MS on a Mariner ESI–TOF spectrometer, using a microbore $C_{18}$ column (see the Experimental section). The arrows on the TIC trace indicate where the PTPs Met-PTP and MetSO-PTP elute. (**B**–**E**) MS (**B** and **C**) and MS/MS (**D** and **E**) spectra of the PTPs selected in the proteolysis mixture of HD-vWF (see **A**). Reaction samples (2 $\mu$g) were analysed by LC-MS on a Micro Q-TOF mass spectrometer, using a capillary $C_{18}$ column. The peptide species with *m/z* values identical with those of Met-PTP and MetSO-PTP were selected and subjected to sequence analysis. The mass values and the amino acid sequence of the fragment ions identified in the *b*- and *y*-series are reported in Table 1.

*y*-series were identified in Met-PTP and MetSO-PTP (i.e. *b*8/*b*8*, *b*9/*b*9*, *y*10/*y*10*, etc.) (Table 1), with an average mass difference of $15.79 \pm 0.05$ a.m.u. This value is compatible with the presence of MetSO in the fragment ions generated from oxidized vWF molecules that are present in HD-vWF sample.

Notably, from the intensity of the monoisotopic species of Met-PTP and MetSO-PTP in the free and $Na^+$-bound forms (Figures 5B and 5C), a relative abundance higher than 10 % was estimated for the oxidatively modified MetSO-PTP. To rule out the possibility that oxidized $Met^{1606}$ (at least in part) could be also present in normal vWF, as a result of the basal oxidative potential in the plasma of healthy subjects or even artefactually generated in HD-vWF during purification and handling, we attempted to identify MetSO-PTP in the LC-MS trace of the Glu-C proteolysis reaction of normal vWF purified from healthy subjects. The data shown in Supplementary Figure S1 (at http://www.BiochemJ.org/bj/442/bj4420423add.htm) unequivocally indicate that, within the limitations of the analytical techniques used, the percentage of MetSO-PTP in normal vWF is lower than 1 %, compared with the unmodified Met-PTP. These results allow us to reasonably interpret the increase of MetSO-PTP in HD-vWF as arising from the oxidative conditions unique to the plasma of HD patients. At this stage of the work, however, either limited availability of plasma samples and low yield of vWF purification impair quantification of $Met^{1606}$ in vWF from individual patients.

**Table 1 MS/MS data of the PTPs Met-PTP and MetSO-PTP identified in HD-vWF**

The PTPs Met-PTP and MetSO-PTP, selected during the LC-MS analysis of the proteolysis reaction of HD-vWF with Glu-C protease (see Figure 5A), were subjected to MS/MS analysis. Ion fragments are listed in order of increasing mass values. Fragment ions containing $Met^{1606}$ in the unmodified or sulfoxide form are shown in bold.

| Met-PTP | | | MetSO-PTP | | |
|---|---|---|---|---|---|
| Fragment ion | $(MH)^+$ * | Amino acid sequence | Fragment ion† | $(MH)^+$ * | Amino acid sequence |
| *y*1 | 148.08 (148.06) | $Glu^{1615}$ | *y*1 | 148.06 (148.06) | $Glu^{1615}$ |
| *y*2 | 263.14 (263.09) | $Asp^{1614}$–$Glu^{1615}$ | *y*2 | 263.06 (263.09) | $Asp^{1614}$–$Glu^{1615}$ |
| *y*3 | 350.19 (350.12) | $Ser^{1613}$–$Glu^{1615}$ | *y*3 | 350.13 (350.12) | $Ser^{1613}$–$Glu^{1615}$ |
| *y*5 | 518.32 (518.21) | $Pro^{1611}$–$Glu^{1615}$ | *y*5 | 518.22 (518.21) | $Pro^{1611}$–$Glu^{1615}$ |
| *b*6 | 623.48 (623.35) | $Gln^{1599}$–$Val^{1604}$ | *b*5 | 524.30 (524.28) | $Gln^{1599}$–$Leu^{1603}$ |
| *y*7 | 689.45 (689.27) | $Gly^{1609}$–$Glu^{1615}$ | *b*6 | 623.37 (623.35) | $Gln^{1599}$–$Val^{1604}$ |
| *b*7 | 786.60 (786.41) | $Gln^{1599}$–$Tyr^{1605}$ | *y*6 | 632.27 (632.25) | $Asn^{1610}$–$Glu^{1615}$ |
| *y*8 | 790.46 (790.32) | $Thr^{1608}$–$Glu^{1615}$ | *y*7 | 689.29 (689.27) | $Gly^{1609}$–$Glu^{1615}$ |
| *y*9 | 889.62 (889.39) | $Val^{1607}$–$Glu^{1615}$ | *b*7 | 786.45 (786.41) | $Gln^{1599}$–$Tyr^{1605}$ |
| ***b*8** | **917.68 (917.46)** | **$Gln^{1599}$–$Met^{1606}$** | *y*8 | 790.33 (790.32) | $Thr^{1608}$–$Glu^{1615}$ |
| ***b*9** | **1016.77 (1016.52)** | **$Gln^{1599}$–$Val^{1607}$** | *y*9 | 889.42 (889.39) | $Val^{1607}$–$Glu^{1615}$ |
| ***y*10** | **1020.61 (1020.43)** | **$Met^{1606}$–$Glu^{1615}$** | ***b*8** | **933.52 (933.46)** | **$Gln^{1599}$–$MetSO^{1606}$** |
| ***b*10** | **1117.81 (1117.57)** | **$Gln^{1599}$–$Thr^{1608}$** | ***b*9** | **1032.53 (1032.52)** | **$Gln^{1599}$–$V^{1607}$** |
| ***y*11** | **1183.73 (1183.49)** | **$Tyr^{1605}$–$Glu^{1615}$** | ***y*10** | **1036.46 (1036.43)** | **$MetSO^{1606}$–$Glu^{1615}$** |
| ***b*12** | **1288.90 (1288.64)** | **$Gln^{1599}$–$Asn^{1610}$** | ***b*10** | **1133.59 (1133.57)** | **$Gln^{1599}$–$Thr^{1608}$** |
| ***b*14** | **1457.08 (1456.73)** | **$Gln^{1599}$–$Ala^{1612}$** | ***b*11** | **1190.58 (1190.59)** | **$Gln^{1599}$–$Gly^{1609}$** |
| | | | ***y*11** | **1199.55 (1199.49)** | **$Tyr^{1605}$–$Glu^{1615}$** |
| | | | ***b*12** | **1304.70 (1304.64)** | **$Gln^{1599}$–$Asn^{1610}$** |
| | | | ***b*14** | **1472.78 (1472.73)** | **$Gln^{1599}$–$Ala^{1612}$** |

*Experimental and theoretical (in parentheses) mass values of singly charged fragment ions.
†Fragment ions derived from MetSO-PTP.

## DISCUSSION

OS is a generic term used for defining the imbalance of the equilibrium existing between the generation of ROS and their scavenging *in vivo* [44]. Shifting this equilibrium in favour of ROS production can lead to oxidation of biomacromolecules (e.g. proteins, lipids and nucleic acids), inducing cell death and tissue injury [45,46]. Biochemical and clinical data accumulated so far indicate that OS is involved in many clinical settings, also associated with pro-inflammatory states and dysfunction of vascular endothelium (i.e. CVD and neurodegenerative diseases, atherosclerosis, cancer, rheumatoid arthritis, inflammatory bowel disease, sepsis, CKD and T2D) [45].

PN and HClO are thought to be the major effectors of OS *in vivo* [41,47,48]. However, a realistic understanding of the relative importance of these two oxidants in health and disease should start from the knowledge of their different reactivity, cellular localization and *in vivo* function. PN is produced *in vivo* from NO (nitric oxide) and superoxide radical ($O_2^{\bullet -}$) [46] mainly by vascular endothelial cells, where vWF is also stored and released; it easily crosses biological membranes and its concentration increases from 0.3 $\mu$M/s, under basal conditions, up to 30–300 $\mu$M/s at inflammatory sites in diseases related to chronic inflammatory states [41,45]. Furthermore, PN reacts directly with cysteine, methionine and tryptophan generating sulfenic acid, MetSO and 2-oxindolylalanine respectively, whereas it reacts indirectly with phenylalanine, histidine and tyrosine [47]. Compared with PN, HClO is a stronger oxidant, mainly involved in microbial killing and is produced *in vivo* (30–400 $\mu$M/h) by the $H_2O_2/Cl^-$ myeloperoxidase system of activated PMNs, together with a burst of LSPs, as part of the mammalian immune defence system [29,48].

Recently, we have investigated the effects of vWF oxidation by PN or HClO on the susceptibility of vWF to proteolysis by physiologically relevant proteases, such as ADAMTS-13 and LSPs, and then related these effects to alterations of the haemostatic process observed in different clinical settings (i.e. T2D and sepsis) [31,34]. In particular, using the minimal vWF substrate for ADAMTS-13 (i.e. vWF74), we showed that oxidation of $Met^{1606}$ in vWF to MetSO hinders cleavage by ADAMTS-13, with a resulting accumulation of the more pro-haemostatic vWF polymers, UL-vWF [34]. Conversely, *in vitro* treatment of vWF with activated PMNs, simultaneously releasing LSPs and ROS, does not reduce but enhances proteolysis of UL-vWF by LSPs [31]. Hence it seems that the same chemical modification (i.e. oxidation of $Met^{1606}$) has opposite effects on the susceptibility of vWF to the proteases responsible for the regulation of its length (i.e. ADAMTS-13 and LSPs) and, ultimately, of its haemostatic potential in different clinical settings. Altogether, these considerations emphasize the different physiopathological meaning of vWF oxidation by PN and HClO and highlight the existence of two different pathways of coupled oxidative/proteolytic reactions involving the ADAMTS-13-vWF and LSPs-vWF systems. Chronic OS by PN, mainly released by perturbed endothelial cells in chronic inflammatory diseases (e.g. vascular aging and diabetes), has a negative effect on the ADAMTS-13/vWF pathway [34], with a resulting accumulation of pro-thrombotic UL-vWF polymers. Conversely, acute OS caused by HClO, rapidly released by activated PMNs during bacterial infection, has a positive effect on the LSPs/vWF pathway [31], thus (partially) compensating the inhibition that $Met^{1606}$ oxidation exerts on ADAMTS-13 proteolysis. Furthermore, the enhanced proteolysis of oxidized vWF by LSPs, reducing the concentration of UL-vWF polymers amenable to interact with bacterial adhesins (see the Introduction), may be regarded as a mechanism aimed at limiting the vWF-mediated adhesion and invasion of bacteria in a highly oxidant milieu (i.e. sepsis), where ADAMTS-13 activity is heavily compromised [31].

Considering the concomitant increase of OS and vWF levels in CKD, in the present study, we chemically characterized

the oxidative state of $Met^{1606}$, as the major site of proteolytic regulation of vWF length. Hence we purified to homogeneity enough quantities of vWF from a pool of plasma from HD patients (Figure 1). As already found with vWF isolated from T2D patients [34], the average carbonyl content of HD-vWF was at least 10-fold higher than in normal vWF (Figure 2A) and favourably correlated with an increased proportion of UL-vWF polymers that were also more resistant to ADAMTS-13 cleavage (Figure 2B). A major achievement of this work relate to the development of a sensitive (2–10 $\mu$g of vWF) and reliable TMS method for detecting MetSO at position 1606 of UL-vWF samples. The experimental procedure was first set up and validated with normal vWF, oxidized *in vitro* with physiological concentrations of PN (Figures 3 and 4), and then used for analysing HD-vWF (Figure 5 and Table 1). MetSO was unequivocally detected at position 1606 of HD-vWF, even though quantitative MS analysis (Figure 5B) indicated that the proportion of vWF molecules containing MetSO at position 1606 was relatively small (i.e. $>10\,\%$). However, this value represents the average extent of $Met^{1606}$ oxidation in a vWF sample obtained from a pool of plasma derived from 30 patients undergoing HD therapy since a variable time period (i.e. from 1 to 15 years; see the Experimental section). Further work is required to correlate the extent of $Met^{1606}$ modification in individual patient plasmas with the severity of CKD and/or with the time period of HD treatment. Moreover, it should be considered that haemostasis is a dynamic process resulting from the delicate equilibrium between finely regulated pro-coagulant and anti-coagulant systems, such that even small perturbation of this equilibrium can cause thrombotic or haemorrhagic effects [49]. For instance, in normal individuals only approximately 10 % of circulating fibrinogen molecules contain the elongated $\gamma$-chain variant (termed $\gamma'$), derived from alternative splicing of mRNA and inserting 20 amino acids at the C-terminus of the $\gamma$ chain. The $\gamma'$ chain binds to thrombin exosite 2, inhibits platelet activation by thrombin and its decreased expression is positively correlated with higher risk of thrombosis [50]. Likewise, *in vivo* nitration of $Tyr^{292}$ and $Tyr^{422}$ in the fibrinogen $\beta$-chain of smokers occurs with yields as low as 0.6–6 %. Nevertheless, the kinetics of fibrin formation and degradation in these patients is markedly altered and tyrosine nitration has been proposed as an important risk factor for thrombosis [51]. In the case of vWF, tensile force acting on vWF molecules increases with the square of multimer length [24]. Therefore UL-vWF polymers are more easily stretched in shear flow [24] and start to form a protein network that efficiently adheres to platelet GpIb receptors, thus increasing the risk of thrombosis [23]. Under physiological conditions, this effect is opposed by shear-induced unfolding of the A2 domain and subsequent cleavage of the newly exposed $Tyr^{1605}$–$Met^{1606}$ bond by ADAMTS-13 [24]. Therefore it is not surprising that under high OS, even relatively small amounts of oxidized UL-vWF multimers, no longer sensitive to proteolysis by ADAMTS-13, may function as nucleators for the generation of networks of vWF fibres, thus amplifying platelet adhesion and thrombus formation. Likewise, UL-vWF polymers might increase the probability of vWF-mediated adhesion of bacteria to vascular vessels and their migration into tissues [27,28], thus expanding infection. Accordingly, previous studies showed that experimental group C *Streptococcus*-induced endocarditis failed to develop in pigs with von Willebrand disease, an inherited bleeding disorder characterized by loss of UL-vWF polymers [52].

In conclusion, in the present study, we have characterized the oxidative state of vWF purified from patients with CKD and developed a convenient MS method of general applicability for detecting MetSO at position 1606 as a 'functional marker' of the susceptibility of vWF to proteolysis in diseases associated with high OS. These results are unprecedented and may contribute to elucidate the molecular root leading to either thrombotic or septic complications in CKD.

## AUTHOR CONTRIBUTION

Vincenzo De Filippis designed the experiments, analysed the results and wrote the paper; Stefano Lancellotti, Fabio Maset, Barbara Spolaore, Nicola Pozzi and Laura Oggianu performed the experiments; Giovanni Gambaro and Lorenzo A. Calò supplied the plasma from HD patients and revised the paper; Raimondo De Cristofaro designed the experiments, analysed the results and revised the paper.

## ACKNOWLEDGEMENTS

V.D.F. thanks Professor Angelo Fontana for providing accessibility to instrumentation for MS/MS analyses, Dr Chiara D'Orlando for helping us with the purification of HD-vWF and Dr Daniele Dalzoppo for critically reading the paper before submission.

## FUNDING

This work was financially supported by the Ministero dell'Istruzione, dell'Università e della Ricerca Scientifica (MIUR) [PRIN2007 grant numbers 2007T9HTFB_002 (to V.D.F.) and 2007T9HTFB_003 (to R.D.C.)].

## REFERENCES

1 Go, A. S., Chertow, G. M., Fan, D., McCulloch, C. E. and Hsu, C. Y. (2004) Chronic kidney disease and the risks of death, cardiovascular events, and hospitalization. N. Engl. J. Med. **351**, 1296–1305
2 United States Renal Data System (2010) USRDS 2010 Annual Data Report: Atlas of Chronic Kidney Diseases and End-Stage Renal Disease in The United States, National Institutes of Health, National Institute of Diabetes and Digestive and Kidney Diseases, Bethesda
3 Himmelfarb, J. and Hakim, R. M. (2003) Oxidative stress in uremia. Curr. Opin. Nephrol. Hypertens. **12**, 593–598
4 Himmelfarb, J., McMonagle, E., Freedman, S., Klenzak, J., McMenamin, E., Le, P., Pupim, L. B. and Ikizler, T. A. (2004) Oxidative stress is increased in critically ill patients with acute renal failure. J. Am. Soc. Nephrol. **15**, 2449–2456
5 Massy, Z. A., Stenvinkel, P. and Drueke, T. B. (2009) The role of oxidative stress in chronic kidney disease. Semin. Dial. **22**, 405–408
6 Walker, L. M., Walker, P. D., Imam, S. Z., Ali, S. F., Muldrew, K. L. and Mayeux, P. R. (2001) Oxidative stress and reactive nitrogen species generation during renal ischemia. Toxicol. Sci. **63**, 143–148
7 Vinas, J. L., Sola, A. and Hotter, G. (2006) Mitochondrial NOS upregulation during renal I/R causes apoptosis in a peroxynitrite-dependent manner. Kidney Int. **69**, 1403–1409
8 Zimmermann, J., Herrlinger, S., Pruy, A., Metzger, T. and Wanner, C. (1999) Inflammation enhances cardiovascular risk and mortality in hemodialysis patients. Kidney Int. **55**, 648–658
9 Annuk, M., Zilmer, M., Lind, L., Linde, T. and Fellström, B. (2001) Oxidative stress and endothelial function in chronic renal failure. J. Am. Soc. Nephrol. **12**, 2747–2752
10 Luke, R. G (1998) Chronic renal failure: a vasculopathic state. N. Engl. J. Med. **339**, 841–843
11 Ueland, P. M., Mansoor, M. A., Guttormsen, A. B., Müller, F., Aukrust, P., Refsum, H. and Svardal, A. M. (1996) Reduced, oxidized and protein-bound forms of homocysteine and other aminothiols in plasma comprise the redox thiol status: a possible element of the extracellular antioxidant defense system. J. Nutr. **126** (4 Suppl.), 1281S–1284S
12 Halliwell, B. (1998) Albumin: an important extracellular antioxidant? Biochem. Pharmacol. **37**, 569–571
13 Bostom, A. G. and Lathrop, L. (1997) Hyperhomocysteinemia in end-stage renal disease: prevalence, etiology and potential relationship to arteriosclerotic outcomes. Kidney Int. **52**, 10–20
14 Ward, R. and McLeish, K. (1995) Hemodialysis with cellulose membranes primes the neutrophil oxidative burst. Artif. Organs **19**, 801–807
15 Małyszko, J. S., Małyszko, J., Hryszko, T., Koźminski, P., Pawlak, K. and Mysliwiec, M. (2006) Markers of endothelial damage in patients on hemodialysis and hemodiafiltration. J. Nephrol. **19**, 150–154
16 Kirmizis, D., Tsiandoulas, A., Pangalou, M., Koutoupa, E., Rozi, P., Protopappa, M. and Barboutis, K. (2006) Validity of plasma fibrinogen, D-dimer, and the von Willebrand factor as markers of cardiovascular morbidity in patients on chronic hemodialysis. Med. Sci. Monit. **12**, CR55–CR62

17 Wagner, D. D. (1990) Cell biology of von Willebrand factor. Annu. Rev. Cell Biol. **6**, 217–246
18 Sadler, J. E. (1998) Biochemistry and genetics of von Willebrand factor. Annu. Rev. Biochem. **67**, 395–424
19 Sadler, J. E. (2009) von Willebrand factor assembly and secretion. J. Thromb. Haemostasis **7** (Suppl. 1), 24–27
20 Schneider, S. W., Nuschele, S., Wixforth, A., Gorzelanny, C., Alexander-Katz, A., Netz, R. R. and Schneider, M. F. (2007) Shear-induced unfolding triggers adhesion of von Willebrand factor fibers. Proc. Natl. Acad. Sci. U.S.A. **104**, 7899–903
21 Siedlecki, C. A., Lestini, B. J., Kottke-Marchant, K. K., Eppell, S. J., Wilson, D. L. and Marchant, R. E. (1996) Shear-dependent changes in the three-dimensional structure of human von Willebrand factor. Blood **88**, 2939–2950
22 Sadler, J. E. (2005) von Willebrand factor: two sides of a coin. J. Thromb. Haemostasis **3**, 1702–1709
23 Ruggeri, Z. M. (2007) The role of von Willebrand factor in thrombus formation. Thromb. Res. **120** (Suppl. 1), S5–S9
24 Zhang, X., Halvorsen, K., Zhang, C. Z., Wong, W. P. and Springer, T. A. (2009) Mechanoenzymatic cleavage of the ultralarge vascular protein von Willebrand factor. Science **324**, 1330–1334
25 Furlan, M., Robles, R. and Lamie, B. (1996) Partial purification and characterization of a protease from human plasma cleaving von Willebrand factor to fragments produced by *in vivo* proteolysis. Blood **87**, 4223–4234
26 Chung, D. W. and Fujikawa, K. (2002) Processing of von Willebrand factor by ADAMTS-13. Biochemistry **41**, 11065–11070
27 Hartleib, J., Kohler, N., Dickinson, R. B., Chhatwal, G. S., Sixma, J. J., Hartford, O. M., Foster, T. J., Peters, G., Kehrel, B. E. and Herrmann, M. (2000) Protein A is the von Willebrand factor binding protein on *Staphylococcus aureus*. Blood **96**, 2149–2156
28 Petri, B., Broermann, A., Li, H., Khandoga, A. G., Zarbock, A., Krombach, F., Goerge, T., Schneider, S. W., Jones, C., Nieswandt, B. et al. (2010) Von Willebrand factor promotes leukocyte extravasation. Blood **116**, 4712–4719
29 Klebanoff, S. J. (2005) Myeloperoxidase: friend and foe. J. Leukoc. Biol. **77**, 598–625
30 Raife, T. J., Cao, W., Atkinson, B. S., Bedell, B., Montgomery, R. R., Lentz, S. R., Johnson, G. F. and Zheng, X. L. (2009) Leukocyte proteases cleave von Willebrand factor at or near the ADAMTS13 cleavage site. Blood **114**, 1666–1674
31 Lancellotti, S., De Filippis, V., Pozzi, N., Oggianu, L., Rutella, S., Scaglione, G. L., Maset, F., Peyvandi, F., Mannucci, P. M. and De Cristofaro, R. (2011) Oxidized von Willebrand factor is efficiently cleaved by serine proteases from primary granules of leukocytes: divergence from ADAMTS-13, J. Thromb. Haemostasis **9**, 1620–1627
32 Brownlee, M. (2001) Biochemistry and molecular cell biology of diabetic complications. Nature **414**, 813–820
33 Reznick, A. Z. and Packer, L. (1994) Oxidative damage to proteins: spectrophotometric method for carbonyl assay. Methods Enzymol. **233**, 357–363
34 Lancellotti, S., De Filippis, V., Pozzi, N., Peyvandi, F., Palla, R., Rocca, B., Rutella, S., Pitocco, D., Mannucci, P. M. and De Cristofaro, R. (2010) Formation of methionine sulfoxide by peroxynitrite at position 1606 of von Willebrand factor inhibits its cleavage by ADAMTS-13: A new prothrombotic mechanism in diseases associated with oxidative stress. Free Radical Biol. Med. **48**, 446–456

Received 6 October 2011/15 November 2011; accepted 18 November 2011
Published as BJ Immediate Publication 18 November 2011, doi:10.1042/BJ20111798

35 Pozzi, N., Lancellotti, S., De Cristofaro, R. and De Filippis, V. (2012) Modeling ADAMTS13–vWF interaction: implications for oxidative stress-related cardiovascular diseases and type-2A von Willebrand disease. Biophys. Chem. **160**, 1–11
36 Foley, R., Parfrey, P. S. and Sarnak, M. J. (1998) Epidemiology of cardiovascular disease in chronic renal disease. J. Am. Soc. Nephrol. **32** (12 Suppl.), S16–S23
37 Mehta, R. L., Bouchard, J., Soroko, S. B., Ikizler, T. A., Paganini, E. P., Chertow, G. M. and Himmelfarb, J. (2011) Sepsis as a cause and consequence of acute kidney injury: program to improve care in acute renal disease. Intensive Care Med. **37**, 241–248
38 van Schooten, C. J., Denis, C. V., Lisman, T., Eikenboom, J. C., Leebeek, F. W., Goudemand, J., Fressinaud, E., van den Berg, H. M., de Groot, P. G. and Lenting, P. J. (2007) Variations in glycosylation of von Willebrand factor with O-linked sialylated T antigen are associated with its plasma levels. Blood **109**, 2430–2437
39 Thorell, L. and Blomback, B. (1984) Purification of the factor VIII complex. Thromb. Res. **35**, 431–450
40 De Cristofaro, R., Peyvandi, F., Palla, R., Lavoretano, S., Lombardi, R., Merati, G., Romitelli, F., Di Stasio, E. and Mannucci, P. M. (2005) Role of chloride ions in modulation of the interaction between von Willebrand factor and ADAMTS-13. J. Biol. Chem. **280**, 23295–13302
41 Ferrer-Sueta, G. and Radi, R. (2009) Chemical biology of peroxynitrite: kinetics, diffusion, and radicals. ACS Chem. Biol. **4**, 161–177
42 Hüttenhain, R., Malmström, J., Picotti, P. and Aebersold, R. (2009) Perspectives of targeted mass spectrometry for protein biomarker verification. Curr. Opin. Chem. Biol. **13**, 518–525
43 Chen, J., Fu, X., Wang, Y., Ling, M., McMullen, B., Kulman, J., Chung, D. W. and Lopez, J. A. (2010) Oxidative modification of von Willebrand factor by neutrophil oxidants inhibits its cleavage by ADAMTS13. Blood **115**, 706–712
44 Forman, H. J., Maiorino, M. and Ursini, F. (2010) Signaling functions of reactive oxygen species. Biochemistry **49**, 835–842
45 Pacher, P., Beckman, J. S. and Liaudet, L. (2007) Nitric oxide and peroxynitrite in health and disease. Physiol. Rev. **87**, 315–424
46 Liaudet, L., Vassalli, G. and Pacher, P. (2009) Role of peroxynitrite in the redox regulation of cell signal transduction pathways. Front. Biosci. **14**, 4809–4814
47 Alvarez, B. and Radi, R. (2003) Peroxynitrite reactivity with amino acids and proteins. Amino Acids **25**, 295–311
48 Hawkins, C. L., Pattison, D. I. and Davies, M. J. (2003) Hypochlorite-induced oxidation of amino acids, peptides and proteins. Amino Acids **25**, 259–274
49 Dahlbäck, B. (2000) Blood coagulation. Lancet **355**, 1627–1632
50 Lancellotti, S., Rutella, S., De Filippis, V., Pozzi, N., Rocca, B. and De Cristofaro, R. (2008) Fibrinogen elongated $\gamma$-chain inhibits thrombin-induced platelet response, hindering the interaction with different receptors. J. Biol. Chem. **283**, 30193–30204
51 Parastatidis, I., Thomson, L., Burke, A., Chernysh, I., Nagaswami, C., Visser, J., Stamer, S., Liebler, D. C., Koliakos, G., Heijnen, H. F. et al. (2008) Fibrinogen beta-chain tyrosine nitration is a prothrombotic risk factor. J Biol. Chem. **283**, 33846–33853
52 Johnson, C. M. and Bowie, E. J. (1992) Pigs with von Willebrand disease may be resistant to experimental infective endocarditis. J. Lab. Clin. Med. **120**, 553–558

Biochem. J. (2012) **442**, 423–432 (Printed in Great Britain) doi:10.1042/BJ20111798

## SUPPLEMENTARY ONLINE DATA

# Oxidation of Met[1606] in von Willebrand factor is a risk factor for thrombotic and septic complications in chronic renal failure

Vincenzo DE FILIPPIS*[1], Stefano LANCELLOTTI†, Fabio MASET*, Barbara SPOLAORE*, Nicola POZZI*[2], Giovanni GAMBARO‡, Laura OGGIANU†§, Lorenzo A. CALÒ‖ and Raimondo DE CRISTOFARO†[1]

*Laboratory of Protein Chemistry, Department of Pharmaceutical Sciences, University of Padova, Padova, Italy, †Haemostasis Research Centre, Institute of Internal Medicine and Geriatrics, Catholic University School of Medicine, Rome, Italy, ‡Division of Nephrology and Dialysis, Department of Internal Medicine and Medical Specialties, Renal Program, Columbus-Gemelli University Hospital, Catholic University, Rome, Italy, §Section of Biology Applied to Human Health, 'Roma Tre' University, Rome, Italy, and ‖Department of Clinical and Experimental Medicine and Postgraduate School of Nephrology, University of Padova, Padova, Italy

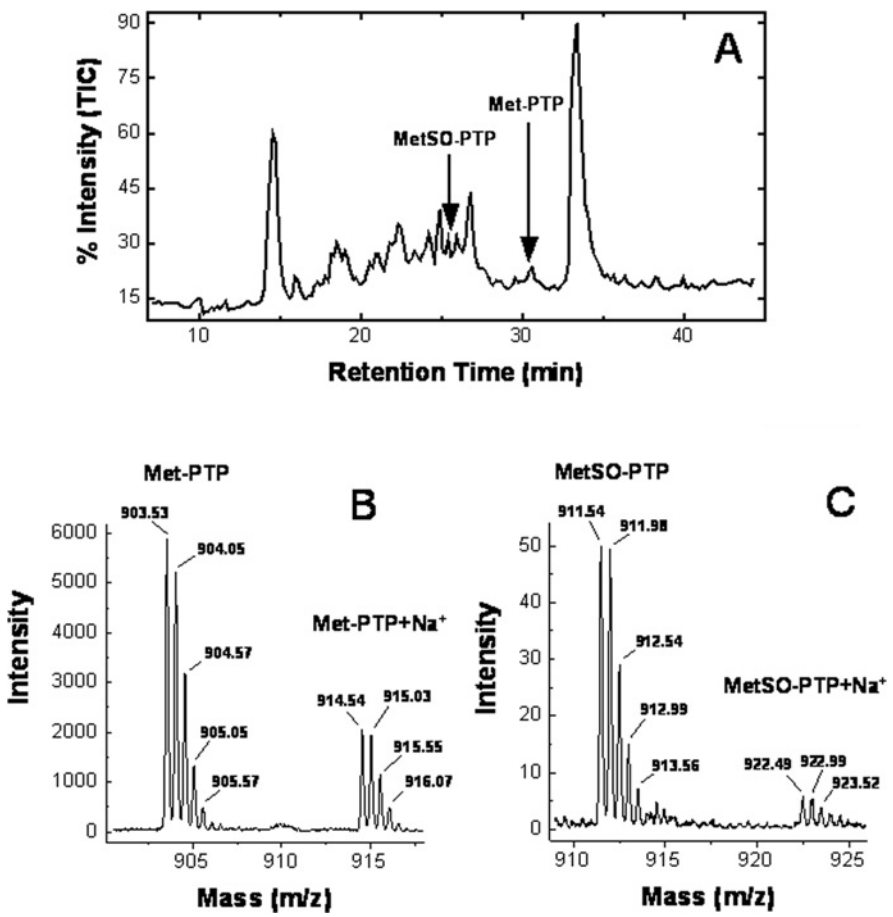


**Figure S1 LC-MS identification of trace amounts of MetSO at position 1606 of normal vWF**

(**A**) LC-MS analysis of the proteolysis reaction of Glu-C protease with normal vWF, as shown in Figure 4(A) of the main text. The arrows on the TIC trace indicate where the PTPs elute. (**B** and **C**) MS spectra of Met-PTP and MetSO-PTP, as identified in (**A**). Instrument parameters were the same as those used in the MS analysis of oxidized vWF samples, as shown in Figures 4 and 5 of the main text. The percentage of MetSO-PTP relative to Met-PTP was estimated from the intensity of the corresponding MS signal and found to be lower than 1 %.

[1] Correspondence may be addressed to either of these authors (email vincenzo.defilippis@unipd.it or rdecristofaro@rm.unicatt.it).
[2] Present address: Department of Biochemistry and Molecular Biology, Doisy Research Center, Saint Louis University, 1100 South Grand Blvd, St. Louis, MO, 63104, U.S.A.

**Table S1 MS data of the fragments obtained by proteolysis of vWF74 and vWF74-MetSO with *S. aureus* Glu-C protease**

The peptide materials eluted that correspond to the chromatographic peaks in Figure 3 of the main text were collected and their monoisotopic masses was determined by MS on an ESI–TOF Mariner spectrometer. The theoretical monoisotopic mass values are shown in parentheses.

(a) vWF74

| Peak number | Fragment sequence | Molecular mass (a.m.u.) |
|---|---|---|
| p1 | $T^{1656}$LPREAPD$^{1663}$ | 897.44 (897.45) |
| p2 | $T^{1656}$LPREAPDLVLQRA$^{1669}$ | 1577.88 (1577.89) |
| p3 | $K^{1616}$IRLPGDIQVVPIGVGPNANVQE$^{1638}$ | 2412.46 (2412.35) |
| p4 | $Q^{1599}$APNLV**YM**VTGNPASDE$^{1615}$ | 1804.92 (1804.83) |
| p5 | $R^{1641}$IGWPNAPILIQDFE$^{1655}$ | 1768.00 (1767.93) |
| p6 | $L^{1639}$ERIGWPNAPILIQDFE$^{1655}$ | 2010.14 (2010.06) |

(b) vWF74-MetSO

| Peak number | Fragment sequence | Molecular mass (a.m.u.) |
|---|---|---|
| p1* | $T^{1656}$LPREAPD$^{1663}$ | 897.44 (897.45) |
| p2* | $Q^{1599}$APNLV**YM(SO)**VTGNPASDE$^{1615}$ | 1821.00 (1820.83) |
| p3* | $T^{1656}$LPREAPDLVLQRA$^{1669}$ | 1577.88 (1577.89) |
| p4* | $I^{1616}$KRLPGDIQVVPIGVGPNANVQE$^{1638}$ | 2412.46 (2412.35) |
| p5* | $R^{1641}$IGWPNAPILIQDFE$^{1655}$ | 1768.00 (1767.93) |
| p6* | $L^{1639}$ERIGWPNAPILIQDFE$^{1655}$ | 2010.14 (2010.06) |

**Table S2 MS/MS data of the PTPs Met-PTP and MetSO-PTP identified in untreated and *in vitro* oxidized vWF**

The PTPs Met-PTP and MetSO-PTP, selected in the LC-MS trace of the proteolysis reaction with Glu-C protease of normal vWF, before and after treatment with peroxynitrite (Figures 4A and 4B of the main text), were subjected to MS/MS analysis. Fragment ions containing $Met^{1606}$ in the unmodified or sulfoxide form are shown in bold.

| Met-PTP | | | MetSO-PTP | | |
|---|---|---|---|---|---|
| Fragment ion | $(MH)^+$ * | Amino acid sequence | Fragment ion† | $(MH)^+$ * | Amino acid sequence |
| *y*2 | 263.07 (263.09) | $Asp^{1614}$–$Glu^{1615}$ | *y*1 | 148.07 (148.06) | $Glu^{1615}$ |
| *y*3 | 350.10 (350.12) | $Ser^{1613}$–$Glu^{1615}$ | *y*2 | 263.08 (263.09) | $Asp^{1614}$–$Glu^{1615}$ |
| *b*4 | 411.17 (411.20) | $Gln^{1599}$–$Asn^{1602}$ | *y*3 | 350.11 (350.12) | $Ser^{1613}$–$Glu^{1615}$ |
| *y*5 | 518.18 (518.21) | $Pro^{1611}$–$Glu^{1615}$ | *y*5 | 518.22 (518.21) | $Pro^{1611}$–$Glu^{1615}$ |
| *b*5 | 524.26 (524.28) | $Gln^{1599}$–$Leu^{1603}$ | *b*5 | 524.26 (524.28) | $Gln^{1599}$–$Leu^{1603}$ |
| *b*6 | 623.32 (623.35) | $Gln^{1599}$–$Val^{1604}$ | *b*6 | 623.32 (623.35) | $Gln^{1599}$–$Val^{1604}$ |
| *y*6 | 632.22 (632.25) | $Asn^{1610}$–$Glu^{1615}$ | *y*6 | 632.22 (632.25) | $Asn^{1610}$–$Glu^{1615}$ |
| *y*7 | 689.23 (689.27) | $Gly^{1609}$–$Glu^{1615}$ | *y*7 | 689.25 (689.27) | $Gly^{1609}$–$Glu^{1615}$ |
| *b*7 | 786.37 (786.41) | $Gln^{1599}$–$Tyr^{1605}$ | *b*7 | 786.39 (786.41) | $Gln^{1599}$–$Tyr^{1605}$ |
| *y*8 | 790.28 (790.32) | $Thr^{1608}$–$Glu^{1615}$ | *y*8 | 790.29 (790.32) | $Thr^{1608}$–$Glu^{1615}$ |
| *y*9 | 889.36 (889.39) | $Val^{1607}$–$Glu^{1615}$ | *y*9 | 889.36 (889.39) | $Val^{1607}$–$Glu^{1615}$ |
| ***b*8** | **917.42 (917.46)** | **$Gln^{1599}$–$Met^{1606}$** | ***b*8** | **933.42 (933.46)** | **$Gln^{1599}$–$MetSO^{1606}$** |
| ***b*9** | **1016.48 (1016.52)** | **$Gln^{1599}$–$Val^{1607}$** | ***b*9** | **1032.48 (1032.52)** | **$Gln^{1599}$–$Val^{1607}$** |
| ***y*10** | **1020.39 (1020.43)** | **$Met^{1606}$–$Glu^{1615}$** | ***y*10** | **1036.41 (1036.43)** | **$MetSO^{1606}$–$Glu^{1615}$** |
| ***b*10** | **1117.52 (1117.57)** | **$Gln^{1599}$–$Thr^{1608}$** | ***b*10** | **1133.53 (1133.57)** | **$Gln^{1599}$–$Thr^{1608}$** |
| ***b*11** | **1174.57 (1174.59)** | **$Gln^{1599}$–$Gly^{1609}$** | ***b*11** | **1190.55 (1190.59)** | **$Gln^{1599}$–$Gly^{1609}$** |
| ***y*11** | **1183.45 (1183.49)** | **$Tyr^{1605}$–$Glu^{1615}$** | ***y*11** | **1199.46 (1199.49)** | **$Tyr^{1605}$–$Glu^{1615}$** |
| ***b*12** | **1288.60 (1288.64)** | **$Gln^{1599}$–$Asn^{1610}$** | ***b*12** | **1304.60 (1304.64)** | **$Gln^{1599}$–$Asn^{1610}$** |
| ***b*14** | **1456.69 (1456.73)** | **$Gln^{1599}$–$Ala^{1612}$** | ***b*14** | **1472.70 (1472.73)** | **$Gln^{1599}$–$Ala^{1612}$** |

*Experimental and theoretical (in parentheses) mass values of singly charged fragment ions.
†Fragment ions derived from MetSO-PTP.

Received 6 October 2011/15 November 2011; accepted 18 November 2011
Published as BJ Immediate Publication 18 November 2011, doi:10.1042/BJ20111798

## 3. CONCLUSIONS

The research carried out during the course of my PhD has focused on different aspects of the pathophysiology of hemostasis and thrombosis.
In particular, the research focused on the role of von Willebrand Factor (VWF), ADAMTS13 and Leukocyte Serine Proteases (LSPs) in physiological and pathological conditions characterized by the presence of elevated oxidative stress, such as sepsis, Diabetes Mellitus (DM) and Chronic Kidney Disease (CKD).
VWF is a plasmatic multimeric glycoprotein stored in platelet α-granules and sub-endothelial connective tissue [1].
The role of VWF in primary hemostasis is to mediate the adhesion and the aggregation of platelets to sites of vascular damage by binding to specific platelet membrane glycoproteins and to constituents of exposed connective tissue [2, 3].
The newly synthesized multimers are called Ultra-Large VWF (UL-VWF), since they can be extremely large (till 20.000 kDa) and hyper adhesive [4].
Upon their secretion into the blood and under shear stress, UL-VWF multimers are proteolytically cleaved by the plasma metalloprotease ADAMTS13, at the peptide bond between Tyr1605 and Met1606 in the VWF A2 domain, as to produce a population of smaller multimers with lower reactivity for platelets [5, 6].
VWF plays an important role in the balance between hemostasis and thrombosis: while the lack of cleavage of VWF by ADAMTS13 causes microvascular thrombosis [7], the excessive cleavage of the molecule by the enzyme may lead to hemorrhagic diathesis [8].
Beside its well known engagement in primary haemostasis, VWF also participates in other biological phenomena of particular relevance for the field of bacterial infection and leukocyte recruitment and extravasation [9].
So, the first part of my research was focused on studying the effect of oxidative stress on the proteolysis of VWF mediated not only by ADAMTS13, but also by leukocyte serine proteases (LSPs).
It was in facts recently shown that LSPs cleave VWF in the A2 domain, near or at the same cleavage site as ADAMTS13 [10], and that oxidation of VWF severely impairs its proteolysis by ADAMTS13 [11].
LSPs were first recognized as degradative enzymes produced by polymorphonuclear cells (PMNs). They can act either intra-cellularly, to degrade ingested host pathogens, or extra-cellularly, in the breakdown of extracellular medium (ECM) components, including VWF, at inflammatory sites to which PMNs are recruited [12, 13].
The human neutrophil elastase (HNE), proteinase 3 (PR3) and cathepsin G (CG) are major components of the neutrophil azurophil granules that participate in the non-oxidative pathway of intra-cellular pathogen destruction [14].
PMNs activation and degranulation results in the production of reactive oxygen species (ROS) and in the release of these proteases into the ECM as proteolytically active enzymes [15].
So, we initially investigated whether or not oxidation of VWF by activated leukocytes affects its cleavage by HNE, PR3 and CG.
Our results showed that, at variance with ADAMTS13, the selective oxidation of Met1606 to Met-SO does not affect or even slightly enhances VWF proteolysis by LSPs.
This was ascertained with both synthetic VWF74-MetSO peptide and full-length VWF, the latter oxidized with HClO or leukocyte MPO, either by using purified proteases or activated PMN cells as source of LSPs and ROS.
All three LSPs have shown to cleave both VWF multimers and synthetic VWF74 peptides with kcat/Km values similar to those of ADAMTS13.
VWF74-MetSO, containing a sulfoxy-methionine residue at position 1606, was cleaved by CG with kcat/Km values even higher than VWF74.
No difference was instead observed for HNE and PR3 in VWF74-MetSO hydrolysis.
Oxidation of VWF multimers by HClO or leukocyte oxidants accelerated their hydrolysis by LSPs.
Thus, on the whole, oxidation by leukocyte ROS leaves unaltered or even improves cleavage of VWF multimers by LSPs under conditions where high concentrations of oxidant species could severely reduce the efficiency of ADAMTS13 proteolysis.
This evidence supports the hypothesis that physiologically, the degradative processing of VWF does not rely on ADAMTS13 proteolysis alone, but arises also from the activity of various serine proteases secreted by activated leukocytes.
On the other hand, the enhanced hydrolysis of VWF by ADAMTS13 in the presence of high oxidative stress remains a point still requiring investigations, particularly in those pathological settings characterized by both high ROS levels and the onset of thrombotic events.
For this reason, the second and the third parts of my PhD were focused on two pathologies characterized by an overall scenario like the one above described: DM and CKD.
In particular, concerning DM, my researches were focused on the study of the role of oxidative stress in acquired thrombotic micro- and macro-angiopathy related to the interaction between VWF and ADAMTS13.
DM is a severe metabolic disease characterized by the presence of high oxidative stress and often complicated by the outcome of thrombotic disorders [16].

By the evaluation of micro- and macro-angiopathy in patients affected by Type 1 (T1DM) and Type 2 Diabetes Mellitus (T2DM), we found a notable increase in the occurrence of both thrombotic disorders among the latter group.
Moreover, T2 diabetic patients even showed significant increases in VWF antigen and activity levels and plasma protein carbonyls content (used as a marker of oxidative stress) when compared to a matched group of control healthy subjects.
No differences appeared instead from ADAMTS13 antigen and activity levels between the groups, meaning that the reduced cleavage of VWF in T2 diabetics did not depend on impaired ADAMTS13 quantity or functionality.
To ensure that to the increased plasma protein oxidation level corresponded an increase in VWF oxidation, we purified VWF from a subgroup of 28 T2 diabetic patients with the highest plasma protein carbonyls level (>200pmol/mg).
We measured the specific VWF carbonyl content and we found it positively correlated with the overall carbonyl content of plasma proteins.
The non linear equation used to analyze the relationship between plasma protein carbonyls and VWF-bound carbonyls allowed us to calculate VWF-bound carbonyls for all samples from T2 diabetic subjects.
The overall plasma proteins carbonyls content and the VWF-bound carbonyls increases were found significantly associated with both micro- and macro-angiopathic complications.
Macro-angiopathies were even found significantly correlated with VWF activity levels, raising the question of whether VWF from T2 diabetics might undergo oxidative modifications, changing its activity pattern.
The answer came from our finding of a positive linear association between the level of VWF-bound carbonyls and the presence of UL-VWF forms (as reflected by the $M_{MW}$ parameter) in T2 diabetic patients with several degrees of micro- or macro-angiopathic complications.
As well as more abundant in high molecular weight forms, VWF from T2 diabetics with the highest carbonyls level even resulted more resistant to the cleavage with ADAMTS13 when compared to a control group after 60 minutes of incubation with the enzyme.
These data provide first evidence that not only high VWF levels, but also its oxidation status and the presence of UL-VWF multimers are associated with thrombotic angiopathies in T2DM.
Elevation of glycemia is known to contemporary induce ROS production and antioxidant systems impairment [17] and the evidences obtained in our study further remark the fundamental role of the oxidative stress in the development of macrovascular diseases in T2DM.
The increase in VWF activity levels that we found associated with oxidative stress and macrovascular thrombosis in T2 diabetic subjects may thus indicate that a huge component of the VWF circulating in the bloodstream is constituted by multimers of high molecular weight, i.e. those characterized by the greatest pro-thrombotic activity.
Likely, the reason of this phenomenon might be due to the ROS-dependent modulation of the signal transduction pathway for the release of high molecular UL-VWF multimers from endothelial cells, where they are stored and where they probably begin their exposure to oxidizing agents [18].
Hence, the increase of ROS in T2DM can dysregulate the release of VWF multimers from endothelial cells, favoring their release into the circulation of patients suffering from this pathology, as verified in our study.
Thus, the obtained evidences led us to conclude that in T2DM, the ROS-mediated induction of UL-VWF release from endothelial cells causes the observed elevation of VWF activity level, which is associated with an increased evidence of major adverse cardiovascular diseases (CVDs).
However, how above said, oxidative stress is not only involved in T2DM clinical settings, but it is also associated with pro-inflammatory and septic states and dysfunction of vascular endothelium characterizing CKD [19].
The concomitant increase of oxidative stress and VWF levels in CKD prompted us to chemically characterize the oxidative state of VWF purified from patients undergoing hemodialysis (HD-VWF) and to compare it with that of healthy subjects.
As already found with VWF isolated from T2DM patients, the average carbonyl content of HD-VWF was at least 10-fold higher than in normal VWF and favorably correlated with the increase of UL-VWF polymers.
Moreover, the incubation with ADAMTS13 of both HD and healthy subjects UL-VWF samples showed a relevant resistance of the former to the enzymatic cleavage.
Targeted Mass Spectrometry (TMS) was used for detecting Met-SO at position 1606 of UL-VWF (the major site of proteolytic regulation of VWF length) in plasma samples of HD patients.
Met-SO was detected at position 1606 of HD-VWF, even though quantitative MS analysis indicated that the proportion of VWF molecules containing Met-SO at position 1606 was relatively small (i.e., >10%). However, this value represents the average extent of Met1606 oxidation in a VWF sample obtained from a pool of plasma derived from 30 patients undergoing HD therapy since a variable time period (i.e., from 1 to 15 years).
Moreover, since haemostasis is a dynamic process resulting from the finely regulated equilibrium between pro-coagulant and anti-coagulant systems, even small perturbation of this equilibrium can cause thrombotic or hemorrhagic effects [20].
In the case of VWF, the shear flow induces the stretching of the multimeric molecules that, in turn, start to efficiently adhere to platelet GpIb receptors, thus increasing the risk of thrombosis [21].

Under physiological conditions, this effect is opposed by shear-induced unfolding of the A2 domain and subsequent cleavage of the newly exposed Tyr1605-Met1606 bond by ADAMTS13 [5].
Hence, it is possible that under high oxidative stress, even relatively small amounts of oxidized UL-VWF multimers, no longer sensitive to proteolysis by ADAMTS13, may generate networks of VWF fibers that amplify platelets adhesion and thrombus formation.
Likewise, UL-VWF polymers might increase the probability of VWF-mediated adhesion of bacteria to vascular vessels and their migration into tissues [9, 22], thus expanding infection. Accordingly, previous studies showed that C *Streptococcus*-induced endocarditis failed to develop in pigs with von Willebrand disease, an inherited bleeding disorder characterized by loss of UL-VWF polymers [23].
In conclusion, the results obtained in my three-years of PhD indicate that the same chemical modification (i.e., oxidation of Met1606) has opposite effects on the susceptibility of VWF to the proteases responsible of the regulation of its length (i.e., ADAMTS13 and LSPs) and of its haemostatic potential in different clinical settings.
In particular, two different pathways of coupled oxidative/proteolytic reactions were identified for VWF.
The first one showed that the rapid and simultaneous release of ROS and LSPs from activated leukocytes results in a positive effect on VWF proteolysis under conditions where high concentrations of ROS could impede the activity of ADAMTS13.
The clinical implications related to such finding concern, in particular, the hemorrhagic diathesis appearing in correspondence of PMNs activation in inflammatory, infectious or onco-hematological settings.
In a more general perspective, this effect could be seen as an anti-bacterial activity of PMNs aimed to impede the efficient VWF-mediated adhesion of bacterial pathogens to the vascular wall and their tissue invasion.
This could (partially) compensate the inhibition that Met-SO formation at position 1606 of VWF exerts on ADAMTS13 proteolysis in conditions of high oxidative stress, which represents the second pathway of coupled oxidative/proteolytic reactions involving VWF.
In this is the case, our findings indicated that chronic oxidative stress, mainly arising from endothelial cells in chronic inflammatory settings such as those characterizing T2DM and CKD, reduces cleavage by ADAMTS13, with a resulting pro-thrombotic effect.
In particular, the involvement of VWF in the pathogenesis of macrovascular thrombosis in T2DM indicates the need of more specific drugs in addition to the classical anti-thrombotic strategies for preventing macrovascular complications in diabetic patients.
The use of aspirin for the primary prevention of cardiovascular events in such subjects, even if widely recommended, provides in facts a lower protection against thrombotic macro-angiopathies than in not diabetic subjects, likely because of the lack of specificity of aspirin in inhibiting the VWF-platelet receptor interaction [24].
Such evidence suggests that the use of more selective VWF inhibitors for the anti-thrombotic prophylaxis, associated to inhibitors of ROS generation and activity, would probably be a successful therapy to apply for the prevention of thrombotic macro-angiopathies in T2DM patients.
Finally, for what concerning patients suffering from CKD, our observations of a critical accumulation of UL-VWF, due to a substantial resistance to the cleavage by ADAMTS13, might constitute a little piece to add in the research of a link among conditions of high oxidative stress and the excess incidence of CVDs in CKD.
Moreover, the same molecular mechanism could event represent a basis for clearing up the reasons of the high frequency with which these patients are so prone to develop sepsis.

## 3.1 REFERENCES


1. Cramer EM et al., *Eccentric localization of von Willebrand factor in an internal structure of platelet alpha-granule resembling that of Weibel-Palade bodies.* Blood, 1985. **66**(3):710-3.
2. Kalafatis M et al., *Localization of a collagen-interactive domain of human von Willebrand factor between amino acid residues Gly 911 and Glu 1,365.* Blood, 1987. **70**(5):1577-83.
3. Pareti FI et al., *Isolation and characterization of two domains of human von Willebrand factor that interact with fibrillar collagen types I and III.* J Biol Chem, 1987. **262**(28):13835-41.
4. Tsai HM et al., *Multimeric composition of endothelial cell-derived von Willebrand factor.* Blood, 1989. **73**(8):2074-6.
5. Tsai HM, *Shear stress and von Willebrand factor in health and disease.* Semin Thromb Hemost, 2003. **29**(5):479-88.
6. Tsai HM et al., *Shear stress enhances the proteolysis of von Willebrand factor in normal plasma.* Blood, 1994. **83**(8):2171-9.
7. Moake JL, *Thrombotic microangiopathies.* N Engl J Med, 2002. **347**(8):589-600.
8. Ginsburg D and Sadler JE, *von Willebrand disease: a database of point mutations, insertions, and deletions. For the Consortium on von Willebrand Factor Mutations and Polymorphisms, and the Subcommittee on von Willebrand Factor of the Scientific and Standardization Committee of the International Society on Thrombosis and Haemostasis.* Thromb Haemost., 1993. **69**(2):177-84.
9. Petri B et al., *Von Willebrand factor promotes leukocyte extravasation*. Blood, 2010. **116**:4712-9.
10. Raife TJ et al., *Leukocyte proteases cleave von Willebrand factor at or near the ADAMTS13 cleavage site*. Blood, 2009. **114**:1666-74.
11. Chen J et al., *Oxidative modification of von Willebrand factor by neutrophil oxidants inhibits its cleavage by ADAMTS13.* Blood, 2010. **115**(3):706-12.
12. Baggiolini M et al., *Cellular mechanisms of proteinase release from inflammatory cells and the degradation of extracellular proteins*. Ciba Found Symp, 1979. **75**:105-21.
13. Janoff A and Scherer J, *Mediators of inflammation in leukocyte lysosomes. IX. Elastinolytic activity in granules of human polymorphonuclear leukocytes*. J Exp Med, 1968. **128**(5):1137-55.
14. Korkmaz B et al., *Neutrophil elastase, proteinase 3 and cathepsin G: physicochemical properties, activity and physiopathological functions*. Biochimie, 2008. **90**(2):227-42.
15. Pham CT, *Neutrophil serine proteases: specific regulators of inflammation*. Nat Rev Immunol, 2006. **6**(7):541-50.
16. Brownlee M, *Biochemistry and molecular cell biology of diabetic complications*. Nature, 2001. **414**:813-20.
17. Giacco F and Brownlee M, *Oxidative stress and diabetic complications*. Circ Res, 2010. **107**:1058-70.
18. Suzukawa K et al., *Nerve growth factor-induced neuronal differentiation requires generation of Rac1-regulated reactive oxygen species*. J Biol Chem, 2000. **275**:13175-8.
19. Massy ZA et al., *The role of oxidative stress in chronic kidney disease.* Semin Dial, 2009. **22**:405-8.
20. Dahlbäck B, *Blood coagulation*. Lancet, 2000. **355**:1627-32
21. Ruggeri ZM *The role of von Willebrand factor in thrombus formation*. Thromb Res, 2007. **Suppl 1**, S5-9.
22. Hartleib J et al., *Protein A is the von Willebrand factor binding protein on Staphylococcus aureus*. Blood, 2000. **96**:2149-56.
23. Johnson CM and Bowie EJ, *Pigs with von Willebrand disease may be resistant to experimental infective endocarditis*. J Lab Clin Med, 1992. **120**:553-8.
24. Ogawa H et al., *Low-dose aspirin for primary prevention of atherosclerotic events in patients with type 2 diabetes: a randomized controlled trial.* Jama, 2008. **300**:2134-41.